Structural Engineering of Evolving Complex Dynamical Networks

A thesis submitted in fulfilment of the requirements for the degree of Doctor of Philosophy

Ali Moradiamani
M.Sc. (Control Engineering), University of Tehran
B.Sc. (Control Engineering), Amirkabir University of Technology

Supervisors:
Dr. Mahdi Jalili
Prof. Lewi Stone

School of Engineering
College of Science, Engineering and Health
RMIT University

September 2019

I certify that except where due acknowledgement has been made, the work is that of the author alone; the work has not been submitted previously, in whole or in part, to qualify for any other academic award; the content of the thesis is the result of work which has been carried out since the official commencement date of the approved research program; any editorial work, paid or unpaid, carried out by a third party is acknowledged; and, ethics procedures and guidelines have been followed.

I acknowledge the support I have received for my research through the provision of an Australian Government Research Training Program Scholarship.

Ali Moradiamani
13/09/2019

List of Publications

Journal articles:

1. **A. Moradi Amani**, M. Jalili, M.A. Fiol, G. Chen, X. Yu, and L. Stone, "Discovering vital nodes for Laplacian spectra of complex networks", IEEE Control Systems Letters (submitted).
2. **A. Moradi Amani**, G. Chen, M. Jalili, X. Yu, and L. Stone, "Distributed rigidity maintenance in distance-based formations using configuration lattice", IEEE Transactions on Control of Network Systems (revision submitted).
3. A Meyer-Bäse, **A. Moradi Amani**, U Meyer-Bäse, S Foo, A Stadlbauer, W Yu, "Pinning observability of competitive neural networks with different time–constants", Neurocomputing, Vol. 329, 2019.
4. N. Gaeini, **A. M. Amani**, M. Jalili, and X. Yu, "Optimization of Communication Network Topology in Distributed Control Systems Subject to Prescribed Decay Rate", IEEE Trans. Cybernetics, 2019.
5. **A. Moradi Amani**, M. Jalili, X. Yu, and L. Stone, "Controllability of complex networks: Choosing the best driver set", Physical Review E, Vol. 98, Issue 3, 2018.
6. **A. Moradi Amani**, N. Gaeini, M. Jalili, X. Yu, "Which Generation Unit Should be Selected as Control Leader in Secondary Frequency Control of Microgrids?", IEEE Journal on Emerging and Selected Topics in Circuits and Systems, Vol. 7 (3), pp. 393-402, 2017.
7. **A. Moradi Amani**, M. Jalili, X. Yu, and L. Stone, "Finding the most influential nodes in pinning controllability of complex networks," IEEE Transactions on Circuits and Systems II: Exp. Briefs, Vol. 64 (6), pp. 685-689, 2017.
8. N. Gaeini, **A. M. Amani**, M. Jalili, and X. Yu, "Cooperative secondary frequency control of distributed generation: The role of data communication network topology," International Journal of Electrical Power & Energy Systems, vol. 92, pp. 221-229, 2017.

Conference articles:

1. **A. Moradi Amani**, M. Jalili, X. Yu, and L. Stone, "A New Metric to Find the Most Vulnerable Node in Complex Networks", IEEE Int. Symp. On Circuits & Systems (ISCAS), Florence, Italy, 2018.
2. **A. Moradi Amani**, N. Gaeini, M. Jalili, X. Yu, "Voltage Control in Distributed Generation Systems Based on Complex Network Approach", Energy Procedia, Vol. 110, pp.334-339, 2017.
3. **A. Moradi Amani**, N. Gaeini, M. Jalili, X. Yu, "Effect of disconnection of generation units on the rate of change of frequency in distributed power systems", Australian Control Conference, Gold Coast, Australia, 2017
4. **A. Moradi Amani**, G. Chen, M. Jalili, X. Yu, "Performance recovery of undirected formations subject to failures in communication links", 43rd Annual Conf. IEEE Indust. Elec. Society (IECON), Beijing, China, 2017
5. N. Gaeini, **A. Moradi Amani**, M. Jalili, and X. Yu, "Secondary cooperative control of distributed generation considering dynamic of nodes and data communication structure," 42nd Annual Conf. IEEE Indus. Elec. Society (IECON), Florence, Italy, 2016.
6. **A. Moradi Amani**, N. Gaeini, M. Jalili, X. Yu, "A New Metric for Measuring Influence of Nodes in Cooperative Frequency Control of Distributed Generation Systems", IEEE Innovative Smart Grid Technologies (ISGT – Asia), Melbourne, Australia, 2016

Abstract

Networks are ubiquitous in nature and many natural and man-made systems can be modelled as networked systems. Complex networks, systems comprising a number of nodes that are connected through edges, have been frequently used to model large-scale systems from various disciplines such as biology, ecology, and engineering. Dynamical systems interacting through a network may exhibit collective behaviours such as synchronisation, consensus, opinion formation, flocking and unusual phase transitions. Evolution of such collective behaviours is highly dependent on the structure of the interaction network. Optimisation of network topology to improve collective behaviours and network robustness can be achieved by intelligently modifying the network structure. Here, it is referred to as "Engineering of the Network".

Although coupled dynamical systems can develop spontaneous synchronous patterns if their coupling strength lies in an appropriate range, in some applications one needs to control a fraction of nodes, known as driver nodes, in order to facilitate the synchrony. This thesis addresses the problem of identifying the set of best drivers, leading to the best pinning control performance. The eigen-ratio of the augmented Laplacian matrix, that is the largest eigenvalue divided by the second smallest one, is chosen as the controllability metric. The approach introduced in this thesis is to obtain the set of optimal drivers based on sensitivity analysis of the eigen-ratio, which requires only a single computation of the eigenvector associated with the largest eigenvalue, and thus is applicable for large-scale networks. This leads to a new "controllability centrality" metric for each subset of nodes. Simulation results reveal the effectiveness of the proposed metric in predicting the most important driver(s) correctly.

Interactions in complex networks might also facilitate the propagation of undesired effects, such as node/edge failure, which may crucially affect the performance of collective behaviours. In order to study the effect of node failure on network synchronisation, an analytical metric is proposed that measures the effect of a node removal on any desired eigenvalue of the Laplacian matrix. Using this metric, which is based on the local multiplicity of each eigenvalue at each node, one can approximate the impact of any node removal on the spectrum of a graph. The metric is computationally efficient as it only needs a single eigen-decomposition of the Laplacian matrix. It also provides a reliable approximation for the "Laplacian energy" of a network. Simulation results verify the accuracy of this metric in networks with different topologies.

This thesis also considers formation control as an application of network synchronisation and studies the “rigidity maintenance” problem, which is one of the major challenges in this field. This problem is to preserve the rigidity of the sensing graph in a formation during motion, taking into consideration constraints such as line-of-sight requirements, sensing ranges and power limitations. By introducing a “Lattice of Configurations” for each node, a distributed rigidity maintenance algorithm is proposed to preserve the rigidity of the sensing network when failure in a sensing link would result in loss of rigidity. The proposed algorithm recovers rigidity by activating, almost always, the minimum number of new sensing links and considers real-time constraints of practical formations. A sufficient condition for this problem is proved and tested via numerical simulations.

Based on the above results, a number of other areas and applications of network dynamics are studied and expounded upon in this thesis.

Keyword: Complex networks, collective behaviours, synchronisability, pinning control, Laplacian spectrum, fault tolerance.

Table of contents

Section II: Controllability of complex networks in the case of node/edge removal

Table of Figures

Abbreviations

ER	Erdős-Rényi
WS	Watts-Strogatz
SF	Scale-Free
DG	Distributed Generation
LMI	Linear Matrix Inequality
MG	Microgrid
PCC	Point of Common Coupling
PLL	Phased-Locked Loop
VSI	Voltage Source Inverter
SG	Smart Grid
WWW	World Wide Web
RoCoF	Rate of Change of Frequency
MCI	Mild Cognitive Impairment
AD	Alzheimer's Disease
ANDI	Alzheimer's Disease Neuroimaging Initiative
AAL	Automated Anatomical Labelling

Chapter 1

Introduction

1.1 Network science

Networks of dynamical units, modelling many natural and human-made systems, may exhibit cooperative phenomena through diverse interactions. Many real systems can be modelled as networks, ranging from biology to ecology, information and technology (Newman 2010). For example, the World Wide Web (WWW) represents an information network. Transportation systems are terminals or stations connected over a network of roads, railways or air. The brain is a network of neurons interacting with each other to process information received from sensing inputs. Social networks are networks of people connected to each other as friends, colleagues or followers. Networks among animals form food chains. The new critical enabler concept of smart grids refers to electricity networks that can intelligently integrate the behaviour and actions of all stakeholders to deliver electricity efficiently, sustainably and economically.

Historically, the study of networks has been mainly a branch of applied mathematics known as *graph theory* (Boccaletti et al. 2006). The root of this theory dates back to 1736 with the problem known as the "Seven Bridges of Königsberg" which was proposed by the Swiss mathematician Leonhard Euler (Euler 1741). This is a problem of seven bridges over four areas in a town as shown in Fig. 1.1. It required finding a round trip for a citizen to pass through the town in such a way that each bridge would be crossed exactly once. Although Euler mathematically proved that such a path does not exist, it was the first time that graphs were

applied to solve a problem. Since then, graph theory has witnessed massive progress. Many practical problems have been solved via graph theory, such as the maximum flow from a source to a sink in a network of pipes. Parallel with graph theory, *network science* has emerged as a multidisciplinary field of science in recent years.

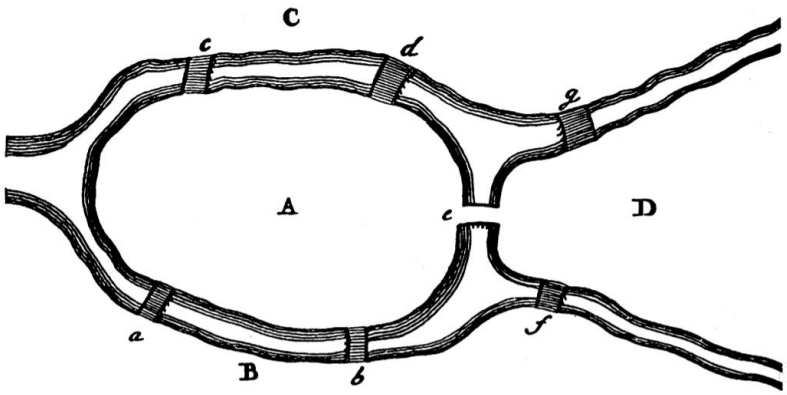

Fig. 1.1. Konigsberg bridge problem (Euler 1741)

In recent decades, network science has gained ever-increasing popularity thanks to massive developments in data processing capabilities and availability of real-world data. Tools borrowed from graph theory have been applied on networks constructed from data collected from real systems. Network science was initiated within the society of Physics by introducing small-world and scale-free network models in two seminal publications by Watts and Strogatz in Nature (Watts and Strogatz 1998) and by Barabási and Albert in Science (Barabasi and Albert 1999). The discovery of small-world and scale-free properties in many real complex systems in different disciplines has attracted a great deal of interest. In a network with small-world features, there is a relatively short path between any two nodes despite their large size. In contrast, there are many networks in nature in which most nodes have very few connections and yet some nodes are hubs, attracting most of the connections; these networks show scale-free properties.

Many real-world complex systems contain nodes with internal dynamics. An example is power grids, where the individual nodes have certain dynamics. An interesting collective behaviour occurs in networks of coupled dynamical agents when they are all doing the same thing at the same time. This is called *synchronisation* or *consensus*.

1.2 Synchronisation as a collective behaviour

Synchronisation processes, as a major collective behaviour observed in coupled dynamical systems, has been extensively studied in different domains, such as biology, ecology, climatology, sociology, technology, and arts (Pikovsky et al. 2003, Yu et al. 2014, Liu and Pan 2015). It has been experimentally shown that synchronisation plays an important role in the pathogenesis of several neurological diseases, such as Parkinson's and Alzheimer's diseases and essential tremor (Uhlhaas and Singer 2006). It is known that synchrony is rooted in human life from the metabolic processes in our cells to the highest cognitive tasks being performed as a group of individuals. For example, the effect of synchrony has been described in experiments of people communicating in a background of shared, non-directive conversation, song or rhythm, or of groups of children interacting to an unconscious beat (Winfree 1967, Arenas et al. 2008).

Study of the synchronisation phenomena is rooted in the discovery of an odd kind of sympathy in two pendulum clocks suspended side by side of each other (Arenas et al. 2008). The Huygens' pendulum clocks swung with exactly the same frequency and 180 degrees out of phase even if they were perturbed. Wiener and Winfree contributed in this field by studying the question of "How is it that thousands of neurons or fireflies or crickets can suddenly fall into step with one another, all firing or flashing or chirping at the same time, without any leader or signal from the environment?" (Wiener 1965). Their contribution was applicable only for all-to-all connected networks which limited its application to large real-world networks. The introduction of Small-World (SW) networks by Watts and Strogatz in 1998 was a revolution for synchronisation theory (Watts and Strogatz 1998).

Synchronisation, also known as consensus or pinning control in engineering applications, has many applications in engineering systems. Power grid networks need to attain synchronisation to guarantee a sound operation of the smart grid in the steady state (Machowski et al. 2011). Pinning control pins the states of all nodes to a desired trajectory by controlling only a small subset of nodes, called driver nodes. Classic stability analysis methods, widely studied by the control community, often fail to handle large complex networks. Inspired by the Lyapunov stability theory, the *master stability function* concept has been proposed to study the local stability of synchronisation in a complex network (Pecora and Carroll 1998). This formalism proposes a sufficient condition for synchronisability and decouples topology and dynamics. Based on this, a topology-dependant metric was suggested for ranking dynamical networks with identical nodes based on their synchronisability (Sorrentino et al. 2007).

Recent research results reveal that synchronisation is highly dependent on the structure of the interaction network as well as dynamics of agents (Porfiri and di Bernardo 2008, Rad et al. 2008, Wu et al. 2009, Posfai et al. 2013, Orouskhani et al. 2016). This has initiated much research on stability and stabilisability of synchronised systems as well as on the optimisation of interaction topology, when possible (Pecora and Carroll 1998, Sorrentino et al. 2007, Jalili et al. 2015). This thesis is inspired by the role of network topology on collective behaviours in complex networks.

1.3 Failure tolerant complex networks

Systems are always subject to faults. For a long time, Fault Detection (FD) and Fault Tolerant Control (FTC) have been interesting research fields in the control community. The main approach is to detect a pre-defined class of faults in the system and to accommodate them by performing modification or re-structuring of controllers. This can preserve the performance of the faulty system still in an acceptable region. Distributed FD and FTC has a long history in control systems (Staroswiecki and Amani 2015). However, there is still a big gap in implementing these algorithms in real-world complex systems with thousands of nodes.

Because complex networks are interconnected, any local fault can easily propagate through them thereby affecting the performance of their collective behaviours. Although many complex systems display a surprising degree of tolerance against faults (Albert et al. 2000), cascading failures have occurred in major infrastructures such as computer and power networks, and will continue to impact our everyday life. Many of these failures work like an avalanche mechanism, triggered by a small initial shock in one point of the system. In addition to failure events in nodes or interconnections, the distributed nature of many complex systems makes them extremely vulnerable to attacks. It has been shown that heterogeneous networks, for instance, are particularly vulnerable to these attacks (Motter and Lai 2002). Robustness against failures and attacks has been an active field of research in recent decades.

When attempting to design complex networks tolerant against failures or attacks, important questions should be addressed, such as “Which components are the most vulnerable points for collective behaviour in a complex network?” or “How can one reduce the failure propagation speed (or even stop it) in a complex network?”. Answering these questions requires combining mathematical graph theory with recent advances in control theory. Although many research results have been reported to address these problems, there is still a

lack of computationally efficient but nevertheless sufficiently accurate methods for working with complex networks. Also, in some applications, such as large-scale power networks, techniques fulfilling real-time requirements of online operation has not been well addressed yet.

1.4 Objectives and contributions

The first objective of this thesis is to derive easily computable and accurate enough metrics to rank nodes of a network based on their influence on collective behaviours. This problem is studied in the case when these nodes are supposed to be drivers of the network and also when they are subject to failure. Metrics should be computationally efficient, i.e. easily applicable to large networks, and also suitable for networks with different topologies. The second objective is to develop an online algorithm to prevent the propagation of failure of nodes in a complex network.

The main contributions of this thesis are:

1) A centrality measure based on sensitivity analysis of the topology of the connection graph which finds (with some approximation) the most influential driver node(s) in pinning control strategy i.e. the strategy for which synchronisation of the whole network to the reference state is attained over the widest range of the coupling parameter. The proposed metric is computationally efficient as it requires only a single eigen-decomposition of the Laplacian matrix of the graph. The metric shows sub-modularity feature so that the best driver set of any size can be derived from the eigenvector associated with the largest eigenvalue of the Laplacian matrix of the network (Moradi Amani et al. 2017, Moradi Amani et al. 2018).

2) A new metric is proposed to identify the spectral impact of node removal in a complex network. This metric is based on the concept of “local multiplicity” and can measure the impact of the removal of any node on any desired eigenvalue of the Laplacian matrix. It is computationally efficient, accurate and applicable to networks with different topologies. Using this metric, the most vulnerable node in the consensus of complex networks are identified as an example (Moradi Amani et al. 2018). It also works accurately in finding vital nodes for the spectral gap and the Laplacian energy.

3) An online algorithm is proposed to recover rigidity of the sensing graph in the formation of agents, as an engineering application of synchronisation. Using this algorithm, the

collective behaviour (formation) remains stable if failure of a sensing link makes the sensing graph non-rigid (Moradi Amani et al.). This is a distributed algorithm which satisfies the real-time requirements of this application and recovers the rigidity by adding a minimum number of links.

1.5 Organisation of the thesis

This thesis consists of three main sections as well as this introduction chapter, a chapter on literature review and a conclusion chapter. Chapters 3 and 4 form section I in which contribution 1 is addressed. Contributions 2 and 3 are addressed in Chapters 5 and 6, respectively forming section II of this thesis. In each chapter, theoretical achievements are first stated and are then supported by simulations.

In **Chapter 3,** the problem of controllability of complex networks using a set of driver nodes is first formulated. Then, based on sensitivity analysis, a new metric is proposed to find the best driver node. It requires a single eigen-decomposition of the Laplacian matrix of the graph. Simulations on a number of synthetic networks show that the proposed metric is accurate for large networks and outperforms heuristics in finding the best driver node. This metric is then extended to find the best driver set of nodes, which again results in a computationally efficient and accurate metric for this unsolved problem of the network community (Moradi Amani et al. 2017, Moradi Amani et al. 2018). Application of these theories to solve problems in distributed generation systems and dementia networks have also been published in various publications I co-authored (Moradi Amani et al. 2017) and (Tahmassebi et al. 2018), respectively. These results are reported in **Chapter 4**.

Chapter 5 focuses on the spectral impact of node removal in a graph. That is when a node (and all its adjacent links) is removed from a network, to what extent will the eigenvalues of the Laplacian matrix change. Immediate application of this problem is to study the effect of node removal on the performance of some collective behaviours, such as the speed of convergence in consensus. The local multiplicity concept, which is indeed a generalisation of the algebraic (or geometric) multiplicity when the graph is seen from a specific node, is applied to address this problem. A new metric is introduced to rank nodes of the network based on the impact of their removal on any desired eigenvalue of the Laplacian matrix. It is applicable to networks with repeated eigenvalues and requires only a single eigen-decomposition; thus, easy to calculate. Simulation results corroborate the accuracy of this metric and demonstrate its

advantage over heuristic techniques. Preliminary studies of this chapter have been reported in (Moradi Amani et al. 2018) while the main contribution has been submitted.

Chapter 6 address the problem of how to prevent the propagation of node/link failure. This chapter focuses on the formation control problem where stability is achieved using distance-based local control actions in agents over a minimally rigid sensing graph. Failure in a link results in loss of rigidity in the sensing graph and instability of the formation. An online distributed rigidity recovery technique using "lattice of configurations" is proposed to solve the rigidity maintenance problem in the case of link breakage. This approach satisfies the real-time requirements of the problem and is not computationally complicated. Another technique based on the combination of sensing and communication networks is proposed for formation recovery in the case of emergency. Results of this chapter have been submitted for publication.

Finally, the thesis concludes with **Chapter 7** where some future directions are proposed.

Chapter 2

Literature review

The study of collective behaviours in complex networks requires knowledge about the structure of the interaction network as well as the dynamics of agents (M. Profiri and M. di Bernardo 2008, Rad et al. 2008, Wu et al. 2009, Posfai et al. 2013, Gates and Rocha 2016, Orouskhani et al. 2016). Mathematical graph theory is a powerful tool to study these aspects from a structural perspective. In addition, dynamical behaviours, such as synchronisability, can be addressed from the control theory point of view. In this chapter, research results on synchronisation and synchronisability of complex networks are reviewed in the context of graph and control theories.

2.1 Complex networks and graph theory

Many networked systems can be modelled as a collection of nodes interacting over a maze of connections, appropriately referred to as a *complex network*. In the context of graph theory, a complex network is modelled as a graph with a set of nodes V connected over a set of edges $E \subset V \times V$ and is given the notation $G = (V, E)$. Nodes can have either static or dynamical behaviours. The set of links E establishes a network among agents, which contains directed/undirected or weighted/unweighted links. The topology of this network can be either

static or evolving over time. Complex network methodology is flexible enough to cover different types of networked systems.

The study of real-world systems requires mathematical models of networks with different structures. One way of modelling that has received considerable attention, is through "random graphs". This approach lies at the intersection of graph theory and probability theory and considers a set of random edges placed between the nodes of a graph. In the late 1950's, two mathematicians, Paul Erdős and Alfréd Rényi described a network with complex topology by this random graph methodology (Erdős and Rényi 1960). They proposed a model for homogenous networks where nodes are connected to each other with probability *p*. Although it was clear that many real-world complex networks have neither regular nor completely random topologies, the Erdős-Rényi random model dominated scientific thinking for some 50 years, because of lack of precise models or computational facilities for large-scale real-world networks (Wang and Chen 2003).

In recent decades, to uncover generic properties of different kinds of complex networks, it was discovered that many real-world networks show small-world effect or scale-free feature (as formally defined below). Some real-world networks, such as social networks and power systems, have the small-world feature in which any two nodes are connected through a path containing only a small number of nodes. In other words, in small-world networks, there is always a short path between any two nodes regardless of the size of the network (Cui et al. 2010). In order to address these networks, Watts and Strogatz introduced the concept of small-world networks in 1998 (Watts and Strogatz 1998). Their proposed model covers networks from a completely regular to completely random topology by changing a rewiring probability *p* (Fig. 2.1). They showed that as *p* increases, networks start to demonstrate small-world features such as high clustering coefficient, a phenomenon observed in many real systems.

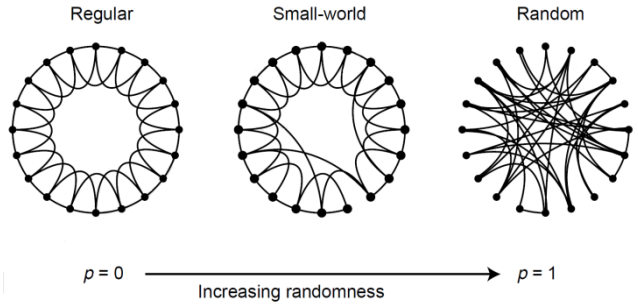

Fig. 2.1. Regular, small-world and random networks for a set of 20 nodes (Watts and Strogatz 1998).

Although networks with Watts-Strogatz (WS) topology is often more realistic than the Erdős-Rényi (ER) model, both of them show almost the same degree distribution. In graph theory, the degree of a node is defined as the number of its connections. The degree distributions of both WS and ER networks peak at an average value and decays exponentially (Wang and Chen 2003). This means that many of the nodes have almost the same number of connections which is the feature observed in *homogenous networks*. However, many real networks, such as the World Wide Web and the Internet, in which the number of nodes grows over time, do not follow such a degree distribution. In order to address these heterogeneous networks, Barabasi and Albert proposed a model resulting in networks with power-law degree distribution (Barabasi and Albert 1999). These networks are often called Scale-Free (SF) networks. In these networks, nodes with higher degrees have more chance to receive new connections than those with lower degrees.

2.1.1 Graph theory notation and terminology

Here, some basic concepts and terminology of graph theory are reviewed.

Definition 2.1: A *graph* $G = (V, E)$ is a non-empty finite set of N nodes or vertices, denoted by the set $V = \{v_1, v_2, \ldots, v_N\}$, and a set of edges $E \subset V \times V$, i.e. a subset of pairs of elements of N.

Two nodes connected by an edge are referred to as adjacent or neighbouring nodes. For example, the pair (i, j) or a_{ij} denotes the edge between nodes i and j. The order of pairs matters to the structure in directed graphs (digraphs), i.e. $a_{ij} \neq a_{ji}$, but not in undirected ones. If there is a directed edge from v_i to v_j, v_i and v_j are called "parent" and "child", respectively. In addition to binary networks, i.e. those with $a_{ij} \in \{0,1\}$, there are weighted networks in which, the edge (i, j) is labelled with the weight $w_{ij} \in \mathbb{R}^+$. This weight can be applied to quantify the amount of different types of interactions between nodes, such as distance, force and impedance. Figure 2.2 displays the graphical representation of three graphs that are (a) undirected, (b) directed, and (c) weighted.

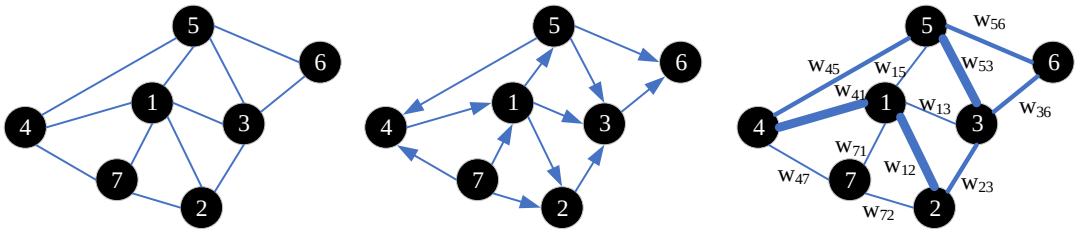

(a) (b) (c)

Fig. 2.2. A graphical representation of (a) undirected, (b) directed and (c) weighted undirected.

In directed graphs, the in-degree and out-degree of a node are numbers of links pointing to or from the node, respectively. In undirected networks, the number of links divided by the total number of nodes, i.e. $2\times E/N$, is the average degree of the graph. The distance between two nodes of a graph is the number of edges along the shortest path connecting them. When there is a path between any pair of nodes, an undirected (directed) graph is called "connected" ("strongly connected"). A directed graph is "weakly connected" if it is connected when all links are converted to undirected. One of the basic concepts in graph theory is *reachability*. Node *j* is reachable from node *i* if there is a path from node *i* to *j*. The concept of connectivity can be defined based on the reachability of nodes.

A graph in which all nodes have the same degree is called "regular". A graph is called "complete" if there is an edge between every pair of distinct nodes. A walk from node *i* to node *j* is a series of nodes and edges which starts with node *i* and finishes with node *j*. The length of the walk is defined as the number of edges in it. A walk with the minimum number of edges between two nodes is referred to as the shortest path. The average shortest path is one of the important properties of a complex network and demonstrates how well information flows throughout the network globally (Wasserman and Faust 1994, Scott 2017).

Existence of closed walks or the cycle structure in a network is conveyed by the "clustering coefficient". The clustering coefficient shows the presence of triangles or loops in a network and quantifies the efficiency of the network in transferring information locally. It can be calculated by (Costa et al. 2007):

$$C = \frac{3N_{\Delta}}{N_3}$$

where C is the clustering coefficient, N_{Δ} and N_3 are the number of triangles and the number of triple combinations of nodes of the network, respectively, which can be calculated as

$$N_{\Delta} = \sum_{k>j>i} a_{ij}a_{ik}a_{jk}$$

$$N_3 = \sum_{k>j>i}(a_{ij}a_{ik} + a_{ji}a_{jk} + a_{ki}a_{kj})$$

The clustering coefficient is also known as a measure of fault tolerance of a network, i.e. the lower the clustering coefficient is, the more fault vulnerable the network will be. In other words, networks with small clustering coefficients indicate poor local connectivity and any fault in one of the nodes may dramatically affect their communication performance (Latora and Marchiori 2001).

Although flexible enough to model many real-world networks, the presence of these interactions in complex networks has raised important questions which have been neglected in the studies of traditional disciplines (Wang and Chen 2003). For example, how do social networks mediate the transmission of disease? How does a failure propagate through a large power network or a global financial network? Is a network with a pre-defined topology robust enough against failures? What is the most efficient network topology in a networked system? These questions have led scholars to some important research problems concerning how the network structure facilitates or constrains the network dynamical behaviour.

2.1.2 Network models

In this thesis, synthetic scale-free, small-world and Erdős-Rényi networks are considered to support the theoretical achievements. Scale-free networks are constructed using the static model proposed in (Goh et al. 2001). In this algorithm, starting with a fully connected core for the graph, at each step a new node is added to the network and creates a number of connections as follows. The edges for the new nodes are linked to an old node i with a probability proportional to $(k_i+B)/\sum_j(k_j+B)$, where k_i is the degree of the node i and B is a constant to control the heterogeneity of the network; as B increases, heterogeneity of the network decreases (Chavez et al. 2005).

Scale-free networks have heterogeneous node degrees. In order to construct networks with almost homogeneous degrees, the model proposed by Watts and Strogatz in their seminal work (Watts and Strogatz 1998) is used. The network construction algorithm is as follows. First, a regular graph is considered in which each node is connected to its m-nearest neighbours (each node has $2m$ connections). Then, the links are rewired with probability p, provided that self-loops and multiple connections are avoided. For some medium values of the rewiring probability, one obtains a network that has both small-world property (the average path length scales logarithmically with the network size), and a rather high clustering coefficient (or transitivity). Watts and Strogatz showed that many real networks (including power grids) have this property (Watts and Strogatz 1998). Degree-homogeneous networks can also be constructed using the model proposed by Erdős and Rényi (Erdős and Rényi 1960). In this model, the nodes are connected with probability p. In other words, random probability values are assigned to all link in a complete network; then links with probabilities less than p are removed.

2.1.3 Spectral Graph theory

Graph theory is the mathematical framework of complex networks in which matrix representation has been always of interest (Amaral and Ottino 2004, Barabasi and Oltvai 2004, Bornholdt and Schuster 2006). A graph $G = (V, E)$ with N nodes and m edges can be described by an adjacency matrix or an incidence matrix.

Definition 2.2. The *adjacency matrix* for a graph G is an $N \times N$ square matrix $A = [a_{ij}]$ in which $a_{ij} = 1$ ($i, j = 1, 2,\ldots,N$) whenever there is a link from node i to j and zero otherwise ($a_{ij} = w_{ij} \in \mathbb{R}^+$ for weighted graphs).

Definition 2.3. A Graph G can be represented by an $N \times m$ matrix $H = [h_{ik}]$ called *incidence matrix* where h_{ik} equals to 1 whenever node i is incident with edge k.

If G is a simple graph, i.e. an undirected and unweighted graph containing no self-loops and no multiple edges, then the eigenvalues α_i ($i = 1,2, \ldots, N$) of its adjacency matrix A satisfies $\sum_i \alpha_i = 0$ and $\sum_i \alpha_i^2 = 2m$. In general, $\sum_i \alpha_i^l$ counts the number of closed walks of length l.

Perron-Frobenius theorem: If an $n \times n$ matrix has nonnegative entries, then it has a nonnegative real eigenvalue λ, which has *maximum* absolute value among all eigenvalues. This eigenvalue λ has a nonnegative real eigenvector.

The Perron–Frobenius Theorem immediately implies that if G is connected, then the largest eigenvalue α_{max} of its adjacency matrix is real and has multiplicity 1 (Lovasz 2007).

2.1.3.1 The Laplacian matrix and its properties

Another important matrix which has outstanding properties and is heavily used in graph theory is the Laplacian matrix. The Laplacian matrix brings important information on the connectivity properties of a graph.

Definition 2.4. The *Laplacian matrix* L associated with a graph G is defined as $L = D - A$ in which A is the adjacency matrix of the graph and $D = [d_{ij}]$ is a diagonal matrix for which $d_{ii} = \sum_j a_{ij}$ and $d_{ij} = 0$ for $i \neq j$.

The Laplacian matrix can be also represented using the incidence matrix. For an edge l connecting nodes i and j of the undirected graph $G = (V, E)$, one can define $h_{li} = 1$ and $h_{lj} = -1$. Then the Laplacian matrix is

$$L = HH^T = \sum_{i=1}^{m} h_l h_l^T$$

where m is the number of edges and h_l refers to the l^{th} column of the incidence matrix H.

Definition 2.5. The set $sp(L) = \{\lambda_1^{m1}, \lambda_2^{m2},\ldots, \lambda_d^{md}\}$ in which λ_i ($i = 1, 2, \ldots, d$) is the i^{th} eigenvalue of L with multiplicity m_i, is called *spectrum* of the Laplacian matrix.

The Laplacian matrix of an undirected graph is a symmetric matrix; thus all its eigenvalues are real and have non-negative values according to the Gershgorin circle theorem (Gershgorin 1931). In other words, The Laplacian matrix of an undirected graph is a positive semi-definite matrix. In addition, all its eigenvectors are real and orthogonal. Since the Laplacian matrix has a zero-row sum, it always admits $\lambda_1 = 0$ as the lowest eigenvalue and corresponding eigenvector $v_1 = (1,1,\ldots,1)$. Therefore, the spectrum of a connected simple graph, i.e. a graph with non-repetitive Laplacian eigenvalues, is of the form of $sp(L) = \{\lambda_1, \lambda_2,\ldots, \lambda_N\}$ where $0 = \lambda_1 < \lambda_2 \leq \ldots \leq \lambda_N$.

Definition 2.6. The second smallest eigenvalue of the Laplacian matrix, λ_2, is known as the *algebraic connectivity* (Fiedler 1973) with the corresponding normalized eigenvector referred to as the *Fiedler vector*.

Algebraic connectivity shows how well-connected the graph is since $\lambda_2(L)$ is monotone increasing in the edge set, i.e. if $G_1 = (V, E_1)$ and $G = (V, E_2)$ are such that $E_1 \subseteq E_2$, then $\lambda_2(L_1) \leq \lambda_2(L_2)$ (Fiedler 1973). It means that the smaller the λ_2 is, the closer the graph is to disconnection. Another important property of the Laplacian eigenvalues is the number of zero eigenvalues. Multiplicities of zero eigenvalues are proved to be the number of isolated components of a graph (Boccaletti et al. 2006). The maximum eigenvalue λ_N is real from Perron-Frobenius theorem and is called the *spectral gap*.

2.2 Controlling complex networks

Control theory, an interdisciplinary branch of engineering and mathematics, has been studied for a long time to influence dynamical systems towards better performances. Traditionally, the control design process has been based on mathematical models of dynamical systems in the form of state-space equations. Extensive research in this area has promoted advanced control systems, such as optimal, robust and adaptive control algorithms. However, with increasing complexity and the distributed nature of complex networked systems, the traditional methodologies may not satisfy real-time constraints required for real systems. This

has started a paradigm shift in which network structure is also considered when dealing with a control problem (Yu et al. 2011).

Complex networks methodology provides a promising addition to existing control theories in order to deal with networked dynamical systems. It essentially studies structural and dynamical aspects of a collection of nodes and links without heavy dependence on the system dimension. Therefore, it may reduce the computational cost of traditional control methodologies applied to networked systems. Here, we briefly overview recent progress in the field of networks synchronisation and control.

2.2.1 Controllability of dynamical systems

Controllability is one of the fundamental concepts in the mathematical control theory. The notion of controllability of a dynamical system was first introduced in (Kalman et al. 1963).

Definition 2.7. State (output) controllability of a dynamical system is defined as the possibility of driving states (outputs) of the system from an arbitrary initial condition to any desired value in a finite time by applying appropriate control signals (Kailath 1980).

The classic and famous method to ensure state controllability of a dynamical system states that the system

$$\dot{\boldsymbol{x}}(t) = A\boldsymbol{x}(t) + B\boldsymbol{u}(t)$$
$$\boldsymbol{y}(t) = C\boldsymbol{x}(t) + D\boldsymbol{u}(t) \qquad (2.1)$$

is full state controllable if and only if Kalman's controllability matrix $[B, AB, \ldots, A^{n-1}B]$ has a full rank (Kailath 1980). $\boldsymbol{x} \in \mathbb{R}^n$ and $\boldsymbol{u} \in \mathbb{R}^p$ are state and input signals, respectively and A, B, C and D are matrices with appropriate dimensions where A and B are called state and input matrices, respectively.

There are important relationships between controllability and stabilisability of both finite- and infinite-dimensional linear control systems. A linear dynamical system is stabilisable if its unstable modes are controllable (Chen 1998). Controllability is also strongly related to the theory of minimal realization and canonical forms of dynamical systems, which have been developed by Kalman, Jordan and Luenberger (Kailath 1980). The problem of minimum energy control for many classes of linear and time-delay systems is also related to the concept of controllability (Klamka 2013).

Although control theory is a mathematically developed branch of engineering, fundamental questions pertaining to the controllability of complex networks make the applicability of traditional approaches questionable. Traditional controllability conditions should be updated considering a new player; that is the network topology. In addition, computationally efficient measures are required to study real-world large-scale complex dynamical networks. These difficulties have been the root of recent research in controllability of complex networks.

2.2.2 Controllability of complex networks

The classic controllability analysis method is often inapplicable in the context of complex networks due to the system dimension (Pasqualetti et al. 2014). It has also been shown that network control fails in practice if the controllability Gramian is ill-conditioned, which can occur even when the corresponding Kalman's controllability matrix is well conditioned (Sun and Motter 2013). Therefore, a new paradigm is required for controllability studies of complex networks. The fact that the field of complex networks originated from mathematical graph theory motivates a graph-inspired understanding of controllability rather than the traditional matrix-theoretical one.

The structural controllability concept (Lin 1974) has been studied in the context of complex networks (Liu et al. 2011) in order to identify a driver set with the minimum number of nodes to control the network. Although the proposed method is simple and easy to implement, it does not consider internal dynamics of nodes. Later, (Cowan et al. 2012) showed that deriving only one node is enough to control the whole network if internal nodal dynamics are considered. Clearly, control of a large network by driving only a single node requires huge amount of energy to be injected into that node, which is impractical, if not impossible, in most real-world applications. Therefore, new metrics are required to identify the best set driver nodes in a complex network.

Controllability of complex networks has been also studied from an energy perspective. The trade-off between control energy and the number of control (driver) nodes is characterised in (Pasqualetti et al. 2014). They also proposed a decoupled control strategy for controlling stable complex networks, which is based on network partitioning. The first step requires extracting the least controllable cluster based on the minimum eigenvalue of the controllability Gramian and then calculating the second smallest eigenvalue of its Laplacian matrix. This

process should be repeated *m* time (*m* being the number of driver nodes) resulting in a computationally complicated process. The controllability Gramian has also been applied to derive the lower and upper energy bounds in control of complex networks (Yan et al. 2012). Metrics based on controllability and observability Gramians are also studied for sensor and actuator placement problems (Summers et al. 2016).

2.2.2.1 Structural controllability

Control performance in complex networks depends on both the structure of the network and the dynamics of nodes. Lin first introduced the concept of *Structural Controllability* for linear time-invariant dynamical systems (Lin 1974). Consider the dynamical system (2.1) with the following state and input matrices:

$$A = \begin{bmatrix} a_{11} & a_{12} & 0 \\ a_{21} & a_{22} & 0 \\ a_{31} & a_{32} & a_{33} \end{bmatrix}, \boldsymbol{b} = \begin{bmatrix} 0 \\ 0 \\ b_3 \end{bmatrix}$$

A graph for pair (*A*,***b***) can be generally obtained as follows (Lin 1974). For every non-fixed entry (here, non-zero entry) of the augmented matrix [*A* | ***b***], there exist a directed graph between states x_i themselves or between x_i and b_j. Diagonal elements of matrix *A* result in self-loops in the graph. An example is shown in Fig. 2.3(a). It is clear from this graph that nodes x_1 and x_2 are nonaccessible. A node x_i is called nonaccessible if and only if there is no possibility to reach x_i from any input b_i. It is concluded in (Lin 1974) that the pair (*A*,***b***) is not structurally controllable if there exists at least one nonaccessible state x_i in its graph. It is also clear that the system is not full state controllable if it is not structurally controllable.

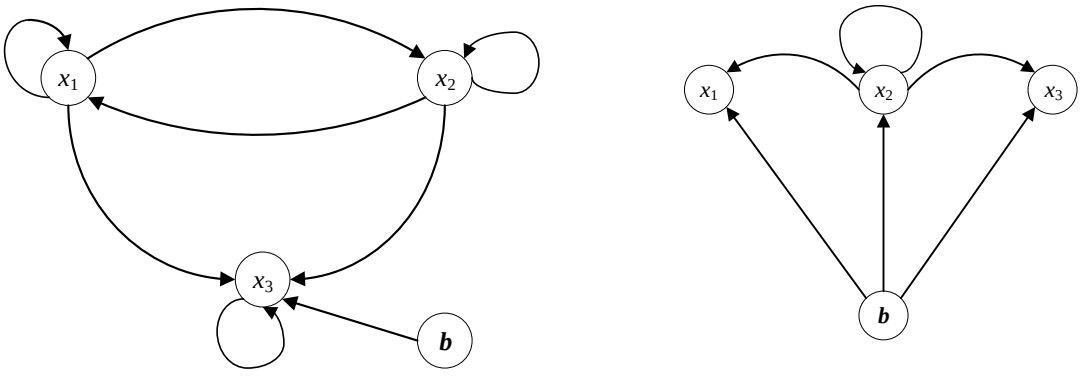

(a) (b)

Fig. 2.3. Structural controllability study using graphs

In addition, there may be "dilation" in the graph which makes the pair (A,$\boldsymbol{b}$) structurally uncontrollable although all nodes are accessible. To introduce the concept of dilation, suppose the dynamical system (2.1) with the following state and input matrices:

$$A = \begin{bmatrix} 0 & a_{12} & 0 \\ 0 & a_{22} & 0 \\ 0 & a_{32} & 0 \end{bmatrix}, \boldsymbol{b} = \begin{bmatrix} b_1 \\ b_2 \\ b_3 \end{bmatrix}$$

for which, the graph of Fig. 2.3(b) represents the pair (A,$\boldsymbol{b}$). Clearly, all x_i's are accessible from $\boldsymbol{b}$. Now, let's consider the set of states $S = \{x_1, x_2, x_3\}$. Consider the set of nodes from which at least one node of S is accessible, defined as $T(S) = \{x_2, \boldsymbol{b}\}$. The graph of pair ($A$,$\boldsymbol{b}$) contains a dilation if and only if there is a subset of S with k states for which there is no more than $k - 1$ nodes in $T(S)$. Therefore, the graph in Fig. 2.3(b) contains dilation. If the graph of pair (A,$\boldsymbol{b}$) contains dilation, then system (2.1) is structurally uncontrollable (Lin 1974).

The dynamical system (2.1) is structurally controllable if the graph related to its pair (A,$\boldsymbol{b}$) is accessible and has no dilation (Lin 1974). This proposes a computationally efficient algorithm to study structural controllability which works with matrices of only 0 and 1 elements. This efficiency paved the way for structural controllability towards complex networks as presented by (Liu et al. 2011). However, in deriving this controllability measure, the internal dynamics of the nodes were ignored. This thesis combines structural proprieties and nodal dynamics in order to address the controllability of complex networks.

2.2.2.2 Synchronisation

In addition to structural and energy-based studies, controllability of complex networks is also addressed in the context of collective behaviours, such as synchronisation, consensus, formation and flocking. Among them, synchronisation has attracted a lot of research activities (Tang et al. 2014). The synchronisation problem in a network of coupled dynamical agents is presented as follows. Let's consider a dynamical network including N identical individual dynamical nodes and an undirected and unweighted connection network. The equations of motion of the network read:

$$\frac{d\boldsymbol{x}_i}{dt} = F(\boldsymbol{x}_i) - \sigma \sum_{j=1}^{N} l_{ij} H \boldsymbol{x}_j; \quad i = 1,2, \dots, N, \tag{2.2}$$

where $\boldsymbol{x}_i \in \mathbb{R}^n$ is the n-dimensional state vector, F: $\mathbb{R}^n \rightarrow \mathbb{R}^n$ defines the individual dynamical systems' state equation, σ represents unified coupling strength and $L = [l_{ij}]$ is the Laplacian

matrix. Non-zero elements of *H* determine the coupled elements of the oscillators. Let's first distinguish between local and global synchronisation:

Definition 2.8. The dynamical system described by (2.2) synchronises *globally* if the following condition is satisfied for any initial conditions,

$$\lim_{t\to\infty}\left\|\boldsymbol{x}_i(t)-\boldsymbol{x}_j(t)\right\|=0; \qquad \forall i,j=1,2,\dots,N \tag{2.3}$$

The dynamical system described by (2.2) synchronises *locally* if (2.3) holds only when $\|\boldsymbol{x}_i(0)-\boldsymbol{x}_j(0)\|<\varepsilon$ for an $\varepsilon>0$. ■

The "synchronisation" topic is widely studied in physics. It is also studied in other disciplines under different terms, such as consensus of multi-agent systems in engineering. Relevant research results, reported in the last two decades (see e.g. (Tang et al. 2014) as a survey), can be classified in the following important topics (Tang et al. 2014):

- Robustness of synchronisation in complex networks
- Controllability of complex networks
- Observability of complex networks
- The synchronisation of multiplex networks
- Explosive Synchronisation of complex networks

Although synchronisation emerges in a network of coupled dynamical nodes under some conditions, control actions facilitating synchrony are required in many applications. There has been much interest in this topic in the control community.

2.2.3 Synchronisability of complex networks

Synchronisability of complex networks can be generally defined as the ease by which nodes of the network synchronise their activities. Although coupled dynamical systems can develop spontaneous synchronous patterns if their coupling strength lies in an appropriate range, in some applications one needs to control a fraction of nodes, known as driver nodes in order to facilitate the synchrony (Sun and Motter 2013, Gao et al. 2014). This control action can provide faster synchronisation over a wider range of coupling strength.

In addition to the structural techniques, pinning control has also been proposed in the literature as a strategy to synchronise coupled dynamical nodes of a network onto a desired common trajectory (Porfiri and di Bernardo 2008, Q. Song and J. Cao 2010). The idea is to actively control a subset of nodes (usually called driver nodes) to achieve the control objective while the control action is propagated to the rest of the network through couplings. The objective of pinning control is to pin all nodes of the system to the following desired state, i.e. $\boldsymbol{x}_1(t) = \boldsymbol{x}_2(t) = \ldots = \boldsymbol{x}_n(t) = \boldsymbol{s}(t)$ (Wang and Chen 2002):

$$\frac{d\boldsymbol{s}(t)}{dt} = F\big(\boldsymbol{s}(t)\big). \tag{2.4}$$

The master stability function (Pecora and Carroll 1998) gives necessary conditions for the local stability of the synchronisation manifold $\boldsymbol{x}_1(t) = \boldsymbol{x}_2(t) = \ldots = \boldsymbol{x}_n(t) = \boldsymbol{s}(t)$. To study local stability of this manifold, states of nodes can be perturbed around equilibrium as $\boldsymbol{x}_i(t) = \boldsymbol{s}(t) + \boldsymbol{\zeta}_i(t)$. The variational equations of (2.2) are

$$\dot{\zeta}_i(t) = \nabla F(s)\zeta_i(t) - \sigma \sum_{j=1}^{N} l_{ij} H\zeta_j\,, \quad i = 1,2,\ldots,N \tag{2.5}$$

where ∇ stands for the Jacobian. For an undirected network, i.e. $L = L^T$, the similarity transformation $\eta_i = \zeta_i.P$ can be defined such that $L = P\ \Gamma P^T$ where Γ is a diagonal matrix including eigenvalues of L and columns of P are their corresponding eigenvectors. As a result, (2.5) is equivalent to

$$\dot{\eta}_i(t) = \nabla F(s)\eta_i(t) - \sigma\lambda_i H\eta_i(t), \quad i = 1,2,\ldots,N \tag{2.6}$$

where λ_i's are eigenvalue of the Laplacian matrix L. The largest Lyapunov exponent of variational equation (2.6) is called the *Master Stability Function* and is shown here by $\Lambda(a)$ in which $a = \sigma\lambda_i$. From the Lyapunov stability theory, the synchronised system is locally stable if $\Lambda(a) < 0$.

Based on the master stability function, one can classify synchronisation systems into two different classes (Jalili 2013): Class I (like *x*-coupled Lorenz Oscillators) in which $\Lambda(a)$ becomes zero at some values $a = a^*$ and stay negative for any $a > a^*$ (see Fig. 2.4 a). On the other hand, class II systems (such as *x*-coupled Rössler oscillators) have negative master stability function only in the range $a_1^* < a < a_2^*$ (Fig. 2.4 b). For the latter class, synchronisability condition is $a_1^* < \sigma\lambda_2 < \sigma\lambda_3 < \ldots < \sigma\lambda_N < a_2^*$ which is satisfied if

$$\frac{\lambda_N}{\lambda_2} < \frac{a_2^*}{a_1^*} \tag{2.7}$$

The left-hand side of this condition is related to the topology of the network, while the right-hand side depends on the dynamics of individual nodes. From this condition, it is concluded that the smaller λ_N / λ_2, the better its synchronisability (Jalili 2013).

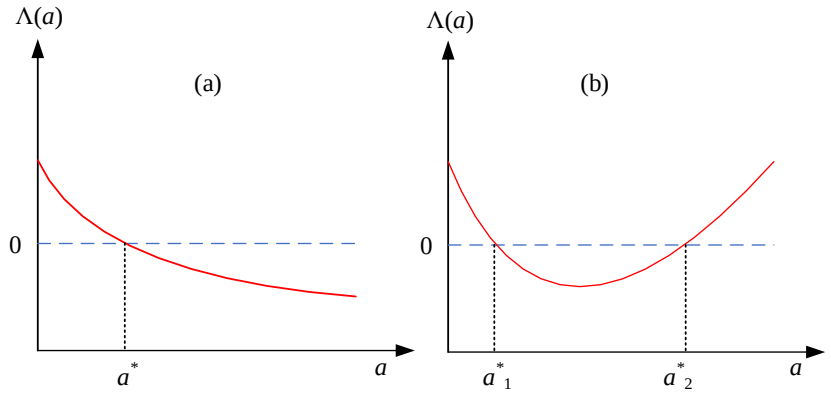

Fig. 2.4. Different types of system considering their Lyapunov exponent Λ(*a*) behaviour

In order to pin (synchronise) the dynamical network (2.2) to the reference dynamics (2.4), the following state feedback controller should be designed:

$$\frac{d\boldsymbol{x}_i}{dt} = F(\boldsymbol{x}_i) - \sigma \sum_{j=1}^{N} l_{ij}\, H\boldsymbol{x}_j + \sigma\beta_i k_i(\boldsymbol{x}_i - \boldsymbol{s}); \quad i = 1,2,\dots,N, \tag{2.8}$$

where k_i is the feedback gain. β_i determines the node where the control signal should be applied; $\beta_i = 1$ for driver nodes and zero otherwise. Therefore, the control system should propose driver nodes (for which $\beta_i = 1$) and their control gains k_i simultaneously, which results in a combinatorial optimisation problem (Summers et al. 2016). There is still a lack of research on selecting the best driver node(s) and their corresponding control gains. This thesis addresses the first problem.

Following the master stability function formalism, local stability of the synchronised solution can be evaluated in terms of N independent blocks with the difference that λ_i's are not eigenvalues of the Laplacian matrix, but they are for the following augmented Laplacian matrix:

$$C = \begin{bmatrix} l_{11} + k_1\beta_1 & l_{12} & \dots & l_{1N} \\ l_{21} & l_{22} + k_2\beta_2 & \dots & l_{2N} \\ \vdots & \vdots & \vdots & \vdots \\ l_{N1} & l_{N2} & \dots & l_{NN} \end{bmatrix} \tag{2.9}$$

which is the Laplacian matrix of the network diagonally perturbed by control gains of driver nodes. Eigenvalues of this augmented Laplacian matrix are ordered as $0 < \lambda_1 \leq \lambda_2 \leq \dots \leq \lambda_N$. From the master stability function formalism, $R = \lambda_N/\lambda_1$ can be considered as the synchronisability metric for the network (Sorrentino et al. 2007, Jalili et al. 2015); i.e. the

smaller R, the better the synchronisability (pinning controllability). Based on this metric, having two sets of driver nodes S_1 and S_2 with the same size, S_1 is argued to provide more effective pinning control than S_2, if the network synchronises to the reference state for a larger range of coupling parameter when nodes in S_1 is chosen as drivers. The metric R depends on eigenvalues of the augmented Laplacian and connects the pinning controllability studies to spectral graph theory.

Pinning controllability can be evaluated in terms of the required control action, the number of nodes to be pinned and the feedback topology (Sorrentino et al. 2007). An important unsolved challenge in this context is to find the set of best drivers, leading to the best pinning control performance. Depending on the choice of pinning controllability metric, one can interpret what "optimality" means. An obvious choice for the optimal set is to select vital nodes, e.g., those with the highest degree, betweenness or closeness centrality. These heuristic methods, although computationally cost-effective, often result in non-effective pinning controllability (Liu et al. 2011, Jalili et al. 2015, Zhou et al. 2015, Moradi Amani et al. 2017). Recently, evolutionary optimisation algorithms have also been applied to find a set of most influential nodes in pinning control, resulting in a better performance than the above heuristic methods (Jalili et al. 2015, Orouskhani et al. 2016). However, evolutionary optimisation algorithms require computing an objective function, i.e. the synchronisation criteria, at every step of the optimisation process, and they often converge only after many steps, where the number of steps grows exponentially with network size. Therefore, such methods can only be applied to relatively small networks.

Using the metric R, pinning controllability can be influenced through network topology (i.e. l_{ij}'s), location of driver nodes (or β_i's) and control gains of driver nodes (i.e. k_i's). In other words, synchronisation of a complex network can be facilitated through:

1) Optimizing network topology by
    a. Adding/removing nodes (Watanabe and Masuda 2010)
    b. Adding / Removing / Rewiring edges (M. Jalili and Yu 2016)
2) Selecting appropriate control nodes (Moradi Amani et al. 2018)
3) Designing proper control gains for drivers

Chapter 3 of this thesis addresses the problem of identifying the best drivers in controllability of complex networks using sensitivity analysis of R. Then, application of these

achievements in solving practical problems in distributed power generation and dementia networks are studied in Chapter 4.

2.3 Controllability in the case of node/edge removal

What is the most vulnerable node of a network to be attacked or to be removed? What is the most influential node in a network? These are typical questions of great interest to the network science community. Removing important nodes from complex networks is a challenge in fighting against criminal organisations and preventing disease outbreaks (Jahanpour and Chen 2013). Central (or vital) nodes are those with significant importance for the functionality of the network. A number of centrality measures have been proposed to quantify the importance of a node in complex networks (Mieghem 2011). The simplest one is the degree centrality, measuring the number of connections a node has, which proposes hubs as vital nodes. However, to answer the above questions comprehensively, terms like "vulnerable", "influential" or "important" should be linked to a particular network function, as the degree is not always the best choice of centrality for many dynamical properties (Liu et al. 2011, Cowan et al. 2012). This thesis focuses on synchronisability of a complex network which is measured by the metric *R*.

"Robustness" and "vulnerability" of a network against failures and attacks have been of much interest especially when security (Motter and Lai 2002) or fault tolerance (Staroswiecki and Amani 2015) of networked systems are considered. It has been shown that scale-free networks are robust against random node removal (Albert et al. 2000), but are fragile to specific removal of the most highly connected nodes (Xiao Fan and Guanrong 2002). Interactions among nodes as well as interconnections between networks facilitate the spread of undesired effects of failures and attacks which may result in catastrophic cascading failures (Motter and Lai 2002, Buldyrev et al. 2010). Therefore, increasing the robustness of the network against failures and attacks has been a hot research field in the recent decade.

In order to increase the robustness of a network or to identify the most vulnerable node(s), domain-specific metrics, i.e. those which directly address synchronisability, should be proposed. Heuristic methods such as degree centrality, betweenness centrality and closeness centrality measures are still of much interest in the analysis of network robustness. In (Iyer et al. 2013), the size of the largest connected component of the network is studied when nodes are removed based on various heuristic centrality metrics. It shows that scale-free and small-

world networks are vulnerable to simultaneous targeted attacks to nodes with a high degree or betweenness centrality. Structural robustness of complex networks against edge removal has been also studied in (Wu et al. 2011) where the redundancy of alternative roots in a network is characterised using a spectral measure called "natural connectivity". It is shown in (Jamakovic and Van Mieghem 2008) that in Erdős-Rényi networks, the node and link connectivity, is related to the second smallest eigenvalue of the Laplacian matrix (also known as algebraic connectivity).

Some centrality measures are connected with the spectral properties of networks (Milanese et al. 2010). For example, (Pecora and Carroll 1998) linked the problem of synchronisation stability of linearly coupled oscillators to the eigenvalues of the Laplacian matrix of the graph. A node removal strategy, called perturbative strategy, was proposed in (Watanabe and Masuda 2010) which sequentially removes the nodes in order to increase the second smallest eigenvalue of the Laplacian matrix of the graph which enhances the synchronisability and convergence performance of the network. The applicability of their results is limited to the class of dynamical systems in which synchronisation is facilitated in networks with large λ_2. A subgraph centrality measure is proposed in (Estrada and Rodriguez-Velazquez 2005) based on the spectra of the adjacency matrix.

In Chapter 5 of this thesis, the effect of node removal on pinning controllability of a complex network is addressed. Based on the "local multiplicity" concept, a metric is proposed to rank nodes based on their influence on λ_i's of Laplacian matric. This is an extension of the centrality metric proposed in (Moradi Amani et al. 2018). Using this proposed metric, the effect of node removal on convergence speed of consensus in networks with different topologies has been studied.

2.3.1 Fault tolerance of complex networks

Interaction between agents in a dynamical network might facilitate the propagation of failure effects. Failure of a node or link, which can be modelled as a node/link removal, can easily affect the performance of the whole dynamical network and even make it unstable. Breakdown of a single node is sufficient to collapse the efficiency of the entire system if the node is among the ones carrying the largest load (Crucitti et al. 2004). Study of this case is of much interest in power grids where failure in a generation unit or a power link may result in a blackout (Kinney et al. 2005). The thesis systematically studies the problem of preventing

failure propagation in a complex network using structural modification. It focuses on the formation control problem. Driving multiple agents to meet a prescribed constraint on their states so as to form a certain shape in the state space, referred to as the formation control problem, has attracted a great deal of research effort in recent years. Along with its applications to environmental monitoring, mobile robots (Das et al. 2002) and spacecraft formation flying (Scharf et al. 2004), theoretical challenges arising from controlling such a network with distributed controllers using only local data remain, which makes this important topic attractive.

A multi-agent formation is composed of a number of interacting agents, each equipped with its own measurement and control devices. The control objective in a formation is to maintain the inter-agent distances constant over time. Multi-agent formation control problems are generally categorized into three groups based on different types of measurements and control variables (Oh et al. 2015). In the simplest case, each agent has an advanced sensing capability, thus being able to sense its own position with respect to a global coordinate system. This category is called position-based control, where each agent can directly go to the desired location without cooperative communications with its neighbours. Clearly, communications among agents can lead to better coordination of their positions, thus enhancing the control performance. In the second category, known as displacement-based control, each agent is able to sense the relative positions of its neighbours with respect to a global coordinate system, meaning that orientations of coordinates of all agents are aligned with the global coordinate framework. Compared with the position-based category, agents require less advanced sensing capabilities but more cooperation with each other. In the third category, referred to as distance-based formation control, each agent has its own local coordinate system which is not necessarily aligned with its neighbours. Here, sensing systems of agents are simple while inter-agent communications play an important role in the control of formation. This thesis takes the approach of the third category, with bidirectional interactions of agents over a sensing network of general topology.

The existing literature on formation control mainly focuses on the stability of formations and the topologies of sensing graphs (see e.g. (Eren et al. 2002, Cortés 2009, Kar and Moura 2009, Krick et al. 2009, Jalili et al. 2015, Liu et al. 2016, Ramazani et al. 2017)). One of the crucial issues for formation shape control, when each agent can only measure in local coordinates, is the rigidity of the underlying sensing network (Eren et al. 2003, Krick et al. 2009). Pure distance measurements can be used in controlling the shape of a formation. If one

presents a formation by a graph $G = (V, E)$, the rigidity theory (Laman 1970, Asimow and Roth 1979, Eren et al. 2002) addresses the question of "active control of which inter-agent distances are sufficient to maintain every possible distance between agents at desired values?" In other words, rigid formation control is concerned with designing distributed control for each agent so that the formation converges to a prescribed rigid shape. In addition to distance, other sensing capabilities of agents can contribute to the control of formations among them, e.g. bearing has attracted much attention in recent years (Eren 2012, Schiano and Giordano 2017). Formations controlled using angles scale up easier than their distance-based counterparts. They are also useful when accurate localization is required (Eren 2012). This thesis focuses on the shape control considering only the distances between agents.

Besides stability, the robustness of a formation against uncertainties and faults is another important issue to consider. Formations are usually subject to faults in nodes, such as mechanical/electrical failures and loss of agents as well as breakdowns in communication or sensing links. One of the early works in this context is reported in (Lewis and Tan 1997), whereby using the "virtual structure" concept and based on simulations, a high-precision formation control scheme for mobile robots was proposed to preserve the formation in the case of failures in nodes. A robust formation control algorithm for a swarm of mobile agents was proposed in (Cheng et al. 2005), which could tolerate sensor errors to a certain extent. Recently, a formation control technique based on gain adaptation was proposed in the presence of arbitrary changes in the sensing graph topology (Fathian et al. 2017).

The *rigidity maintenance* problem, in particular, is to preserve the rigidity of the sensing graph in a formation during motion, taking into consideration of constraints such as line-of-sight requirements, sensing ranges and power limitations. A rigid multiagent network was partitioned into two sub-teams in (Carboni et al. 2015) preserving rigidity. The rigidity theory was extended to rigidity eigenvalues in (Zelazo et al. 2015), which is used to generate a local control action on each agent in order to maintain the rigidity property while some constraints such as collision avoidance are met. Maintenance of bearing rigidity in a formation of unmanned aerial vehicles was studied in (Schiano and Giordano 2017), where a decentralized gradient-based control law was developed to preserve rigidity despite constraints in the sensing range. The above control algorithms are all designed assuming that each node always has enough neighbours in its sensing range such that a rigid formation is achievable.

Chapter 6 of this thesis presents a distributed rigidity maintenance algorithm to recover rigidity of the sensing graph in the presence of link breakage. The proposed algorithm satisfies

real-time requirements of the problem and can recover rigidity with activating the minimum number of new sensing links in most of the time.

2.4 Summary

In this chapter, synchronisability of complex networks was defined and the recent literature on this topic was reviewed. The master stability function formalism relates local synchronisability of a complex network to the eigen-ratio of its Laplacian matrix, i.e. the largest eigenvalue divided by the second smallest one. This connects the synchronisation of complex networks to spectral graph theory. From the control theory perspective, structural- and energy-based approaches to the controllability of dynamical systems were revisited. Although traditional controllability approaches are mathematically well developed, they should be revised considering network structure when they are extended to complex networks. This is the main motivation of this thesis. The problem of identifying the best driver to improve synchronisability of complex networks was formulated. Effect of removal in nodes or links on synchronisability of complex networks was also considered. Finally, the rigidity maintenance problem and its importance in the formation control problem, as an engineering application of synchronisation, was addressed and related literature was reviewed.

Section I: Enhancing controllability of complex networks by selecting appropriate drivers

Chapter 3

Choosing the best driver nodes in controllability of complex networks

In this chapter, an analytical approach is introduced to find the best driver node(s) in a complex network. The eigen-ratio of the augmented Laplacian matrix is considered as the pinning controllability index. This index has been frequently used in the literature as a metric of pinning controllability of dynamical networks (Sorrentino et al. 2007, De Lellis et al. 2008, Tang et al. 2013, Jalili et al. 2015). Our approach for obtaining the set of optimal drivers is based on the sensitivity analysis of the eigen-ratio (Milanese et al. 2010). It requires a single computation of the eigenvectors and thus is applicable to large-scale networks. Achievements of this chapter have been published in IEEE Transactions on Circuits and Systems II and Physical Review E (Moradi Amani et al. 2017, Moradi Amani et al. 2018).

3.1 Identification of the best driver node

Let us consider a dynamical network including *N* identical individual dynamical nodes and an undirected and unweighted connection network. The equations of motion of the network read:

$$\frac{d\boldsymbol{x}_i}{dt} = F(\boldsymbol{x}_i) - \sigma \sum_{j=1}^{N} l_{ij} H\boldsymbol{x}_j; \quad i = 1,2,\dots,N, \tag{3.1}$$

where $\boldsymbol{x}_i \in \mathbb{R}^n$ is the n-dimensional state vector, F: $\mathbb{R}^n \rightarrow \mathbb{R}^n$ defines the individual dynamical systems' state equation and σ represents the unified coupling strength. $L = [l_{ij}]$ is the Laplacian matrix, that is a zero-row sum matrix with off-diagonal elements equal to −1 if there is a link, and 0 otherwise (Mieghem 2011). The diagonal elements of L are the corresponding degree of the nodes. H is the projection matrix determining the coupled elements of the oscillators. The objective of pinning control is to pin all nodes to the following desired state (Wang and Chen 2002):

$$\frac{d\boldsymbol{s}(t)}{dt} = F\big(\boldsymbol{s}(t)\big). \tag{3.2}$$

Indeed, the reference state is considered to have identical dynamics as the individual dynamical systems. In order to pin the dynamical network to $\boldsymbol{s}(t)$, linear state feedback controllers are applied only to driver nodes, and the equations of motion read as

$$\frac{d\boldsymbol{x}_i}{dt} = F(\boldsymbol{x}_i) - \sigma \sum_{j=1}^{N} l_{ij}\, H\boldsymbol{x}_j + \sigma\beta_i k_i(\boldsymbol{x}_i - \boldsymbol{s}); \quad i = 1,2,\dots,N, \tag{3.3}$$

where k_i is the feedback control gain, $\beta_i = 1$ when node i is a driver node, and otherwise $\beta_i = 0$. When $\boldsymbol{x}_1(t) = \boldsymbol{x}_2(t) = \dots = \boldsymbol{x}_N(t) = \boldsymbol{s}(t)$, one can state that the network has been synchronised to the reference state. Inspired by the master stability function approach (Pecora and Carroll 1998), the local stability of the synchronised system can be evaluated in terms of the following N decoupled blocks (Jalili et al. 2015, Yu et al. 2017):

$$\dot{\boldsymbol{\eta}}_i(t) = \nabla F(s)\boldsymbol{\eta}_i(t) - \sigma\lambda_i H\boldsymbol{\eta}_i(t), \quad i = 1,2,\dots,N \tag{3.4}$$

where ∇ represents the Jacobian, $\boldsymbol{\eta}_i = \boldsymbol{x}_i - \boldsymbol{s}$ and $a_i = \sigma\lambda_{ci}$ with λ_{ci} being the i^{th} eigenvalue of the augmented symmetric Laplacian matrix:

$$C = \begin{bmatrix} l_{11} + k_1\beta_1 & l_{12} & \dots & l_{1N} \\ l_{21} & l_{22} + k_2\beta_2 & \dots & l_{2N} \\ \vdots & \vdots & \vdots & \vdots \\ l_{N1} & l_{N2} & \dots & l_{NN} \end{bmatrix} \tag{3.5}$$

Provided that the network is connected, the eigenvalues of the symmetric matrix C are real and can be ordered as $0 < \lambda_{c1} \leq \lambda_{c2} \dots \leq \lambda_{cN}$. It has been shown that the eigen-ratio $\eta = \lambda_{c1}/\lambda_{cN}$ accounts for pinning controllability, and larger values indicate better controllability (Sorrentino et al. 2007, De Lellis et al. 2008, Tang et al. 2013, Jalili et al. 2015). Interestingly, this technique

decouples the dynamical properties of the open-loop network from spectral properties of the network as well as from the set of the drivers (Sorrentino et al. 2007). In other words, the pinning controllability can be evaluated through spectral properties of matrix *C* regardless of the dynamics of the individual nodes. According to equation (3.5), selecting node *i* as a driver can be represented as a perturbation on the related diagonal element l_{ii} in the original Laplacian matrix *L*, i.e. by setting $\beta_i = 1$. Here, it is assumed that perturbations, caused by control gains k_i, on all diagonal elements of the matrix *C* are uniform and $k_i > 0$. In order to obtain theory for the optimal driver set, the perturbations need to be much smaller than the diagonal entries of the original Laplacian matrix *L*, i.e. much smaller than the smallest degree of the network. For larger perturbations, the accuracy of the method might decline.

3.1.1 Eigenvalue sensitivity analysis

From the eigenvalue perturbation theory (Wilkinson 1965, Nelson 1976), changes in the eigenvalue λ_m of the matrix *L* caused by perturbation in the parameter *p* is:

$$\frac{d\lambda_m}{dp} = \boldsymbol{y}_m^T \frac{dL(p)}{dp} \boldsymbol{x}_m; \quad m = 1,2,\dots,N \tag{3.6}$$

where $\boldsymbol{y}_m^T$ and $\boldsymbol{x}_m$ are the left and right eigenvectors of *L* corresponding to λ_m, respectively and $\boldsymbol{y}_m^T \boldsymbol{x}_m = 1$. Selecting node *i* as the driver affects only a diagonal element of *L* which results in

$$\frac{d\eta}{dl_{ii}} = \frac{(y_1^i x_1^i)\lambda_N - (y_N^i x_N^i)\lambda_1}{(\lambda_N)^2} \tag{3.7}$$

where the superscript *i* indicates the i^{th} element of the vector. The vector $\boldsymbol{x}_1 = \mathbf{1}_N$ is the eigenvector of *L* corresponding to λ_1 where $\mathbf{1}_N$ is a vector with *N* elements all equal to 1. For undirected graphs we have $\boldsymbol{y}_n = \boldsymbol{x}_n$; therefore equation (3.7) can be written as:

$$\frac{d\eta}{dl_{ii}} = \frac{1}{\lambda_N}\left[1 - \eta\left(\boldsymbol{x}_N^i\right)^2\right] \tag{3.8}$$

It shows that node *i* with the maximum value of $(\boldsymbol{x}^i{}_N)^2$ results in the smallest $d\eta/dl_{ii}$ meaning that η is closer to the maximum value. That is the node which is associated with the largest component $(\boldsymbol{x}^i{}_N)^2$, will have the largest value of $\eta = \lambda_{c1}/\lambda_{cN}$, resulting from a perturbation to the diagonal $l_{ii.}$ This leads us to define the "controllability centrality" $\Psi(i)$ for node *i* as (Moradi Amani et al. 2017):

$$\Psi(i) = \left(\boldsymbol{x}_N^i\right)^2, \quad i = 1,2,\dots,N \tag{3.9}$$

where $\boldsymbol{x}_N$ is the eigenvector corresponding to the largest eigenvalue of the Laplacian matrix of the graph. Thus, the node with the maximum value of controllability centrality is the best driver node for the network.

3.2 Best driver selection in synthetic networks

The metric obtained in the previous section is applied to a number of synthetic networks and its performance is compared with some heuristic methods. As network modes, scale-free, small world and Erdös-Rényi networks are considered, with the construction algorithms explained in section 2.1.1.

3.2.1 Networks with scale-free topology

As heuristic methods, three approaches are considered: selecting hubs (nodes with the highest degree) as drivers, setting drivers as nodes with the highest closeness centrality or those with highest betweenness centrality. Figure 3.1 compares the performance of the proposed controllability centrality measure with heuristic methods in finding the most influential driver node. The networks are scale-free with N = 1000 and different values for parameter B and varying average degree. First, the exact ranking of the nodes is numerically obtained based on their influence on the pinning controllability. To this end, the augmented Laplacian matrix is considered when one of the nodes is taken as a driver, and the eigen-ratio is obtained. This is repeated for all nodes, resulting in a ranking of nodes (the most influential nodes are also identified). This gives the ground-truth, which is compared with the predictions made by the methods. For each case, 100 network realizations are considered and report the accuracy of the methods (Fig. 3.1). For example, an accuracy of 50% means that the method can correctly predict the most influential node in 50% of the cases. The results reveal significant outperformance of the proposed controllability centrality measure over the heuristics. For example, with B = 0 and an average degree of 2, controllability centrality has an accuracy of 72%, while others have an accuracy of at most 31%. Among the heuristic methods, degree-based one shows the worst performance, those based on closeness and betweenness are the bests for networks with small and high average degree, respectively. In some cases, the heuristic methods can never correctly predict the most influential nodes (i.e., accuracy of

almost zero). Furthermore, as the networks become less heterogeneous (B increases), the gap between controllability centrality and other methods decreases, indicating that controllability centrality is more effective in heterogeneous networks.

These methods are further compared in terms of their accuracy in predicting the top-T most influential nodes (Fig. 3.2). The results indicate that as T increases, the heuristic methods get a closer performance to controllability centrality. Indeed, when T is not small, it is highly likely that the set of top-T most influential drivers are among the most central nodes (i.e., those with the highest degree, closeness or betweenness centrality measures). For example, the top-10 most influential drivers are those with the highest degrees in more than 90% of the cases in networks with $B = 0$. Often, for $T > 2$, choosing the nodes based on their degree results in better pinning controllability than choosing based on closeness or betweenness centrality measures.

3.2.2 Networks with small-world topology

Figure 3.3 shows the accuracy of the methods in Watts-Strogatz networks with $N = 1000$, average degree of 4 and varying rewiring probability p. controllability centrality and the degree-based method are clearly better predictors than the closeness- and betweenness-based methods. In many cases, controllability centrality results in slightly better accuracy than the degree-based method. For $p > 0.4$, the top driver node is never the one with the highest closeness centrality. As p increases, the networks become less homogeneous, and thus, the accuracy of controllability centrality increases (similar to scale-free networks).

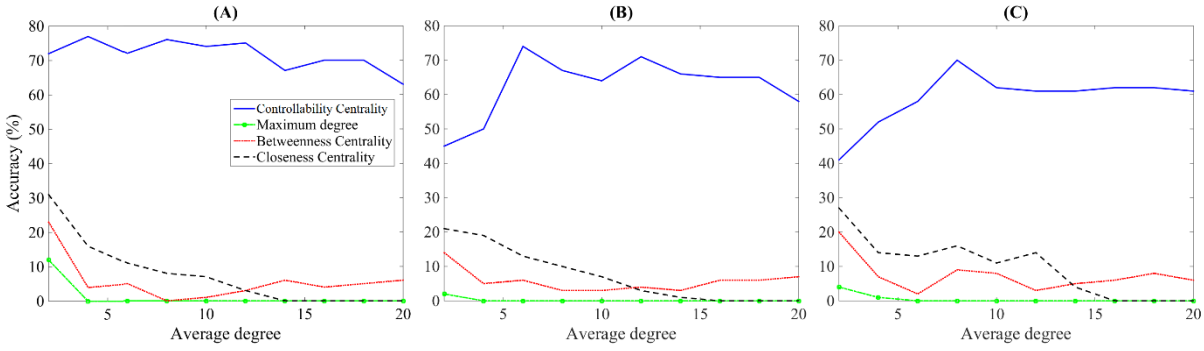

Fig. 3.1: Accuracy of controllability centrality in scale-free networks. Accuracy of controllability centrality (solid), maximum degree (dash-dot), maximum betweenness centrality (dot) and maximum closeness centrality (dashed) in finding the most influential driver node in networks with N=1000 nodes with A) $B = 0$, B) $B = 5$, and C) $B = 10$ (as B increases, the heterogeneity of the network decreases). The average degree of the networks varies from 2 to 20 and the results show the accuracies over 100 realizations.

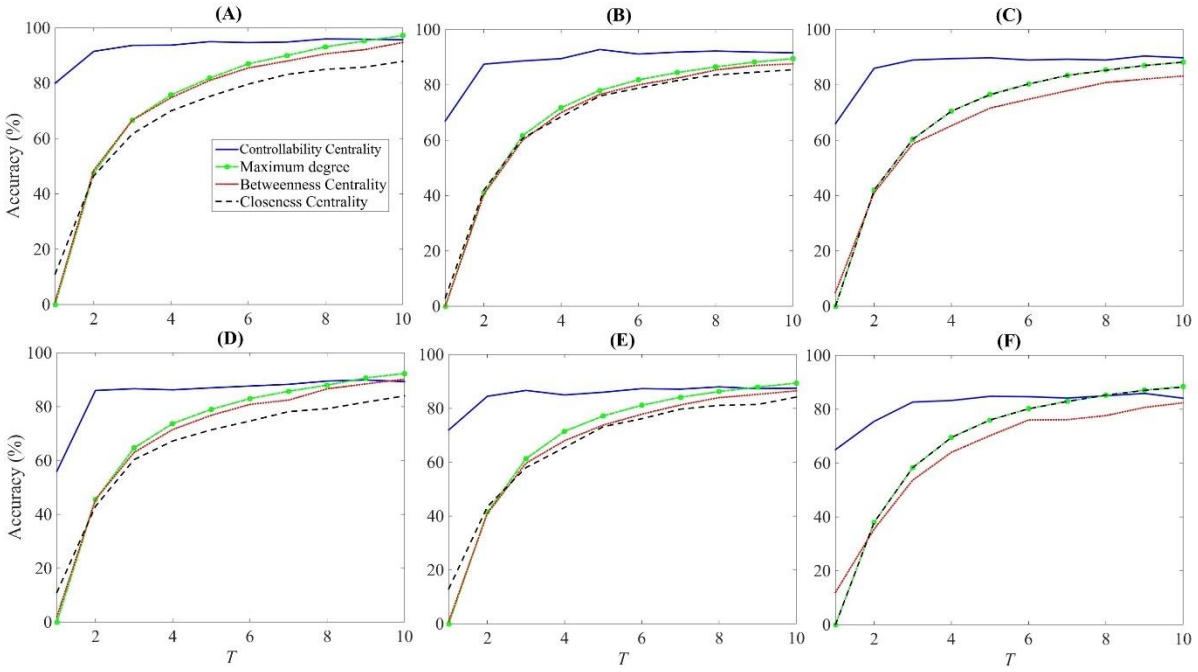

Fig. 3.2: Accuracy of controllability centrality in finding the top-T most influential driver nodes in scale-free networks. Accuracy of controllability centrality (solid), maximum degree (dash-dot), maximum betweenness centrality (dot) and maximum closeness centrality (dashed) in networks with N=1000 nodes. Networks have scale-free structures with B=0 and A) m=5, B) m=10 and C) m=20 as well as B=5 and D) m=5, E) m=10 and F) m=20 (m is the average degree. In addition, as B increases, the heterogeneity of the network decreases). Results are averaged over 100 realizations.

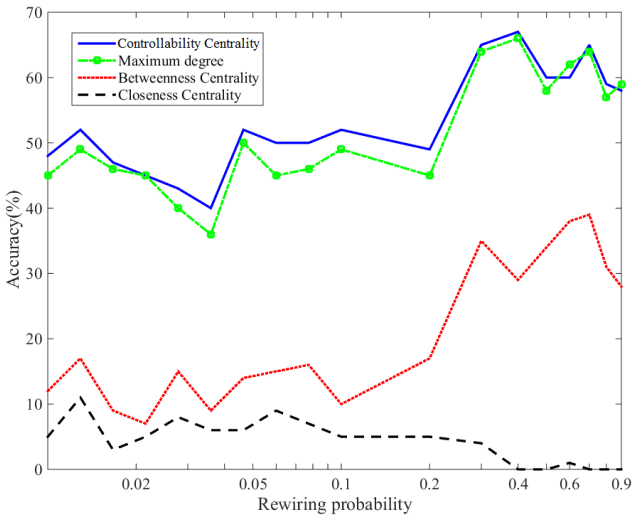

Fig. 3.3: Accuracy of controllability centrality in Watts-Strogatz complex networks. Accuracy of controllability centrality (solid), maximum degree (dash-dot), Betweenness centrality (dot) and Closeness centrality (dot) in finding the most influential driver node on the controllability of Watts-Strogatz complex networks with N=1000 nodes. Watts-Strogatz networks are generated from a regular network with a rewiring probability from 0.01 to 0.9 (which is shown on horizontal axes and is logarithmically scaled). Results are averaged over 100 realization

Having only a single driver node might require a very high control gain, which might not be practical in some cases. Therefore, the proposed controllability centrality is extended to select the best driver set in the next section.

3.3 Choosing the best driver set

Identifying the optimal set of N_d drivers for complex networks results in a combinatorial optimisation problem as selection of nodes and designing their control gains should be done simultaneously (Summers et al. 2016). In order to obtain a set of μ nodes (S_μ) that if selected as driver will have the maximal influence on the pinning controllability, the subset which issues the strongest effect on the eigen-ratio $\eta(l_{ii})$ where $i \in S_\mu$ is investigated. The amplitude of the gradient of η can be written as:

$$|\nabla\eta|^2 = \nabla\eta^T.\nabla\eta = \sum_{i\in S_\mu}\left(\frac{\partial\eta}{\partial l_{ii}}\right)^2 \tag{3.10}$$

Considering $\eta << 1$ and using equation (3.8), this can be simplified to:

$$|\nabla\eta|^2 = \sum_{i\in S_\mu}\frac{1}{\lambda_N^2}\left[1-\eta\left(\boldsymbol{x}_N^i\right)^2\right]^2 \approx \frac{1}{\lambda_N^2}\left[\mu - 2\eta\sum_{i\in S_\mu}\left(\boldsymbol{x}_N^i\right)^2\right] \tag{3.11}$$

Therefore, controllability centrality can be defined for the subset S_μ in the same way as it is defined in equation (3.9) for a single node:

$$\Psi(S_\mu) = \sum_{i\in S_\mu}\left(\boldsymbol{x}_N^i\right)^2 \tag{3.12}$$

The optimisation problem to find the subset of μ nodes with maximum influence on η reads as:

$$\underset{S_\mu}{\text{maximize}} \quad \Psi(S_\mu) \tag{3.13}$$

In other words, among subsets of μ nodes, the one maximizing $\Psi(S_\mu)$, i.e. minimizing equation (3.12), is the most influential subset to be considered as the driver for pinning controllability.

3.3.1 Computational efficiency

Currently, there is no computationally efficient solution to find the set of optimal N_d drivers. One can find the global optimal solution through a brute force search on all possible combinations of nodes in sets of size N_d and choosing the set with the best performance. However, as it requires computing a synchronisation criterion, e.g. the eigen-ratio η, for all possible combinations, this combinatorial process is not practical for many cases, especially for large-scale networks (Summers et al. 2016).

Interestingly, the controllability centrality proposed in (3.13) is independent of the control gain k_i. This is valid only for uniform control gains among driver nodes and when the conditions of the perturbation theory hold, that is control gains are sufficiently small. It also shows the sub-modularity feature as it is a monotone increasing function, as:

$$\Psi(S_{\mu+1}) = \left(\boldsymbol{x}_N^{\mu+1}\right)^2 + \Psi(S_\mu) \tag{3.14}$$

meaning that all interesting properties of sub-modular functions can be applied to this case as well. Based on the sub-modular property, in order to add a new driver node to the subset previously controlling the network, the best candidate is the node with the highest controllability centrality. In other words, once the eigen-decomposition of the Laplacian L (i.e., the case without any drivers) is performed, the best driver set of μ nodes is the set of top-μ nodes ranked by the controllability centrality measure. This is a significant result as it only requires a single eigen-decomposition and has complexity comparable to many standard heuristic methods.

3.4 Simulation results of the best driver set selection

In order to assess the performance of the proposed metric, the proposed controllability centrality measure is applied on synthetic scale-free and small-world networks and its performance is compared with the heuristic methods. The synthetic networks are constructed with size $N = 1000$ and different average degree and heterogeneity levels. First, the true optimal driver set, which is referred to as the ground-truth, is obtained and is used to compare the precision of different methods. The ground-truth optimal set is obtained by examining all possible combinations. Let's consider obtaining the optimal driver set with μ nodes. First, all μ-combinations of N nodes are selected one-by-one and the variation of η by perturbing any of them is obtained. The perturbations considered on the diagonal elements of the original Laplacian matrix take into account uniform and non-zero control gains for the drivers. The μ-combinations are then sorted in descending order based on the amount of the variation of η; the one at the top is selected as the best set. Extensive numerical simulations are run to obtain the ground-truth optimal sets for the networks for $\mu = 1, 2, \ldots, 10$. The precision of each method for a given μ is obtained as follows. 100 realizations of each network type are considered and the set with μ nodes predicted by that particular method is obtained. Then, the precision is obtained as $P = (n_p/n)100\%$, where n is the total number of runs for each case ($n = 100$ here) and n_p is the number of times that all nodes in the set predicted by the method match to those

in the ground-truth optimal set. For example, P = 90% for an algorithm indicates that the algorithm correctly predicts all nodes of the ground-truth optimal set in 90% of the runs.

Figure 3.4 shows the precision P as a function of μ for scale-free networks with different average degrees and B. The proposed controllability centrality metric has significantly better precision than the other heuristic methods. It has always a precision of higher than 70% and even in some cases close to 100%. This is a significant performance indicating the proposed methods, although being computationally efficient, can correctly predict all nodes in the ground-truth optimal sets in most cases. The heuristic methods have a close to zero precision for $\mu > 2$ in less heterogeneous networks, i.e. $B = 5$, while the controllability centrality has still high precision in such cases. The closeness-based method has the poorest performance among the heuristics. Figure 3.5 shows P as a function of rewiring probability p in small-world networks with N = 1000 and m = 2. The controllability centrality can correctly predict the ground-truth in almost half of the cases in these networks. Except for p = 0.2 for which the controllability centrality is slightly better than the degree- and betweenness-based methods, its precision is significantly higher than these heuristics in other cases. Similar to scale-free networks, the method based on closeness centrality has the worst precision in homogeneous networks. The proposed approximate method indeed works much better in heterogeneous networks than degree-homogeneous ones, as the nodes and subset of nodes are more distinguishable from each other in such networks. The precision of the proposed metric is acceptable although it is based on the first-order approximation of equation (3.6). It is worth noting that the approximation provided by this first-order equation is closer to the actual value when perturbation on diagonal elements of equation (3.5) is smaller; i.e. when the perturbed node has higher degree. Therefore, it is expected to have less precision for this approximation in networks with homogenous and/or low-degree nodes. This is also evident from our simulations, as the precision for scale-free networks is much higher than that of Watts-Strogatz networks.

One may surprise with such a poor quality of heuristic methods. Indeed, the criterion used here is rather strong and to be counted as a precise set of size μ, all μ nodes suggested by the algorithm must be included in the optimal set. Although the heuristic methods may correctly find many of the optimal nodes (e.g. in many cases, they can correctly find 7-9 nodes for μ = 10), they fail to recover the ground-truth optimal set in majority of the cases. However, the proposed metric can correctly find all nodes within the optimal set with much higher precision, especially in scale-free networks for which its precision is above 80% in majority of the cases.

In other words, we do not show how effective a pinning control scheme can be in improving the synchrony as enough evidence has already been provided in the literature. Our aim is to find the best driver(s).

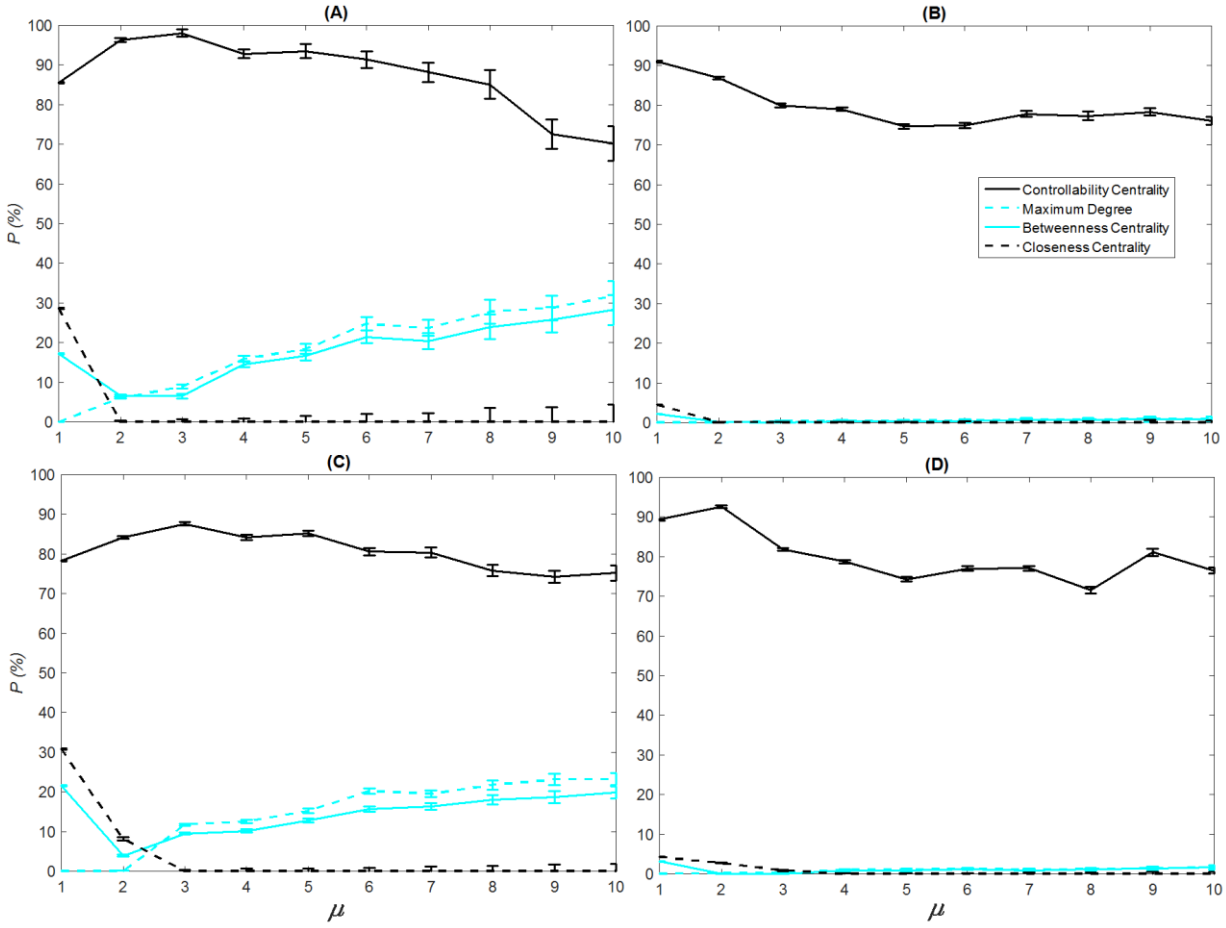

Fig. 3.4: Precision P of the proposed controllability centrality in networks with scale-free structures. The precision of the proposed metric (solid black line), and heuristic methods including considering hub nodes with maximum degree (dashed cyan line), maximum betweenness (solid cyan line) and maximum closeness (dashed black line). Graphs show P for finding a driver set of μ nodes (μ = 1, 2, ..., 10). Networks have scale-free structure with N = 1000 and A) m = 2 and B = 0, B) m = 10 and B = 0, C) m = 2 and B = 5, and D) m = 10 and B = 5. (see text for description of these parameters). Data show mean values with error bars corresponding to standard error over 100 realizations.

In conclusion, we introduced a pinning controllability centrality measure to obtain a driver set of μ nodes. The method is based on a single eigen-decomposition of the original Laplacian matrix (without information of drivers), indicating its computational efficiency. Although being simple to compute, its precision in identifying the ground-truth optimal set correctly is significantly better than heuristic methods.

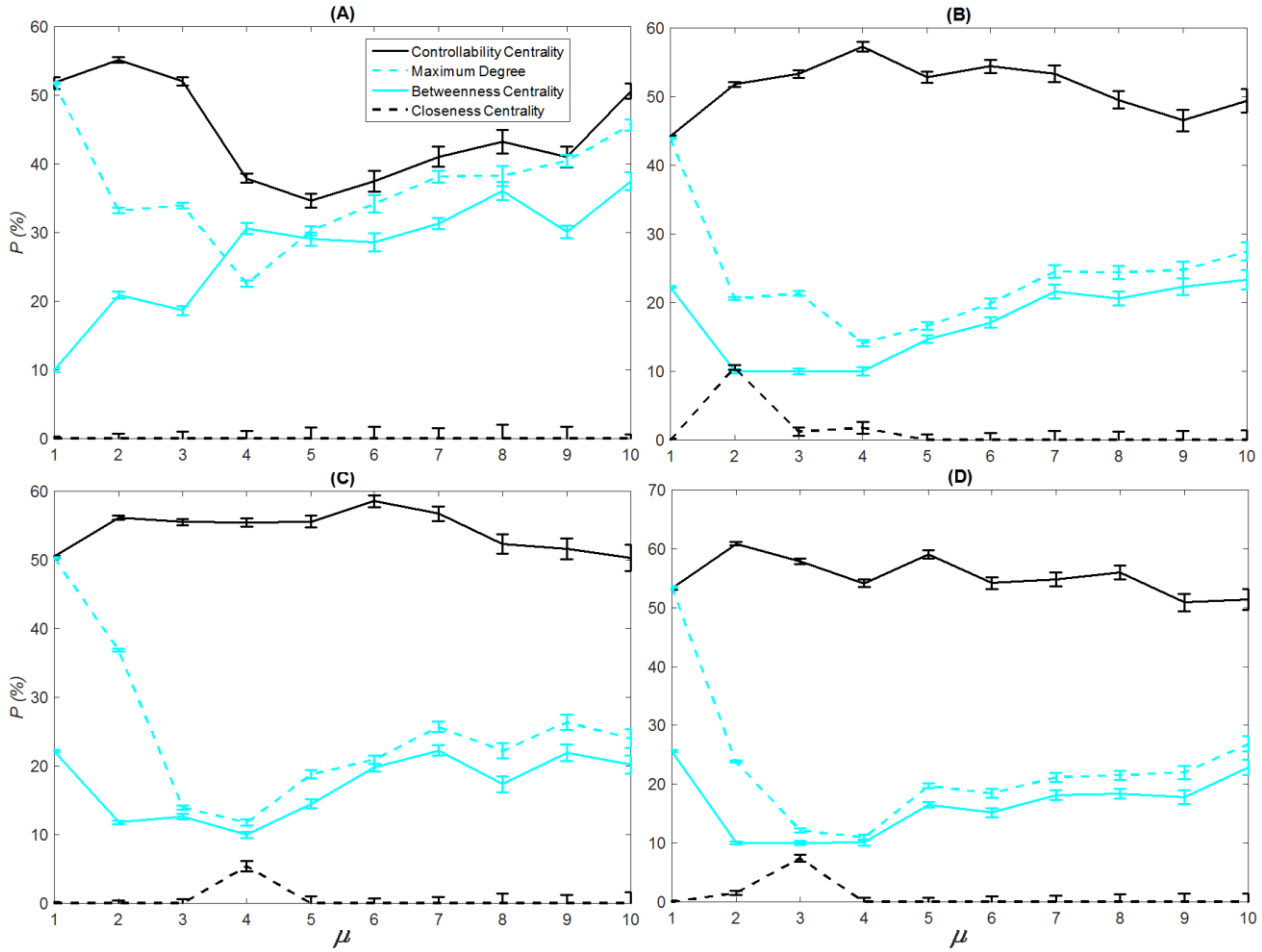

Fig. 3.5: Precision P of the proposed controllability centrality in networks with Watts-Strogatz structures. The precision of the proposed metric (solid black line), and heuristic methods including considering hub nodes with maximum degree (dashed cyan [light grey in Black&White print] line), maximum betweenness (cyan [light grey in Black&White print] line) and maximum closeness (dashed black line). Graphs show P for finding a driver set of μ nodes (μ = 1, 2, ..., 10). Networks have Watts-Strogatz structure with N=1000 nodes and m=2 and rewiring probability of A) p=0.2, B) p=0.5, C) p=0.7 and D) p=0.9. Data show mean values with error bars corresponding to standard error over 100 realizations.

The proposed perturbation-based metric assumes uniform control gain for all drivers. Although the diagonal elements of matrix C have both k_i and β_i (the gain and location of drivers), our perturbation technique does not distinguish k_i and β_i, as only one parameter can be considered in the perturbation. Such an approach may raise an argument about the accuracy of the proposed metric when the control gains vary. Indeed, according to equation (3.12), the optimal driver set is k_i-independent when the perturbations are uniform and much smaller than the smallest degree of the network. To test this, we study how the accuracy of the proposed metric changes by varying the control gains. We run simulations for networks with scale-free structures with N = 100 nodes and average degree m = 5 with minimum degree of 1. The control gain k_i is changed from 0.001 to 50 having driver sets of different cardinality μ = 1, 2,…, 6. Deriving the ground-truth and calculating the accuracy is performed in the same way done above. Our numerical results (Fig. 3.6) show that for control gains sufficiently smaller than the

minimum degree of the graph, the proposed perturbation theory is highly accurate and the theory perfectly matches the simulation, i.e. accuracy is 100%. Even after increasing the control gain by 50 times the minimum degree of the graph, the accuracy of the proposed metric is still well above 85%. Indeed, when the control gain increases, the accuracy of the proposed perturbation-based method slightly declines, as the first-order approximation used here becomes less accurate. Future direction to our research could be to further consider optimising the control gains together with the location of driver nodes, i.e. designing pinning control with optimal control cost.

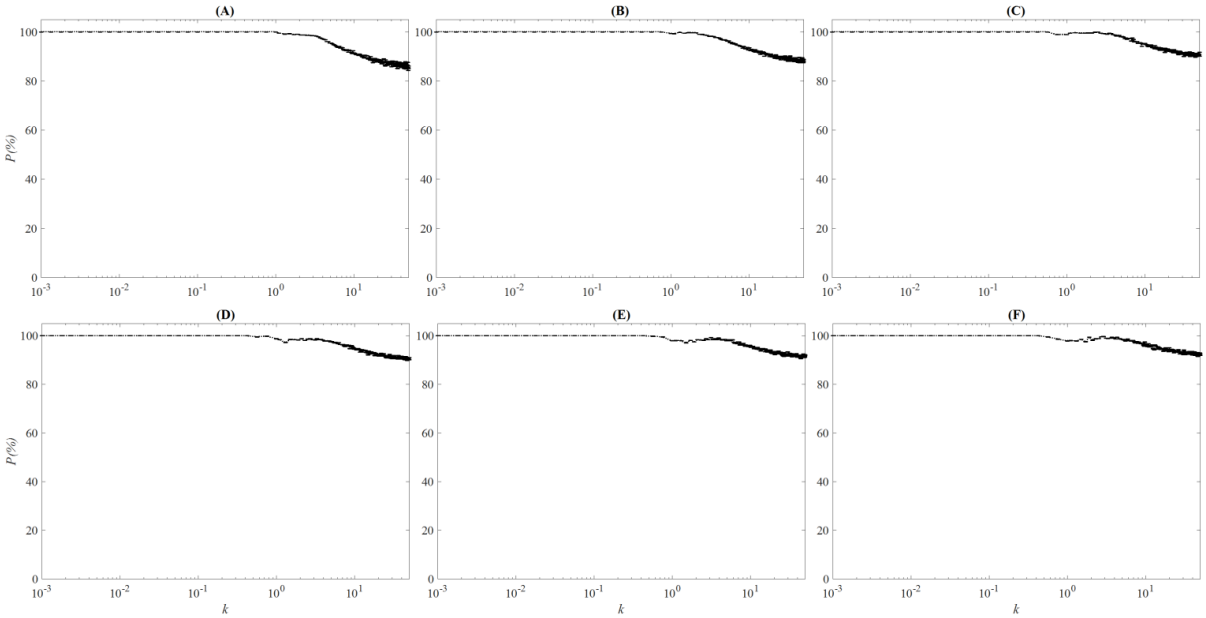

Fig. 3.6: Precision P of the proposed controllability centrality metric for different control gains k. Graphs show P as a function of control gain k for different value of μ. The networks have scale-free structure with $N = 100$, $m = 2.5$ and $B = 0$. The driver sets have A) $\mu = 1$, B) $\mu = 2$, C) $\mu = 3$, D) $\mu = 4$, E) $\mu = 5$ and F) $\mu = 6$ nodes. The control gain k is applied uniformly to all drivers and varies from $k = 0.001$ to $k = 50$. Data show mean values with error bars corresponding to standard error over 300 realizations.

3.5 Summary

Pinning control of complex networks has many potential applications in science and engineering. Pinning controllability of a network is defined as the ease by which pinning control (or synchronisation) can be achieved in the network. A challenge in designing efficient pinning control is to find a set of optimal driver nodes to which the control signal should be fed. In this chapter, a controllability metric (eigen-ratio of the augmented Laplacian matrix of the connection graph) was considered and a novel metric, called controllability centrality, for the centrality of nodes for pinning controllability (the nodes with high controllability centrality are good candidates for drivers) was introduced. controllability centrality was computed based

on the eigenvectors of the Laplacian matrix. The proposed metric was compared with a number of heuristic methods including taking the hub nodes (i.e. those with the highest degree, closeness or betweenness centrality) as the driver. Although these heuristics are not based on eigen-decomposition, they have been natural choices for drivers in the previous works. Our results showed that the proposed metric outperforms heuristic approaches in synthetic scale-free, small-world and random networks.

Chapter 4

Choosing the best driver set in application

In the recent decade, complex networks have been frequently used to model large-scale systems, including modern power grids. In this chapter, the metrics proposed in chapters 3 are applied to solve some important problems in real applications. The first problem is in the distributed secondary frequency control of power generation systems and the second one is in dementia networks which. The results have been published in IEEE Journal on Emerging and Selected Topics in Circuits and Systems (Moradi Amani et al. 2017), Neurocomputing (Meyer-Bäse et al. 2019) and the Medical Imaging conference (Tahmassebi et al. 2018).

4.1 Best leader identification in the distributed secondary frequency control

A revolution in the paradigm of power generation and distribution has started by moving from centralized large power generation units towards distributed generation and renewable energy sources (Yu et al. 2011). Recent technological advances in small generators, power electronics, and energy storage devices, as well as economic unfeasibility of large power plants caused by system and fuel costs and environmental problems, push this movement (Marwali et al. 2004). Many countries, including Australia, have set clear targets for their electricity generation from renewable resources. The impact of distributed generation units, especially renewable sources on the performance of the network is a concern in the power system society

(Slootweg and Kling 2002, Pham et al. 2009, Tielens and Van Hertem 2012). Controlling the network's frequency and voltage levels in a large-scale power grid composed of many renewable sources is a challenging task.

A microgrid, as the main building block of future smart grids (Yu et al. 2011), includes a number of distributed generation units, such as renewables from wind to solar sources and energy storage units, which are connected over a low-voltage or medium-voltage AC bus (Slootweg and Kling 2002). It should be operated in such a way that local loads like hospitals, technology firms, university campuses and houses are reliably supplied. The microgrid normally works in the grid-connected mode, in which its AC bus is connected to the main power grid. However, in the case of disturbance or fault in the network, the microgrid will be isolated from the main grid and starts working in islanded mode (Bidram et al. 2014). Each microgrid has a dedicated control system, which is responsible for preserving the quality of the power delivered to loads in different normal or emergency working scenarios (Bidram and Davoudi 2012). Due to presence of multiple small generation units with different capabilities and characteristics as well as lack of a dominant generator in the islanded mode, the control system with faster response than traditional interconnected grids is necessary to guaranty sound operation of the network (Katiraei and Iravani 2006).

Similar to traditional power systems, the control system of a microgrid can have a hierarchical structure. The lowest level includes primary (local) controllers which are often implemented inside generation units. This part should stabilise the frequency and voltage after any change in load or supply (Guerrero et al. 2013). Most of the microsources like photovoltaic arrays, small wind generators and microturbines are not suitable to be directly connected to the AC bus of the microgrid. Therefore, power electronic interfaces (known as inverters), are required to connect them to the microgrid (Lopes et al. 2006). These inverters work as the final elements of the primary control system. The secondary controller is responsible for the performance of the whole microgrid and is implemented at a higher level (Bevrani et al. 2014). This control restores the frequency of the microgrid to the nominal condition (Kundur et al. 1994). Tertiary control in the highest level regulates the power flow to/from microgrids and optimizes the operation of the whole power system (Bidram and Davoudi 2012).

4.1.1 Distributed secondary control

Secondary control of a microgrid is traditionally implemented in centralized schemes, in which the central controller gathers information from all local controllers, applies a control

algorithm and sends back control signals to the actuators (Rocabert et al. 2012). However, such a centralised control structure has drawbacks, such as scalability, the requirement for a high-performance controller unit and single point of failure in the system (Ge et al. 2015). These drawbacks along with the progress in the communication technologies have made the distributed scheme more reasonable. The distributed secondary controller can be implemented in either cooperative control (Bidram et al. 2013) or decentralized control schemes (Schafer et al. 2015). Distributed approaches outperform the traditional centralized ones because of their modularity, scalability and robustness (Ge et al. 2015). Regardless of specific control scheme, a data communication network is needed between the primary and secondary controllers (Bidram et al. 2014). In recent approaches, local controllers interact with one another over this communication network to coordinate their task for achieving the desired performance (Vasquez et al. 2013). Such coordination schemes have also been studied in other disciplines, such as consensus in multi-agent systems or synchronisation in complex networks (Olfati-Saber et al. 2007, Arenas et al. 2008). It has been shown in all of these studies that the structure of the communication network plays an important role in coordination of the system (Belykh et al. 2005, Mesbahi and Egerstedt 2010, Jalili et al. 2015, Gaeini et al. 2016).

During the grid-connected operation, all generation units use the voltage and frequency of the grid as the reference. However, in islanded mode, when the microgrid losses these reference signals, preserving the stability of the network is subject to many unexpected events (Moradi Amani et al. 2013). In this case, the secondary control should assign one (or more) generation source(s) to regulate the voltage and frequency of the microgrid. This node(s) will perform as master node(s) and other nodes will be set by the secondary control to follow them (Bevrani et al. 2014). Therefore, one of the most challenging problems to set the proper functioning of the secondary control in islanded mode of a microgrid is to find the master node(s) for voltage and frequency. The problem of finding the best masters depends on both the dynamics of generation units as well as the topology of the physical power network and that of the data communication network (Yu et al. 2009, Jalili 2013).

In this chapter, the technique proposed in chapter 3 is used to introduce a metric to rank all generation nodes based on their effects on the frequency of a microgrid. The proposed metric is derived using sensitivity analysis of the largest eigenvalue of the state matrix of the power system. The microgrid is assumed to contain both synchronous machines, which are directly connected to the AC bus, and renewable energy sources, which are connected through power electronic equipment. A distributed secondary frequency control system is assumed to regulate

the frequency of the microgrid. As the data communication network for implementing this control system, a number of synthetic network structures with scale-free and small-world properties are considered. It is shown that the ranking obtained by the proposed metric is highly correlated with the true ranking. However, the computational complexity of the proposed method is much less than obtaining the true rankings. Our numerical simulations also reveal that the proposed metric results in much higher accuracy than a number of heuristic methods including selecting the master nodes as hub ones with the highest degree, betweenness centrality or closeness centrality values.

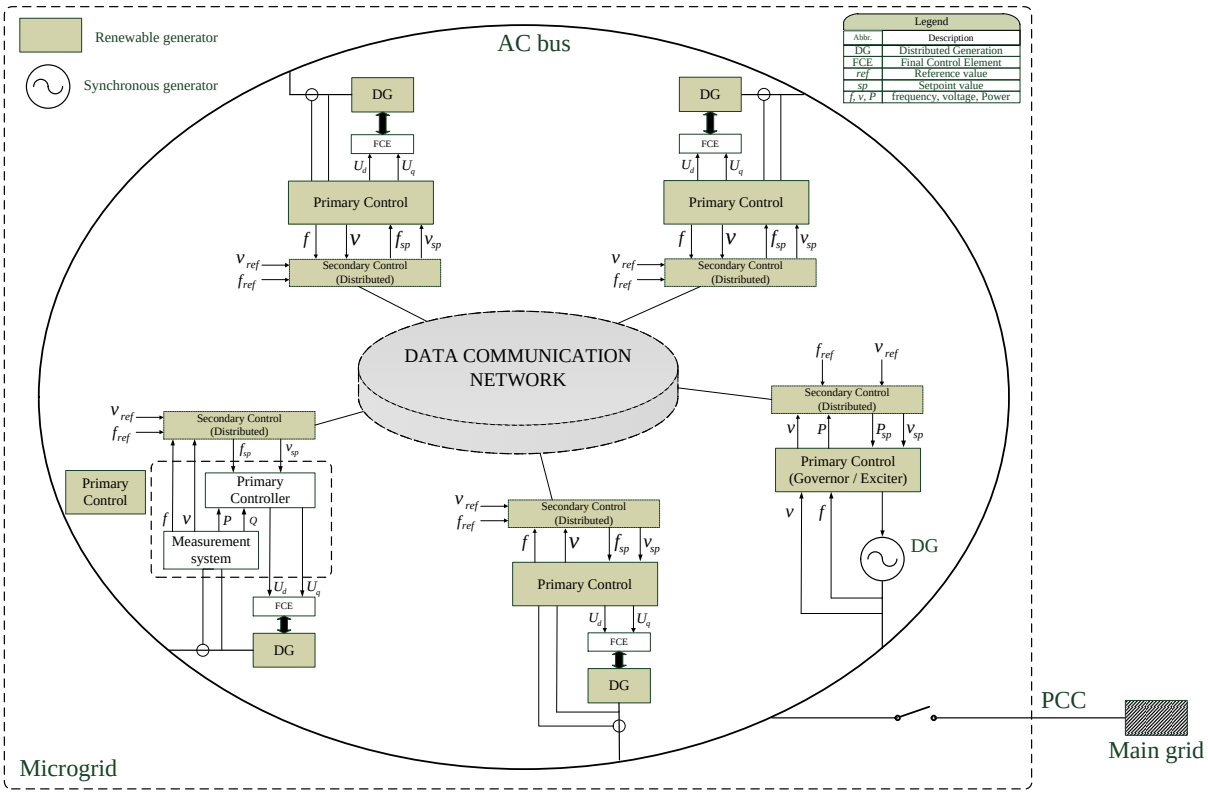

Fig. 4.1: Typical control structure of a distributed generation system.

The primary control strategy implemented in inverters depends on their role in the network. When the inverter is set to feed a certain amount of active and reactive power into the network, PQ (active and reactive power) control mode should be used (Lopes et al. 2006). This mode is also suitable when the microgrid is in grid-connected mode. In the case of a fault, when the microgrid is disconnected from the main grid, one inverter or a subset of inverters should be switched into Voltage Source Inverter (VSI) control. In this case, the control objective is to feed the load with predefined values for voltage and frequency. In other words, inverters working in VSI control mode are responsible to maintain the voltage and frequency of the

microgrid in islanded mode (Rocabert et al. 2012). In this thesis, this situation (i.e., microgrid in the islanded condition) is considered.

Figure 4.1 shows a typical structure of the control system in a microgrid. All Distributed Generation Systems (DGS) are connected to an AC bus that is normally connected to the main grid at the Point of Common Coupling (PCC). Each DG is equipped with a dedicated primary control system, which is mainly responsible to prevent voltage and frequency deviation in the case of any imbalance between generation and consumption (Bidram and Davoudi 2012). This controller continuously monitors the voltage and frequency of the network. In the case of any voltage and frequency deviations, it starts increasing the generation of active and/or reactive powers to prevent them from further deviation. The primary controller is a fast-acting system and can stop the frequency and voltage drops in many of the cases. However, it may not necessarily recover the system to the voltage and frequency set-point. Each microgrid has also a secondary control system, which regulates the voltage and frequency to desired values following any disturbance. It is traditionally implemented in a centralized scheme; however, a distributed scheme (Fig. 4.1) is more desirable in modern power grids. In this section, dynamical equation for frequency stability analysis of a microgrid is derived when energy sources are connected to the bus either directly or through electronic interfaces.

4.1.2 Secondary frequency control

Let's consider a microgrid with N generation units connected to the network through inverters (numbered as 1,2, … l) and some synchronous machines (numbered as l + 1, …, N). Dynamical equation of the frequency of a microgrid will be:

$$\dot{\delta}_i = u_i - \sum_{\substack{j=1 \\ j\neq i}}^{N} T_{ij}\left(\delta_i - \delta_j\right) + G\delta_i \qquad i = 1,2,\dots,l$$

$$M_i\ddot{\delta}_i + D_i\dot{\delta}_i + \frac{\dot{\delta}_i}{R_i} = u_i - \sum_{\substack{j=1 \\ j\neq i}}^{N} T_{ij}\left(\delta_i - \delta_j\right) \qquad i = l+1,\dots,N \qquad (4.1)$$

where δ_i shows either the power angle if $i = l$+1, …, N or the voltage angle for i = 1, 2, …, l. M_i is the inertia of the i^{th} generation unit for synchronous machines and D_i is the damping factor of the load. T_{ij} is a coefficient representing the power transfer between generation units i and j and is calculated as $T_{ij} = E_iE_j / Z_{ij}$ where E_i and E_j are voltages at generation units i and j, respectively and Z_{ij} is the impedance of the line connecting them. Finally, u_i represents the control signal for the i^{th} unit. Defining vectors of the system states as $\varepsilon = [\delta_1,\dots, \delta_l, \delta_{l+1},\dots, \delta_N]^T$

and $\xi = [\delta_{l+1}, \ldots, \delta_N]$ as well as the input vector as $u = [u_1, u_2, \ldots, u_N]$, the augmented dynamical equation of the microgrid can be written as (Moradi Amani et al. 2017):

$$\begin{bmatrix} \dot{\varepsilon} \\ \dot{\xi} \end{bmatrix} = \begin{bmatrix} -I_N^l \times L_P & I_{N-l}^l \\ -M^{-1} I_N^{N-l} \times L_P & -Z \end{bmatrix} \begin{bmatrix} \varepsilon \\ \xi \end{bmatrix} + \begin{bmatrix} I_N^l \\ M^{-1} \end{bmatrix} u \tag{4.2}$$

where,

$$I_N^l = \begin{bmatrix} I_{l\times l} & 0 \\ 0 & 0 \end{bmatrix}_{N\times N},\ I_{N-l}^l = \begin{bmatrix} 0_{l\times(N-l)} \\ I_{(N-l)\times(N-l)} \end{bmatrix},\quad I_N^{N-l} = [0_{(N-l)\times l} \quad I_{(N-l)\times(N-l)}]$$

$$M = [m_{ij}]_{(N-l)\times(N-l)},\ m_{ij} = \begin{cases} M_i, & i = j = l+1, \ldots, N \\ 0, & otherwise \end{cases}$$

$$Z = [z_{ij}]_{(N-l)\times(N-l)},\ z_{ij} = \begin{cases} \frac{1}{M_i}(D_i + \frac{1}{R_i}), & i = j = l+1, \ldots, N \\ 0, & otherwise \end{cases} \tag{4.3}$$

If one considers each generation unit of the microgrid as a node of the graph, T_{ij} shows the power of the link between nodes i and j. In this way, the microgrid can be shown as a graph with the adjacency matrix $A_p = [T_{ij}]$. For this graph, the Laplacian matrix is defined as L_P and can be simply obtained from A_p, as $L_P = D - A_p$ where D is a diagonal matrix with appropriate dimension whose $(k,k)^{th}$ element is the summation of elements of k^{th} row of A_p (*i.e.*, degree of node k in the graph).

To stabilise the frequency of the microgrid in the case of deviation in the generation or consumption, the control signal u (as shown in equation (4.1)) should be designed such that the whole system remains stable. This control signal is traditionally designed using a centralized scheme, in which each microgrid has a secondary control system that gathers information from all DGS's and sends back commands to them. However, distributed control schemes are more practical when executive constraints are considered. Advancements in communication network technology also contribute to increasing the implementation of distributed algorithms. In this thesis, the following cooperative secondary control signal is considered in each DG:

$$u_i = -k_i \sum_{j=1, j\neq i}^{N} a_{ij}(\varepsilon_i - \varepsilon_j) + b_{ii}\varepsilon_i,\ \ i = 1,2, \ldots, N \tag{4.4}$$

where k_i represents the feedback gain for the i^{th} DG. The secondary control system considered for each DG in Fig. 4.1 generates the set-point for the primary control based on its own data as well as data received from other generation units. The DGs communicate with one another on a data communication network, represented by adjacency matrix $A = [a_{ij}]$. $a_{ij} \neq 0$ shows that

there is a communication link between the i^{th} and j^{th} DG's, and a_{ij} = 0 when there is no connecting link. In addition, to show the master node for the frequency of the microgrid, the coefficient b_{ii} is defined; one has $b_{ii} \neq 0$ when the i^{th} DG should play the master role in the frequency control of the microgrid, and otherwise $b_{ii} = 0$. Using the control signal as expressed by equation (4.4), the closed-loop control system will be:

$$\begin{bmatrix} \dot{\varepsilon} \\ \dot{\xi} \end{bmatrix} = \begin{bmatrix} -I_N^l \times [L_P + KL_D + B] & I_{N-l}^l \\ -M^{-1} I_N^{N-l} \times [L_P + KL_D + B] & -Z \end{bmatrix} \begin{bmatrix} \varepsilon \\ \xi \end{bmatrix} \tag{4.5}$$

where K and B are diagonal matrices whose $(i,i)^{th}$ elements are k_i and b_{ii}, respectively. Therefore, the frequency of the microgrid is stable if the state matrix in (4.5) is Hurwitz, i.e., all its eigenvalues have negative real parts. This indicates that the dynamics of the frequency of a microgrid depends on Laplacian matrix of the power network (L_P), Laplacian matrix of data communication networks (L_D) used in distributed secondary control, parameters of DG's which are included in Z, local control gains of DG's as diagonal elements of the matrix K and the matrix B which defines driver nodes. The Laplacian of the data communication network (L_D) can be obtained from A using the same method explained for obtaining L_P for the physical power network graph. L_D is a zero row-sum matrix with positive diagonal entries. The Laplacian matrix has been shown to play a critical role in the synchronisation of complex networks. Synchronisability and pinning controllability of dynamical networks are related to spectral properties of the Laplacian matrix of the connection graph (Pecora and Carroll 1998, Sorrentino et al. 2007, Jalili et al. 2015, M. Jalili and Yu 2016). It is also known that the eigenvalue with the largest real part (called dominant eigenvalue) of the state matrix of equation (4.5) shows how fast the system can restore the frequency deviations. The smaller the real part of the dominant eigenvalue is, the faster the response of the system will be. Therefore, it can be considered as a measure for the convergence rate of the system.

4.1.3 Leader identification using eigenvalue perturbation analysis

From equation (4.5), one may state that all L_P, L_D, K, Z and B can be used to tune the dominant eigenvalue. However, from a practical point of view, some of them are difficult (if not impossible) to tune (change) to control the performance of the system. For example, L_P depends on the physical structure of the power network representing the physical connections between the individual units, which is usually fixed and difficult (if not impossible) to change during operation. Parameters of generation units, which form matrix Z, are fixed by the vendor

during the manufacturing process. Any increase in the feedback gains *K* may cause saturation in control elements and generate noise activation problems. Therefore, the most practical way to affect this eigenvalue is to change either the communication network structure (L_D) (Gaeini et al. 2016) or select appropriate node as the master, i.e., changing *B*. This means that the secondary control system should select the best data communication structure as well as the best master node according to the structure of the power system and parameters of the generation units. It is worth mentioning that appearance and disappearance of a DG unit in a microgrid is a common event because of uncertainties in renewable energy sources and large number of small capacity generation units. Therefore, secondary control should always monitor the structure of the power network and select the best communication network based on that. This selection can be performed either using an online design procedure or from a pre-designed bank of structure; although, the latter being more reasonable in large microgrids.

In microgrids with a small number of generation units, secondary control can always find the best master node in a timely manner by analysing the effect of nodes on the eigenvalues of the state matrix of equation (4.5). However, this method fails to satisfy real-time constraints in microgrids with large number of DGs. Therefore, one needs time effective algorithms to find the best master node of the system. In this thesis, an efficient algorithm is proposed to obtain the best master node. The metric introduced in chapter 3 is used for this purpose. One only requires a single eigen-decomposition in order to obtain this metric. Thus, the proposed algorithm for the secondary control can easily rank all DGs and select the best one (i.e., the one with the highest score of the proposed metric) as the master node in large-scale microgrids.

In the state matrix of equation (4.5) structures of the power and data communication networks (L_P and L_D, respectively) as well as the parameters of the generation units (*M* and *Z*) are assumed to be fixed. The only tunable parameter in this matrix is b_{ii} which shows that the i^{th} DG is the master node if $b_{ii} = 1$ (note that there is only a single master node). Applying the perturbation principle (3.6) on the sensitivity analysis of the n^{th} eigenvalue of the state matrix of equation (4.5), one obtains:

$$\left|\frac{d\lambda_n}{db_{ii}}\right| = \begin{cases} \boldsymbol{y}_n^T \begin{bmatrix} \frac{dB}{db_{ii}} & 0 \\ 0 & 0 \end{bmatrix} \boldsymbol{x}_n = \boldsymbol{y}_n^i \boldsymbol{x}_n^i, & i = 1,2,\dots,l \\ \boldsymbol{y}_n^T \begin{bmatrix} 0 & 0 \\ \frac{dB}{db_{ii}} & 0 \end{bmatrix} \boldsymbol{x}_n = m_i^{-1} y_n^{N+1} x_n^i, & i = 1,2,\dots,N-l \end{cases} \tag{4.6}$$

in which, $\boldsymbol{y}_n^k$ and $\boldsymbol{x}_n^k$ are the k^{th} element of $\boldsymbol{y}_n^T$ and $\boldsymbol{x}_n$, respectively and the sign |.| shows the absolute value. Now, the most influential node, on the stability and performance of the microgrid, is defined as the node whose perturbation causes the maximal effect on the real part of the dominant eigenvalue λ_1. Therefore, for the i^{th} generation unit in the microgrid, the value of this metric (η_i) is defined as:

$$\eta_i = Re(\frac{d\lambda_1}{db_{ii}}) \tag{4.7}$$

where '*Re*' is an abbreviation for the real part of a complex number. This metric can be calculated from the eigenvectors of the Laplacian matrix of the data communication network as follows:

$$|\eta_i| = Re\begin{cases} \boldsymbol{y}_1^i \boldsymbol{x}_1^i, & i = 1,2,\dots,l \\ \boldsymbol{y}_1^{(N+i-l)} \boldsymbol{x}_1^{i-l}, & i = l+1,\dots,N \end{cases} \tag{4.8}$$

In an undirected communication network, where the right and left eigenvectors of the Laplacian matrix are the same and real, this equation simplifies to:

$$|\eta_i| = Re\begin{cases} \left(\boldsymbol{x}_1^i\right)^2, & i = 1,2,\dots,l \\ \boldsymbol{x}_1^{(N+i-l)} \boldsymbol{x}_1^{i-l}, & i = l+1,\dots,N \end{cases} \tag{4.9}$$

Remark 1: In the case that $i = 1,\dots,l$, where $|\eta_i| = (\boldsymbol{x}_1^i)^2$, η_i can be either $(\boldsymbol{x}_1^i)^2$ or $-(\boldsymbol{x}_1^i)^2$. This means that to find the node that maximizes η_i, both the maximum and minimum values of $(\boldsymbol{x}_1^i)^2$ should be considered. In other words, the node that maximizes the value of η_i can be either the node maximizing $(\boldsymbol{x}_1^i)^2$ or the one minimizing it. To select the best one from these two candidates, the deviation on the dominant eigenvalue of the state matrix described in equation (4.5) should be computed and compared; the winner is the nodes resulting in the largest deviation. The same condition is for the case $i = l+1,\dots,N$. Thus, the secondary control system can find the master node *r* for frequency control of a microgrid using the following algorithm:

1) Calculate Laplacian matrices L_P and L_D from the connection graphs.

2) For the state matrix as expressed by equation (4.5), calculate the right and left eigenvectors corresponding to the dominant eigenvalue λ_1.

3) Calculate $|\eta_i|$ from equation (4.9) for both renewable energy sources ($i = 1, \dots, l$) and synchronous machines ($i = l + 1, \dots, N$).

4) Rank all nodes based on η_i. As explained in *Remark* 1, nodes with the highest and the lowest values of η_i are candidates for the most influential node.

5) Find the best node by examining the deviation in the dominant eigenvalue of (4.5) caused by each of these two candidate nodes.

Thus, one needs three eigen-decompositions in order to estimate the most influential leader; one for finding the two candidates (those maximizing and minimizing equation (4.7)), and two for examining each of them. This is still much simpler than computing the global optimal (examining all nodes one-by-one, and thus computing the eigenvalues N times) while resulting is satisfactory performance.

Now, Let's consider a power network of 200 generation units including 50 synchronous generators and 150 renewable energy sources. Power outputs of synchronous generators and 20% of the renewable sources (30 units) are considered to be controllable, while those of other units cannot be controlled. To control the frequency of this network, the cooperative control rule, as expressed by equation (4.4), is applied. It is assumed that the generation sources with controllable power outputs are candidates to be frequency leader of the network, while others will be in droop mode, following the leader. Therefore, the secondary control system should find the best node among 80 generation units as the frequency leader of the microgrid. Simulations in this section have two parts. In the first part, it is shown that the proposed metric (equation (4.9)) is accurate enough to find the most appropriate generation unit as the frequency leader. In the second part, the performance of this metric is compared with heuristic methods, such as taking the node with the highest degree or betweenness centrality as the master node and show that the proposed metric is more accurate than the heuristics. It is noteworthy that although other methods such as evolutionary algorithms (Jalili et al. 2015, Orouskhani et al. 2016) and spectral graph analysis (Yu et al. 2013) have been proposed to find near-optimal drivers, the real-time constraints of the secondary control system of power networks make them impractical. Therefore, the comparison is restricted to the above-mentioned heuristics, which can be implemented in a real-time fashion.

The microgrid considered in this simulation has dynamical equation (4.1) in which $M_i \in [0.1, 0.25]$ and $z_{ii} = 2.5$ for all synchronous generation units. All nodes are assumed to have a state feedback controller with gain $k_i = 10$. As stated before, L_P in equation (4.2) representing the Laplacian matrix of the physical power network, is normally assumed to be fixed. This is mainly due to the fact that any small modification in the physical power network (e.g., creating

new wirings) is costly and might not be practical in many cases. Therefore, any fixed structure for the power network can be considered in the simulations. Here, without loss of generality, the physical power network of the microgrid is assumed to be fully connected with the power transfer coefficient (T_{ij} defined in equation (4.1)) in the range of 0.1 and 0.3. The frequency of this microgrid is controlled using a cooperative control scheme as in equation (4.4). The Laplacian matrix of the data communication network is shown by L_D in equation (4.5). The secondary control should find the frequency leader based on the structure of the data communication network.

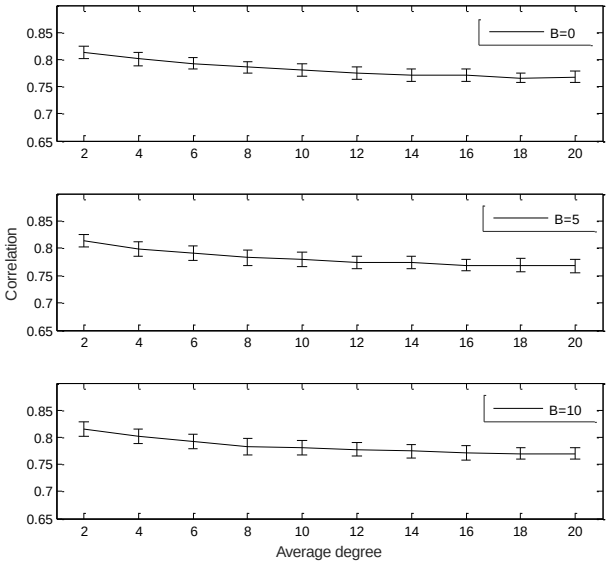

Fig. 4.2: Correlation between the ground-truth and the proposed rankings in scale-free networks. The data communication network is scale-free with N =80 nodes, different average degree and varying B (higher B indicates lower degree heterogeneity in the network). Data show mean values and standard deviations (represented by bars) over 100 realizations.

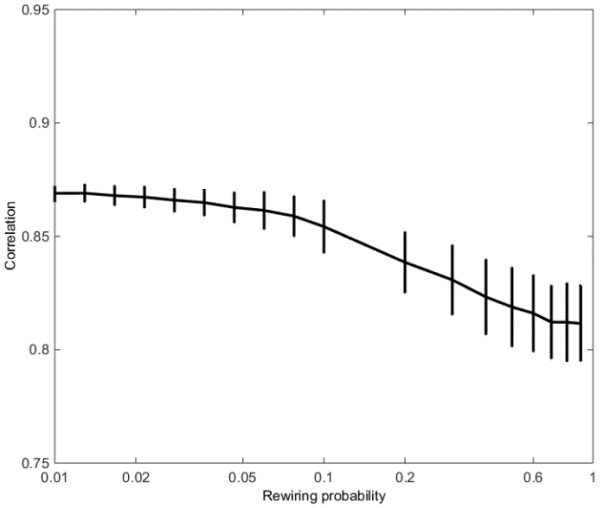

Fig. 4.3: Correlation between the ground-truth and the proposed rankings in Watts-Strogatz networks. The data communication networks are constructed using the Watts-Strogatz model with N = 80, m = 2, and different values of rewiring probability. Data show mean values and standard deviations (represented by bars) over 100 realizations.

To show the reliability of the proposed metric, different synthetic networks with scale-free, Watts-Strogatz and Erdős-Rényi structures are considered as the communication network. In the first step, to show the reliability of the proposed metric, it is applied to rank the generation units when the communication network L_D has a scale-free structure. All units are also ranked according to deviation in the dominant eigenvalue of the state matrix of equation (4.5). In order to obtain the true rankings, first, the nodes are considered to be the master node one-by-one, and the dominant eigenvalue is obtained. Then, the nodes are ranked based on the deviation they cause in the dominant eigenvalue (i.e., the smaller the real part of the dominant eigenvalue, the higher the rank of the node). This requires N eigen-decomposition (one for each node). Figure 4.2 shows Pearson correlation coefficients between these two rankings. It is seen that the correlation is higher than 0.8 no matter how heterogeneous the data communication

network is (i.e., it does not depend on B). However, as the average degree increases, the correlation coefficient slightly drops. Figure 4.3 shows the Spearman correlations as a function of rewiring probability for Watts-Strogatz networks. Again, high correlation values are obtained although it declines as the rewiring probability increases.

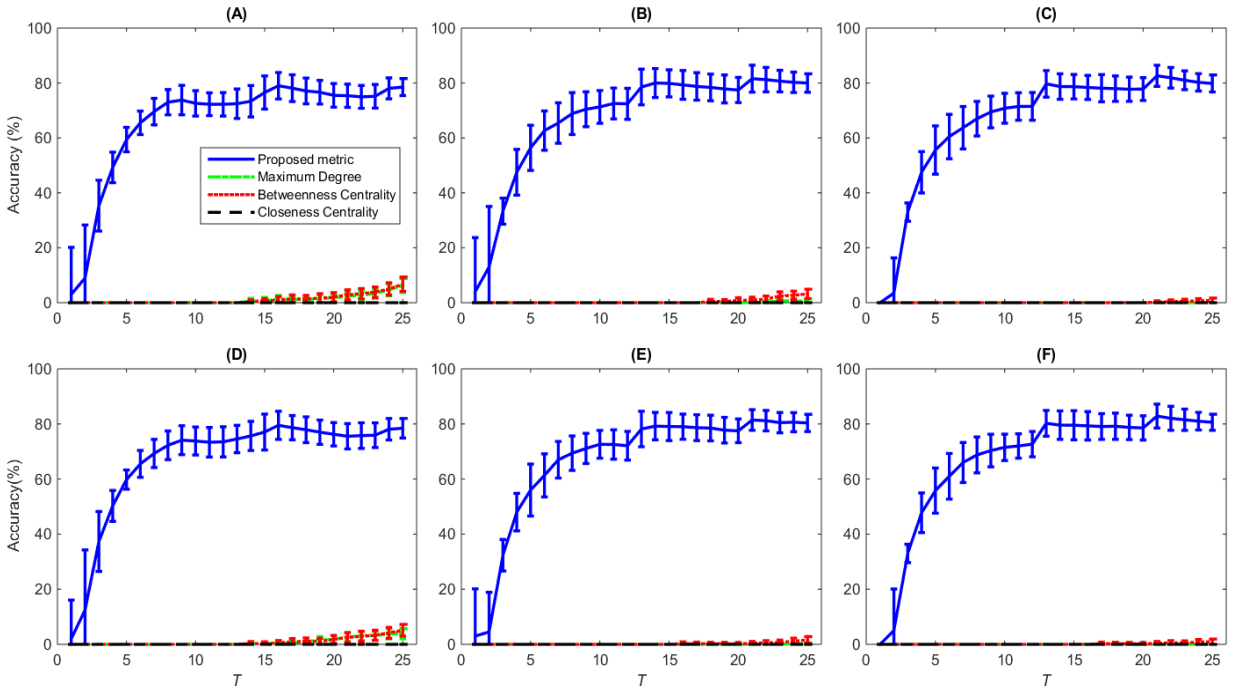

Fig. 4.4: Accuracy of different measures in finding top-T frequency leaders in scale-free networks. The scale-free networks are with $N = 80$, $B = 0$ and average degree of A) 2, B) 10, C) 20, $B = 10$ and average degree of D) 2, E) 10, and F) 20. The top-T nodes are determined either by the proposed metric (equation (14)), those with the highest degree, betweenness or closeness centrality values. The graphs show the mean values with bars corresponding to the standard deviations over 100 realizations.

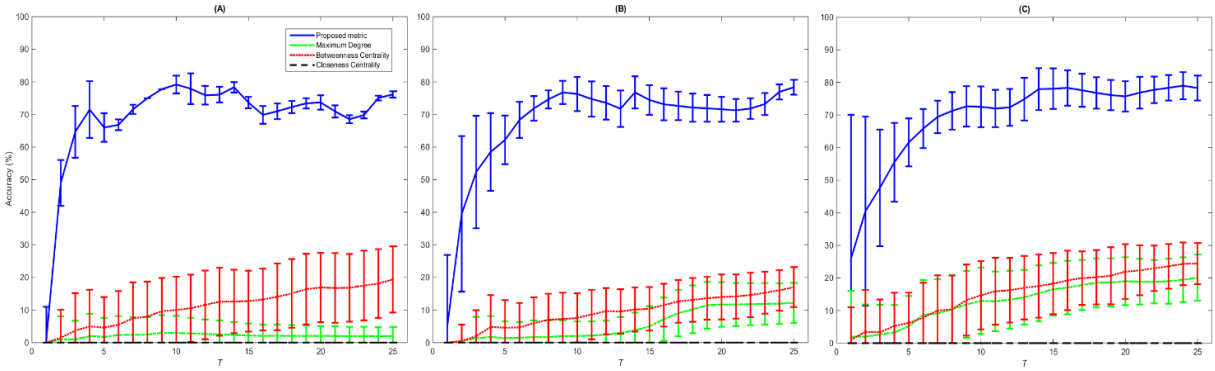

Fig. 4.5: Accuracy of different measures in finding top-T frequency in Watts-Strogatz networks. Networks are with $N = 80$ nodes with rewiring probability of A) $p = 0.01$, B) $p = 0.1$ and C) $p = 0.9$. The top-T nodes are determined either by the proposed metric (equation (14)), those with the highest degree, betweenness or closeness centrality values. The graphs show the mean values with bars corresponding to the standard deviations over 100 realizations.

In order to further study the effectiveness of the proposed metric, in the second step, we compare its accuracy in finding the best frequency leaders with heuristic methods. As heuristic methods, the nodes with the highest degree, betweenness and closeness centrality are chosen as leaders. These heuristics are rather simple to compute and have been previously shown to

be effective in synchronisation and pinning controllability of dynamical networks. To find the accuracy of the methods, the true top-T master nodes are first derived, that is obtained by numerically calculating the dominant eigenvalue for each node, one by one. Then, the top-T nodes predicted by the methods, are obtained and the accuracy is defined as the percentage of them that are also present in the true top-T list.

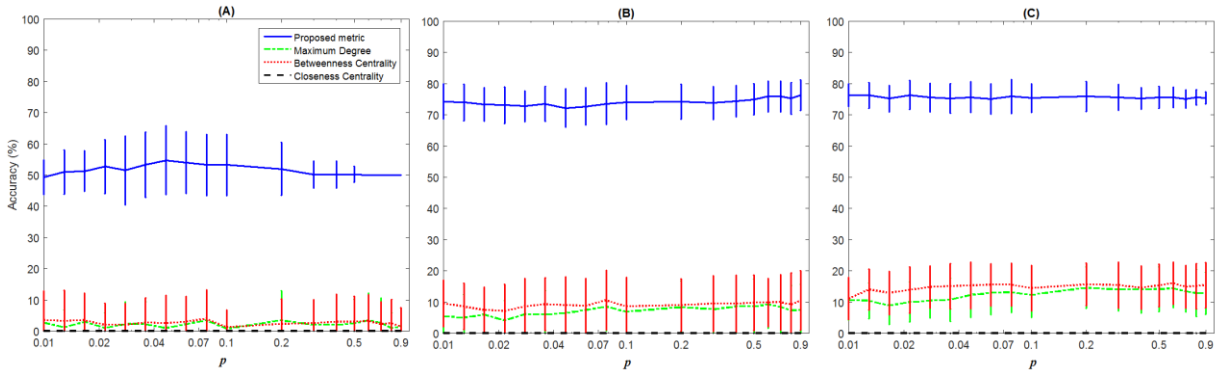

Fig. 4.6: Accuracy of different measures in finding top-T frequency leaders in Erdős-Rényi networks for A) T = 4, B) T = 10 and C) T = 20. Networks are with N = 80 nodes with connection probability p that varies from 0.01 to 0.9 logarithmically. The top-T nodes are determined either by the proposed metric (equation (14)), those with the highest degree, betweenness or closeness centrality values. The graphs show the mean values with bars corresponding to the standard deviations over 100 realizations.

Figures 4.4 and 4.5 compare the performance of the proposed measure with heuristic methods in scale-free and Watts-Strogatz networks, respectively. Accuracies of all methods are compared in finding the best frequency leaders. As it is seen, the proposed metric is much more accurate than the heuristic methods. While the heuristic methods have almost zero accuracies for small values of T and maximum accuracy of around 6% for large values of T, the proposed metric show high accuracy with up to 80% for large T. Generally, as T increases, the accuracy of the algorithms also increases.

Figure 4.5 compares the accuracy of the methods in Watts-Strogatz networks with three different rewiring probabilities. Again, as T increases, the accuracy of the methods increases, except for the one based on closeness centrality for which the accuracy is almost zero for all cases. The methods based on degree and betweenness centrality show a linear increase by increasing T, while the proposed method shows an exponential increase reaching to the accuracy of around 70% for $T > 5$. The proposed method has the best performance followed by the one based on betweenness centrality and then degree. Figure 4.6 shows the results when the data communication network has Erdős-Rényi structure. It is shown that the accuracies of all metrics are almost independent of the average degree, and the proposed metric has the best performance with the accuracy of more than 70% for T = 10 and T = 20, while others have accuracies of less than 20%.

From Figs. 4.4, 4.5 and 4.6, one can conclude that the proposed metric can accurately find the best frequency leaders in the microgrids. Adding the low computational cost of this metric to its rather high accuracy, this metric satisfies the real-time constraints of secondary frequency control calculation as well as the accuracy needed for its sound operation.

4.2 Rate of Change of Frequency in distributed power generation systems

Equation (4.5) shows that any modification in the Laplacian matrix of data communication networks (L_D) used in distributed secondary control affects the frequency performance of the microgrid. It is supposed that outage of a generation unit will not affect the structure of the power grid (L_P) since its local loads should still be supplied through the microgrid. The effect of the outage of a node on the data communication network L_D is considered as node removal, i.e. the node itself, as well as all communication links connecting it to the neighbours, is removed. This node removal affects the eigenvalues of L_D. On the other hand, Rate of Change of Frequency (RoCoF) of the microgrid can be measured by the dominant eigenvalue of the state matrix (4.5), i.e. the smaller the dominant eigenvalue the faster the frequency response. It is clear from (4.5) that while L_P, K, Z and B are supposed to be unchanged by disconnecting a generation unit from the microgrid, variation in the dominant eigenvalue of (4.5) is proportional to the variation of the dominant eigenvalue of L_D. Therefore, it would be enough to rank generation units based on their effect on the dominant eigenvalue of L_D. The following lemma is useful in this way:

***Lemma* 2.1** (Watanabe and Masuda 2010): Let us represent the eigenequation for the second smallest eigenvalue (λ_2) of the Laplacian matrix (L) of an undirected unweighted graph as $L\boldsymbol{u}_2 = \lambda_2 \boldsymbol{u}_2$ where $\boldsymbol{u}_2$ is the normalized eigenvector of L corresponding to λ_2. Removing node i of the network affects λ_2 by:

$$\Delta\lambda_2 \approx \frac{\sum_{j\in N_i} u_2^j(u_2^i - u_2^j)}{1-(u_2^i)^2} \tag{4.10}$$

where $u_2{}^i$ is the i^{th} element of $\boldsymbol{u}_2$ and N_i indicated the neighbourhood of node i.

4.2.1 Approximating change in RoCoF in the case of generation outage

Now, suppose that variation in the dominant eigenvalue of (4.5) is shown by $\Delta\alpha$. Using the lemma and considering that $\Delta\alpha$ is proportional to $\Delta\lambda$, all nodes can be ranked based on their effect on RoCoF. For instance, the node whose removal causes the largest value of $\Delta\lambda_2$ in (4.10), will cause the highest variation in RoCoF of the microgrid.

In this section, a power network of 200 generation units, including 50 synchronous generators and 150 renewable energy sources is considered. Power outputs of synchronous generators, as well as 20% of the renewable sources (30 units), are considered to be controllable, while those of other units cannot be controlled. A cooperative distributed control, expressed by equation (4.4), is applied to control the frequency of the network. Therefore, 80 generation units are candidates to participate in the secondary control of the microgrid.

The microgrid considered in this simulation has the same dynamical equation as the one in section 4.1. To show the reliability of the proposed metric, different synthetic networks with scale-free and Watts-Strogatz structures are considered as communication networks. To derive figure 4.7, first the generation nodes are ranked based on metric (4.10) when data communication network has scale-free structure with $m = 5$ and $B = 0$. Then, the node with the highest rank and the node of 5^{th} rank are removed from the data network one at a time (the 5^{th}-ranked node is selected to show the difference more clearly). After removing each node, a frequency deviation is generated in the power system in order to check how fast the control system can recover it. Recovery rates are shown in Fig. 4.7(A) when the node with the highest rank is removed and in Fig. 4.7(B) when the node with 5^{th} rank is deleted. Clearly, RoCoF is more affected in (A) rather than (B), meaning that node with the highest rank influence RoCoF more that node with rank 5.

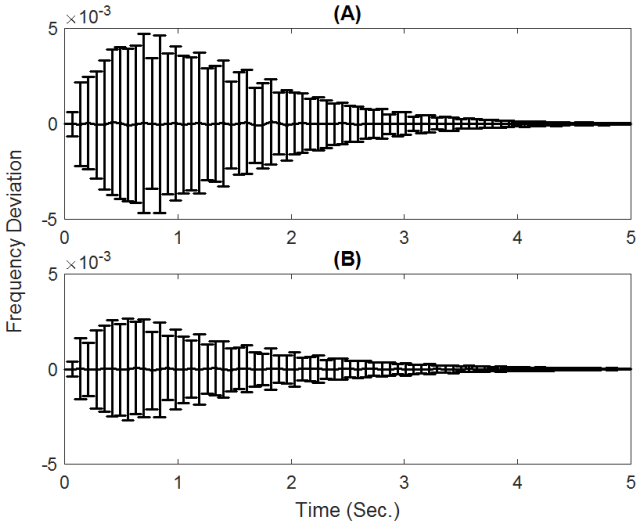

Fig. 4.7: Comparing frequency recovery rate of a microgrid with scale-free control network. Nodes with (A) 1st (B) 5th rank are removed from the network. Nodes are ranked based on equation (4.10). Data show mean values and standard deviations (represented by bars) over 100 realizations.

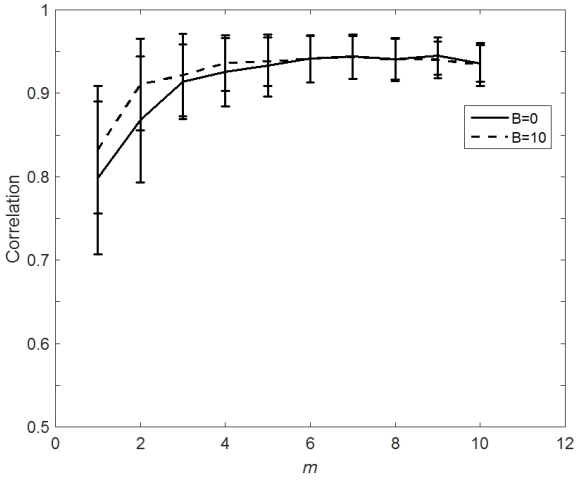

Fig. 4.8: Correlation between the proposed and degree-based rankings. Data network is supposed to have a scale-free structure with the average degree (m) and degree of heterogeneity B. Data show mean values and standard deviations (represented by bars) over 100 realizations.

Correlation between the nodes ranked using equation (4.10) with the ranking is done using degree centrality of the nodes is shown in Fig. 4.8. The average degree of the scale-free data communication network is changed from 1 to 10 when heterogeneity factor *B* is zero or 10. Figure 4.8 shows that these two rankings are highly correlated especially for networks with higher average degrees. In other words, connection/disconnection of nodes with higher degrees in the data communication networks will affect RoCoF more.

The same studies are conducted when data communication network has Watts-Strogatz structure. Here, networks with rewiring probabilities p = 0.01, p = 0.1 and p = 0.9 are considered. Again, first nodes are ranked based on equation (4.10). Then, the node with the highest ranks and the node with rank 5 are removed one at a time at the frequency recovery changes are compared. The upper row of Fig. 4.9 shows frequency recovery when a node with the highest rank is removed while the lower row is that for the node of rank 5. According to Fig. 4.9, removal of the former has stronger effect on the frequency recovery than removal of the latter especially when the structure of the network in nearer to small world, i.e. for small values of rewiring probability *p*. Finally, Fig. 4.10 shows that the ranking which is made using equation (4.10) is highly correlated with the ranking made through degree centrality for higher rewiring probabilities.

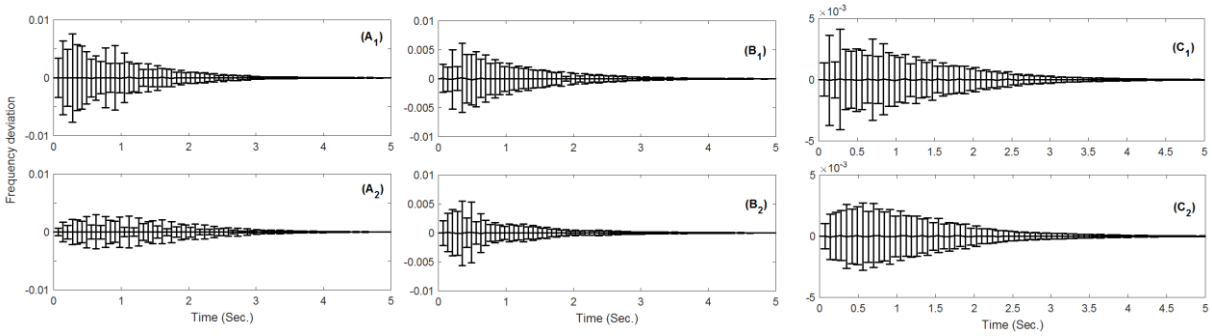

Fig. 4.9: Comparing frequency recovery rate of a microgrid with Watts-Strogatz control network. Nodes with (A_1, B_1, C_1) 1st (A_2, B_2, C_2) 5th rank is removed from the network. Data network is supposed to have (A) p = 0.01, (B) p = 0.1 and (C) p = 0.9. Nodes are ranked based on equation (4.10).

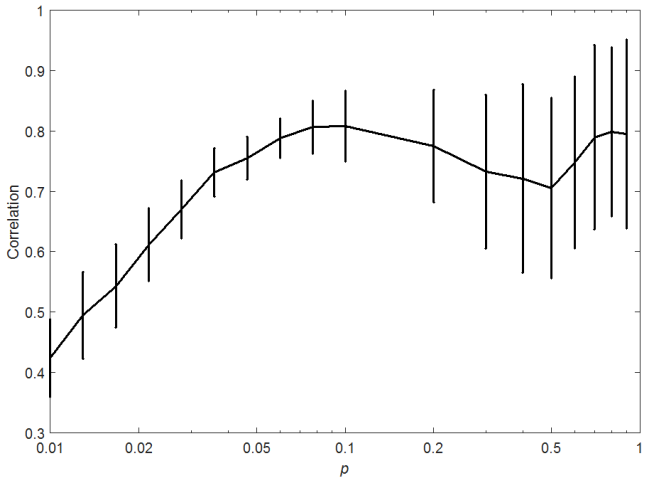

Fig. 4.10: Pearson's linear correlation between the proposed and degree centrality rankings. The data communication networks are constructed using the Watts-Strogatz model with $N = 80$, $m = 2$, and different values of rewiring probability. Data show mean values and standard deviations (represented by bars) over 100 realizations.

4.3 Determining disease evolution driver nodes in dementia networks

With the increasing availability of medical data, improved computing power and network speed, modern medical imaging is facing an unprecedented amount of data to analyse and interpret. Novel mathematical concepts, such as graph-theoretical techniques can capture brain connectivity and its topology. Networks of these graphs are mostly based on Pearson correlation and capture either the structural and/or functional brain connectivity. From these graphs, new descriptors can be derived to quantify induced changes in topology or network organisation or to serve as theory-driven biomarkers to predict dementia at the level of individual patients. Graphs applied to dementia research, even for longitudinal data, are static networks which cannot capture the dynamical processes governing the temporal evolution of dementia. Therefore, a new paradigm in dementia research - dynamical graph networks - is required to advance this field and overcome the obstacles posed by static graph theory in terms of disease prediction, evolution, and its associated connectivity changes (Tahmassebi et al. 2018).

Here, functional connectivity networks in dementia are modelled and analysed as two-time scale sparse dynamic graph networks with hubs (clusters) representing the fast sub-system and the interconnections between hubs and the slow subsystem. Alterations in brain function as seen in dementia can be dynamically modelled by determining the clusters in which disturbance inputs have entered and the impact that they have on the large-scale dementia dynamic system.

Controlling regions in dementia networks represent key nodes to control the dynamics of the network. It is crucial to understand how this complex network is controlled to enable an understanding of the progressive abnormal neural circuits in dementia. Figure 4.11 demonstrates the schematic presentation of an unweighted-undirected graph of complex networks in the brain.

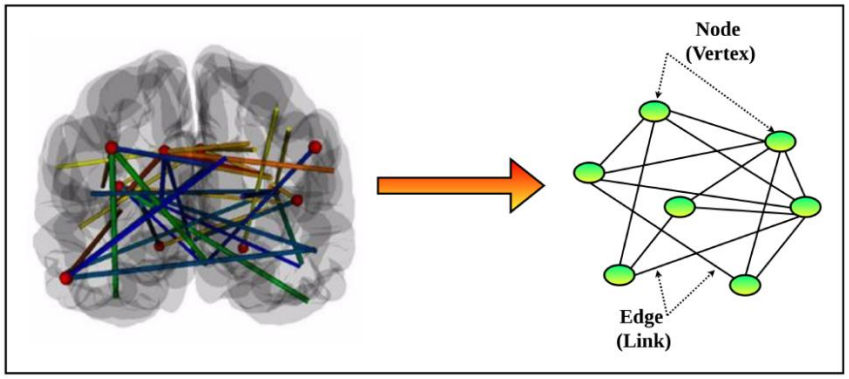

Fig. 4.11. Schematic illustration of an unweighted-undirected graph of complex networks in brain. Nodes can be brain regions or voxels. Edges or links are the functional or structural connections between nodes.

While static graph analysis has revealed the loss of strong connections in dementia patients compared to healthy controls, the dynamic graph analysis shows different slow modes between dementia patients and connectivity networks in healthy controls. The connectivity networks in healthy controls have smaller eigenvalues than in dementia patients for both functional and structural data and those eigenvalues remain operative. The contribution of the larger eigenvalues over time decreases quickly and the range of the eigenvalues for each subject represents an important biomarker for disease prediction. To further contribute to the theoretical progress of the analysis of the dynamical behaviour in dementia, the metric proposed in chapter 3 is applied to select the best driver node in connectivity graphs that show a transaction from normal subjects to Alzheimer's subjects.

The theoretical results in finding the most influential nodes on controllability are applied on functional (FDG-PET) and structural (MRI) connectivity graphs for control (CN), mild cognitive impairment (MCI) and Alzheimer’s disease (AD) subjects (Ortiz et al. 2015). These data were obtained from the Alzheimer's Disease Neuroimaging Initiative (ADNI) database. For the structural MRI data, the connections in the graph show the inter-regional covariation of grey matter volumes in different areas while for the functional PET data, the connections do not show the correlation in activity but in the glucose uptake between different regions. The

model proposed in (Ortiz et al. 2015) considered only 42 out of the 116 regions from the Automated Anatomical Labelling (AAL) in the frontal, parietal, occipital, and the temporal lobes. Nodes in graphs represent the regions while the links show if a connection is existing between these regions or not. Undirected and unweighted graphs are considered and the controllability centrality metric is applied to them. Except for the functional connectivity graph for CN, the controllability centrality metric can be applied to all the other graphs. The largest connected graph in the functional connectivity graph for AD is considered. Figure 4.12 shows the most influential driver nodes found on the functional connectivity graph using controllability centrality metric, i.e. the metric proposed in (3.9). For CN due to the disconnectivity of the graph, we are not able to theoretically determine the best driver nodes. For MCI the best driver node is located in the inferior left occipital lobe (Occipital-Inf-L), and for AD in the superior right occipital lobe (Occipital-Sup-R). Early-onset AD is characterized by changes in the functional connectivity in the occipital lobe. Figure 4.12 shows the most influential driver nodes found on the structural connectivity graph.

For all three networks, the most influential node is located in the temporal lobe (Temporal-Pole-Mid-L). These results agree with the clinical findings which show that the MCI patients who are at risk to develop AD show medial temporal lobe atrophy. Detection of this important driver node being at the same time the most influential one may represent an important biomarker of the diagnosis of AD and its transition from MCI to AD (Tahmassebi et al. 2018).

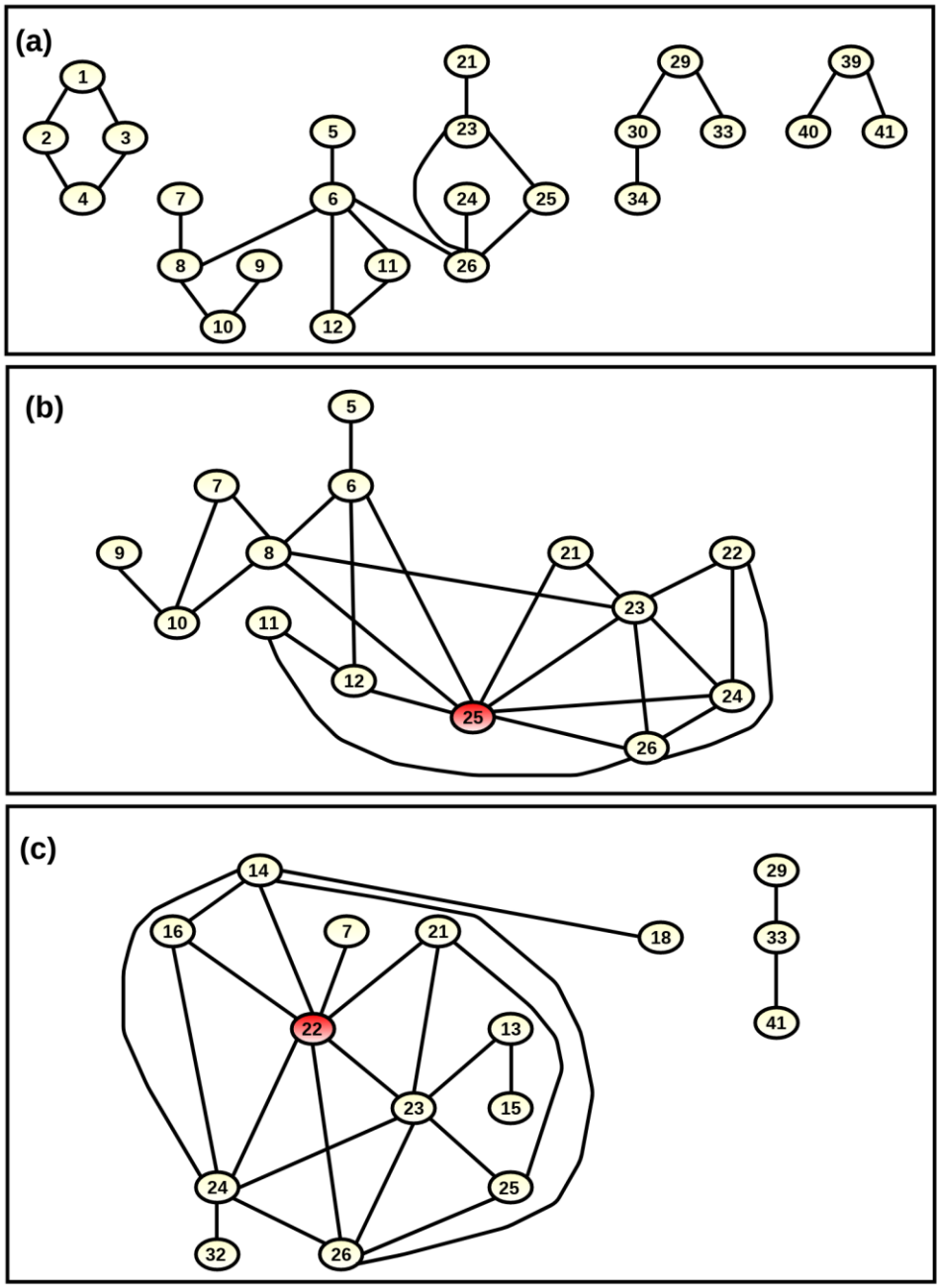

Fig. 4.12. The most influential nodes (shown in red) in brain connectivity graphs for (a) CN, (b) MCI and (c) AD.

4.4 Summary

In this chapter, application of the mathematical achievements of chapter 3, i.e. identifying the best driver node (or set) to control a complex network, was applied to problems in distributed power generation and dementia networks. First, the problem of finding the frequency leader in the cooperative secondary control of a microgrid was addressed. The microgrid was assumed to be composed of both synchronous and VSI-connected generation units. The proposed model showed that the stability and performance of the distributed

secondary frequency control depends on *i*) the structure of the physical power network, *ii*) parameters of generation units, *iii*) structure of the data communication network (on which the distributed control was implemented), and *iv*) the node which was selected as the frequency leader of the microgrid. The first two factors are often fixed in the construction process of the power grids, and their change is costly. Whereas, the last two factors (i.e., the topology of the data communication network and the frequency master node) can be easily tuned. Assuming a communication network with fixed topology, a novel metric to select one of the nodes as frequency leader was proposed.

The problem of finding the generation unit with the maximum influence on the RoCoF was also studied and a new metric to find this unit was proposed. The metric was based on the eigenvalue perturbation analysis of the state matrix of the microgrid. Using this metric, the power management system of the microgrid could rank all generation units and choose the one with the largest influence on the stability of the system as the frequency master, while other nodes following it. The metric is simple to compute and can be easily used in microgrids with a large number of small size generation units including renewables.

Finally, structural and functional connectivity graphs in healthy controls, patients with mild cognitive impairment, and those suffering from Alzheimer's disease were analysed in order to determine the most influential driver nodes or so-called "disease epicentres". The location of the most influential driver nodes provides the scientific community with a novel biomarker that can be employed in differentiating dementia types and to monitor disease evolution. Our results were in good agreement with preliminary clinical findings.

Section II: Controllability of complex networks in the case of node/edge removal

Chapter 5

Impact of node removal on collective behaviours in complex networks

Removal of a node or link in a complex network can be caused due to physical and/or functional defects, such as mechanical/electrical failures or attacks. Node/link removal might impact the spectrum of the network, and thus its synchronisability and collective behaviour. Identifying the node with the maximum influence on the synchronisability is a challenge for both network designers and attackers. In this chapter, a computationally efficient metric is proposed base on spectral graph analysis which can rank nodes based on their influence on the eigenvalues of the Laplacian matrix. Our proposed metric predicts the changes that a node removal makes in the eigenvalues of the Laplacian matrix. Results of this chapter have been published partly in IEEE International Symposium on Circuits and Systems (ISCAS) (Moradi Amani et al. 2018) and another article has been submitted.

5.1 A numerical study on graph spectral impact of node removal

Suppose a set of N identical dynamical nodes V, connected over an undirected and unweighted network (V,E) with a set of edges E. Equations of the motion of this network is as follows:

$$\frac{d\boldsymbol{x}_i}{dt} = F(\boldsymbol{x}_i) - \sigma \sum_{j=1}^{N} l_{ij} H\boldsymbol{x}_j; \quad i = 1,2, \dots, N, \tag{5.1}$$

where $\boldsymbol{x}_i \rightarrow \mathbb{R}^n$ is the n-dimensional state vector, F: $\mathbb{R}^n \rightarrow \mathbb{R}^n$ defines the individual systems' dynamical equation, which is considered to be identical for all nodes, and σ represents the unified coupling strength. Based on the master stability function formalism discussed in chapter 2, local synchronisability of this system depends on spectral properties of the Laplacian matrix of the graph. Among eigenvalues of the Laplacian matrix, λ_N and λ_2, i.e. the largest and the second smallest ones, play significant roles: λ_2 and $R = \lambda_N/\lambda_2$ can be synchronisability metrics for different classes of systems. It was discussed in chapter 2 that the smaller the eigen-ratio R (or the larger λ_2 for classes of systems) is, the better the synchronisability of the network will be.

Synchronisability analysis of a complex network using λ_2 or R needs knowledge about the largest and the second smallest eigenvalues of the Laplacian matrix. For instance, to study the effect of node removal on synchronisability, its impact on the values of λ_N and λ_2 should be first determined. As a preliminary study, Figure 5.1 shows the variation in the eigenvalues (i.e. $\Delta\lambda_N$ and $\Delta\lambda_2$) caused by node removal in synthetic networks with scale-free, Watts-Strogatz and Erdős-Rényi structures. In each network, one node and all its adjacent links are removed, and the terms $\Delta\lambda_N = \lambda_N - \lambda^R_N$ and $\Delta\lambda_2 = \lambda_2 - \lambda^R_2$ are measured where λ^R_N and λ^R_2 are the largest and the second smallest eigenvalues of the Laplacian matrix after node removal. Then, the original network is considered, and the process is repeated for another node. Fig. 5.1 shows the mean values along with the standard errors performed over 100 realizations.

Figure 5.1(A) depicts $\Delta\lambda_N$ and $\Delta\lambda_2$ in a network with scale-free structure as a function of the average degree (expressed by m) and for different values of B. It is shown that the heterogeneity degree (B) does not affect $\Delta\lambda_2$ considerably while it has inverse effect on $\Delta\lambda_N$, i.e. removing a node in more homogenous networks ($B = 0$) affects λ_N more than the case of more heterogeneous ones ($B = 10$). It is also clear in Fig. 5.1(A) that effect of node removal on both λ_N and λ_2 becomes stronger as the average degree increases. In addition, variation of

spectral gap is generally bigger than variation of algebraic connectivity when a node is removed.

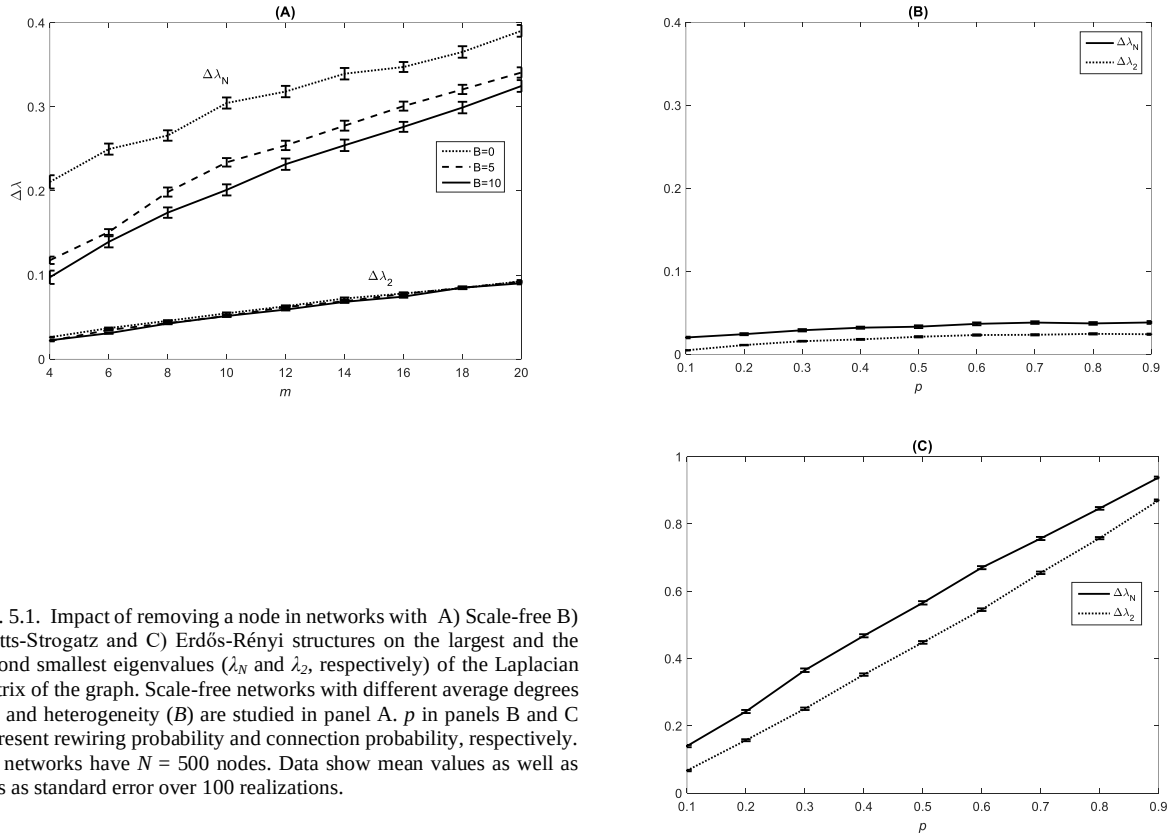

Fig. 5.1. Impact of removing a node in networks with A) Scale-free B) Watts-Strogatz and C) Erdős-Rényi structures on the largest and the second smallest eigenvalues (λ_N and λ_2, respectively) of the Laplacian matrix of the graph. Scale-free networks with different average degrees (m) and heterogeneity (B) are studied in panel A. p in panels B and C represent rewiring probability and connection probability, respectively. All networks have N = 500 nodes. Data show mean values as well as bars as standard error over 100 realizations.

Variation of the largest and second smallest eigenvalues of the Laplacian matrix is relatively small and almost independent of the rewiring probability (p) in Watts-Strogatz networks (Fig. 5.1B). In networks with Erdős-Rényi structures, $\Delta\lambda_N$ and $\Delta\lambda_2$ increase with connection probability almost with the same rates (Fig. 5.1C). These results are used in defining our metric in the next section.

This study gives a general view of the effect of node removal on the synchronisability of a class of dynamical networks where synchronisability is related to the spectral gap. From mathematical graph theory (Mieghem 2011), removing a node from a complex network can be modelled as removal of the related row and column of the Laplacian matrix as well as a perturbation on diagonal elements related to the neighbours of the removed node. For a single node removal in a large network, this perturbation may be negligible. Therefore, one can approximate the effect of removing node k by removing the k^{th} row and column of the Laplacian matrix and use the eigenvalue interlacing theorem (Theorem 5.2) to study the spectral impact of node removal. However, this approximation is not precise when the network is not large enough, and thus a Laplacian eigenvalue interlacing theorem should be developed. In addition,

a metric to rank nodes based on their removal impact on the network spectrum is useful for identification of vulnerable nodes in synchronisation of complex networks. These two problems are studied in the next sections.

5.2 Eigenvalue interlacing for Laplacian matrix

Laplacian is a zero row-sum symmetric (positive semidefinite) matrix with eigenvalues as $0 = \lambda_1 < \lambda_2 \leq \ldots \leq \lambda_n$ when the graph is connected. In general, the multiplicity of $\lambda_1 = 0$ shows the number of components of the network. It is worth noting that to simplify the notations, the vector $\boldsymbol{x}$ is considered in $\mathbb{R}^n$ in the rest of this chapter to get rid of the Kronecker product.

5.2.1 Rayleigh Principle

For any symmetric matrix P, the Rayleigh quotient R_P: $\mathbb{R}^n$–{0} → $\mathbb{R}^n$ is defined as:

$$R_P(\boldsymbol{x}) = \frac{<\boldsymbol{x},P\boldsymbol{x}>}{\|\boldsymbol{x}\|^2} \tag{5.7}$$

one can restrict the study to normalized vectors $\|\boldsymbol{x}\| = 1$ when dealing with the possible values of $R_P(\boldsymbol{x})$. Therefore, from now on, $R_P(\boldsymbol{x})$ is simply computed as $<\boldsymbol{x},P\boldsymbol{x}>$ or $\boldsymbol{x}^T P\boldsymbol{x}$.

Assume that $P = L$, the Laplacian matrix. Then, it is well known that

$$0 \leq R_L(\boldsymbol{x}) \leq \lambda_n \tag{5.8}$$

Indeed, L can be written as $L = Q^T \Lambda Q$, where Λ = diag (λ_1, λ_2, …, λ_n) and Q forms an orthonormal basis from corresponding eigenvectors. Therefore, writing x in such a basis, $\boldsymbol{x} = Q\boldsymbol{\alpha}$ results in

$$\begin{aligned} R_L(\boldsymbol{x}) &= \boldsymbol{x}^T Q\Lambda Q^T \boldsymbol{x} = (Q^T\boldsymbol{x})^T \Lambda (Q^T\boldsymbol{x}) = \boldsymbol{\alpha}^T\Lambda\boldsymbol{\alpha} \\ &= \lambda_1\alpha_1^2 + \lambda_2\alpha_2^2 + \cdots + \lambda_n\alpha_n^2 \end{aligned} \tag{5.9}$$

Then, as $\lambda_1 = 0$, the above range for $R_L(\boldsymbol{x})$ follows. Besides, if G is connected, the corresponding eigenvector $\boldsymbol{u}_1$ is any non-zero multiple of $\mathbf{1}_N = (1,1,\ldots,1)$, i.e. $\boldsymbol{u}_1 \in$ span $\{\mathbf{1}_N\}$.

Lemma 5.2. If G is connected, the smallest non-zero eigenvalue of the Laplacian matrix is

$$\lambda_2 = \min_{<\boldsymbol{x},\mathbf{1}>=0} R_L(\boldsymbol{x}) = \min_{<\boldsymbol{x},\mathbf{1}>=0} \boldsymbol{x}^T L\boldsymbol{x}. \tag{5.10}$$

5.2.2 Effect of node removal on the spectrum of the Laplacian matrix

The first achievement of this section is an eigenvalue interlacing theorem for the Laplacian matrix of a graph. It is worth noting that the well-known eigenvalue interlacing theorem, which is defined based on deleting a row and column of a real symmetric matrix, is only applicable when the effect of node removal is investigated on eigenvalues of the adjacency matrix. In the Laplacian matrix, node removal does not exactly result in only a row and column removal and needs further studies. Here, an interlacing theorem for the eigenvalues of the Laplacian matrix is proposed when a node (and all its adjacent links) is removed from a graph. Here, the Theorem 5.1 and its proof as well as the Theorem 5.2 are first reviewed. These theorems are applied to prove the interlacing theorem 5.3.

Theorem 5.1. (Godsil and Royle 2001) For any symmetric $n \times n$ matrix P

$$\lambda_{j+1} = \max_{\dim(V)=n-j} \min_{\boldsymbol{x}\in V} R_P(\boldsymbol{x}) = \min_{\dim(V)=j+1} \max_{\boldsymbol{x}\in V} R_P(\boldsymbol{x}) \tag{5.11}$$

for all $j = 0, 1, \ldots, n-1$.

Proof: To prove the first equality, let's start with

$$\max_{\dim(V)=n-j} \min_{\boldsymbol{x}\in V} R_P(\boldsymbol{x}) = \max_{\dim(V)=n-j} \min_{\boldsymbol{x}\in V} (\lambda_1 x_1^2 + \lambda_2 x_2^2 + \cdots + \lambda_n x_n^2). \tag{5.12}$$

From $\boldsymbol{x} \in V$, $\dim(V) = n - j$ and $\boldsymbol{x} \in \mathbb{R}^n$, one can conclude that $\boldsymbol{x}$ is orthogonal to at least one subspace $\tilde{V}$ of dimension j. Suppose $\tilde{V}$ is covered by the set canonical basis $\{\boldsymbol{e}_i; i = 1, 2, \ldots, j\}$ and its orthogonal complement V is covered by $\{\boldsymbol{v}_i; i = 1, 2, \ldots, n-j\}$. Therefore, there exists $\boldsymbol{x} \in \mathbb{R}^n$ orthogonal to $\{\boldsymbol{e}_1,\ldots,\boldsymbol{e}_j,\boldsymbol{v}_1,\ldots,\boldsymbol{v}_{n-j}\}$, which have a form of $\boldsymbol{x} = (0,0,\ldots,0, a_1, a_2,\ldots, a_{n-j+1})$ where the first j elements are zero. Suppose $\boldsymbol{x}$ is a normalized vector (otherwise one can normalize it) such that $a_1^2 + a_2^2 + \ldots + a_{n-j+1}^2 = 1$. Therefore,

$$R_P(\boldsymbol{x}) = a_1^2\lambda_{j+1} + a_2^2\lambda_{j+2} + \cdots + a_{n-j}^2\lambda_j \geq \lambda_{j+1} \tag{5.13}$$

which results in

$$\min_{x\in V} R_P(\boldsymbol{x}) = \lambda_{j+1} \tag{5.14}$$

and completes the proof for

$$\max_{\dim(V)=n-j} \min_{x\in V} R_P(x) = \lambda_{j+1} \tag{5.15}$$

To prove the other equality in (5.11), suppose subspace U is a subspace of dimension $j+1$ with basis $\{\boldsymbol{u}_1, \boldsymbol{u}_2,\ldots, \boldsymbol{u}_{j+1}\}$. Then there exists:

$$\min_{\dim(V)=j+1} \max_{\substack{x\in V \\ ||x||=1}} R_P(\boldsymbol{x}) \leq \max_{\substack{x\in U \\ ||x||=1}} R_P(\boldsymbol{x}) \leq \lambda_{j+1} \tag{5.16}$$

Now, suppose another subspace W with dimension $n-(j+1)+1$ and with basis $\{\boldsymbol{u}_j, \boldsymbol{u}_{j+1},\ldots, \boldsymbol{u}_n\}$. There should be at least one vector $\boldsymbol{x}$ in W∩V with $\| \boldsymbol{x} \| = 1$ because:

$$dim(V \cap W) = dim(V) + dim(W) - dim(V \cup W) \geq j + 1 + n - (j + 1) + 1 - n = 1$$

As $\boldsymbol{x} \in W$, there is $R_P(\boldsymbol{x}) = \boldsymbol{x}^T P \boldsymbol{x} \geq \lambda_{j+1}$ which converts inequalities in (5.16) to equality and completes the proof. ■

Theorem 5.2. (Eigenvalue Interlacing Theorem) (Godsil and Royle 2001): Let A be a real symmetric $n \times n$ matrix with eigenvalues $\lambda_1 < \lambda_2 \leq \ldots \leq \lambda_n$. For some $m < n$, let S be a real $n \times m$ matrix with orthogonal columns, S^TS = I, and consider the matrix $Q = S^TAS$ with eigenvalues $\mu_1 \leq \mu_2 \leq \ldots \leq \mu_m$. Then, the eigenvalues of Q interlace those of A, that is

$$\lambda_i \leq \mu_i \leq \lambda_{n-m+i}; \quad i = 1,2,\ldots,m, \tag{5.17}$$

In a particular case when $m = n-1$, Q becomes a submatrix of P where k^{th}, $k \in \{1,2,\ldots,n\}$ row and column are removed and interlacing becomes $\lambda_1 \leq \mu_1 \leq \lambda_2 \leq \mu_2 \leq \ldots \leq \mu_{n-1} \leq \lambda_n$. In addition, when node v is removed, the Laplacian matrix of the network can be written as $\bar{L} = L_{\setminus v} + \Phi$, in which $L_{\setminus v}$ is achieved by removing v^{th} row and column of L and $\Phi = [\varphi_{ij}]$ is defined as

$$\phi_{ij} = \begin{cases} -1, & i = j \in N_v \\ 0, & otherwise \end{cases} \tag{5.18}$$

Now, we prove the following theorem:

Theorem 5.3. Suppose L and $\bar{L}$ are Laplacian matrices of the original graph and the graph when a node and all its adjacent links are removed from it, respectively. The spectrum of these Laplacian matrices satisfies the following inequalities,

$$\lambda_k(L) - 1 \leq \lambda_k(\bar{L}) \leq \lambda_{k+1}(L) \tag{5.19}$$

Proof: First, we show that for any symmetric $n \times n$ matrices P and $P + E$, we have

$$\lambda_1(E) \leq \lambda_k(P + E) - \lambda_k(P) \leq \lambda_n(E) \tag{5.20}$$

for all $k \in \{1,2,\ldots,n\}$. From Theorem 5.1, we have

$$\lambda_k(P + E) = \min_{\dim(V)=k} \max_{\substack{x\in V \\ ||x||=1}} x^T(P + E)x = \min_{\dim(V)=k} \max_{\substack{x\in V \\ ||x||=1}} (x^TPx + x^TEx)$$

$$\leq \min_{\dim(V)=k} \max_{\substack{x\in V \\ ||x||=1}} (x^TPx) + \lambda_n(E) = \lambda_k(P) + \lambda_n(E)$$

which proves the right-side inequality and can also be applied to prove the left-side inequality:

$$\lambda_k(P) = \lambda_k\big((P+E)-E\big) \le \lambda_k(P+E) + \lambda_n(-E) = \lambda_k(P+E) - \lambda_1(E)$$

Now, applying (5.20) on $\bar{L} = L_{\setminus v} + \Phi$ with $P = L_{\setminus v}$, $E = \Phi$ and Φ defined in (5.18) results in

$$-1 \le \lambda_k(\bar{L}) - \lambda_k(L_{\setminus v}) \le 0.$$

on the other hand, from interlacing theorem 5.2. we have

$$\lambda_k(L) \le \lambda_k\big(L_{\setminus v}\big) \le \lambda_{k+1}(L).$$

Combining two recent inequalities completes the proof. ■

Theorem 5.3, which can be called the "Eigenvalue Interlacing of Laplacian matrix" theorem, is also reported in (Lotker 2007); but our proof is much simpler. It defines bounds on the eigenvalues of the Laplacian matrix of a graph when a node is taken out of it. Applying this theorem on the algebraic connectivity and the spectral gap of a graph shows that removing any node from the network results in reduction of λ_n. However, this does not necessarily happen for algebraic connectivity. Although a node removal strategy has been proposed for increasing the algebraic connectivity in large networks (Watanabe and Masuda 2010), no general rule can be achieved from this theorem about effect of node removal on λ_2. Simulations also show that sometimes node removal may result in reduction in λ_2.

5.3 Identification of vital nodes for Laplacian spectrum

Eigenvalue interlacing theorem for the Laplacian matrix does not result in a practical metric although supported mathematically. In fact, in many real-world applications, one needs an applicable metric to find the most vulnerable nodes based on their impact on synchronisability. These nodes can then be further protected to increase the reliability of the whole network. Here, using a concept called "local multiplicity", a new metric to rank nodes based on their spectral impact is proposed. It is shown that the metric can be applied on networks with many different topologies.

5.3.1 Local spectrum of a graph

The spectrum of the Laplacian matrix L can be generally presented as

$$sp(L) = \{\lambda_0^{m_0}, \lambda_1^{m_1}, \dots, \lambda_d^{m_d}\} \qquad (5.20)$$

where the eigenvalues λ_0, λ_1,… and λ_d are in ascending order and the superscript denote algebraic multiplicities $m_i = m(\lambda_i)$ for $i = 0, 1, \ldots, d$. Generally, $m_0 + m_1 + \ldots + m_d = n$ and also $\lambda_0 = 0$ and $m_0 = 1$ for a connected graph.

For each λ_i, let U_i be the matrix whose columns form an orthonormal basis of its eigenspace $\mathcal{E}_i = \text{Ker}\,(L - \lambda_i I)$. The dimension of $\mathcal{E}_i$ is called geometric multiplicity of λ_i of L. For every $i = 0, 1, \ldots, d$, the orthogonal projection of $\mathbb{R}^n$ onto the eigenspace $\mathcal{E}_i$ can be done using the following matrices E_i which are called *principal idempotents* of L (Fiol 2002):

$$E_i = \frac{1}{\phi_i}\prod_{\substack{j=0 \\ j\neq i}}^{d}(L - \lambda_i I) \quad where \quad \phi_i = \prod_{\substack{j=0 \\ j\neq i}}^{d}(\lambda_i - \lambda_j) \tag{5.21}$$

These idempotents are known to satisfy the following properties:

$$(a)\ E_i E_j = \delta_{ij} E_i$$

$$(b)\ LE_i = \lambda_i E_i$$

$$(c)\ p(L) = \sum_{i=0}^{d} p(\lambda_i) E_i \text{ , for any polynomial } p \tag{5.22}$$

The principal idempotents of L can be also defined in the matrix form $E_i = U_i\, U_i^T$ (Fiol 2002).

The *local multiplicities* of the eigenvalue λ_i are defined as the squared norm of the projection of $\boldsymbol{e}_u$ (u^{th} canonical basis of $\mathbb{R}^n$ where $u \in V$) in the eigenspace $\mathcal{E}_i$. That is,

$$m_u(\lambda_i) = \|E_i \boldsymbol{e}_u\|^2 = < E_i \boldsymbol{e}_u, \boldsymbol{e}_u > = E_i^{uu} \tag{5.23}$$

where the superscript '*uu*' shows the $(u,u)^{th}$ element of E_i. In fact, $m_u(\lambda_i) = \cos^2 \beta_{ui}$ in which β_{ui} is the angle between $\boldsymbol{e}_u$ and $\mathcal{E}_i$ (Cvetković and Doob 1985). Local multiplicities are a generalization of the algebraic (or geometric) multiplicities when the graph is seen from node u and satisfy the following properties (Fiol and Carriga 1997):

$$\sum_{i=0}^{d} m_u(\lambda_i) = 1$$

$$\sum_{u\in V} m_u(\lambda_i) = m_i \text{ for } i = 0,1,\ldots,d. \tag{5.24}$$

The local multiplicity concept facilitates the spectral analysis of a graph using a local approach. Here, it is used to rank the nodes based on their impact on the spectrum of the Laplacian. Suppose $\boldsymbol{e}_u$ and $\boldsymbol{e}_v$ are the u^{th} and v^{th} canonical bases of $\mathbb{R}^n$ related to nodes u and v, respectively. Also, consider the case where the angle between $\boldsymbol{e}_v$ and $\mathcal{E}_i$ is bigger than that of $\boldsymbol{e}_u$, i.e. $\beta_2 > \beta_1$, or in other words $E_i^{vv} < E_i^{uu}$ (see Fig. 5.2, assuming that angles are between 0 and $\pi/2$). Removing node u can be modelled as transferring from $\mathbb{R}^n$ space to $\mathbb{R}^{n-\{u\}}$. In large

networks, it is reasonable to assume that the removal of a node has a small effect on the eigenvectors of L (Restrepo et al. 2006). Therefore, considering the eigenvalue λ_i, one can argue that when node u is removed, the projection of $\boldsymbol{e}_u$ on $\mathcal{E}_i$ vanishes. In other words, for any $x \in \mathcal{E}_i$, $Lx = \lambda_i x$; therefore, since $E_i \boldsymbol{e}_u \in \mathcal{E}_i$, we have

$$< LE_i e_u, e_u > = \lambda_i < E_i e_u, e_u >= \lambda_i E_i^{uu} \qquad (5.25)$$

which clearly shows that the impact of the removal of $\boldsymbol{e}_u$ is proportional to E_i^{uu}. It means that node u with the maximum E_i^{uu} is the best candidate to be removed when maximum variation in λ_i is desired.

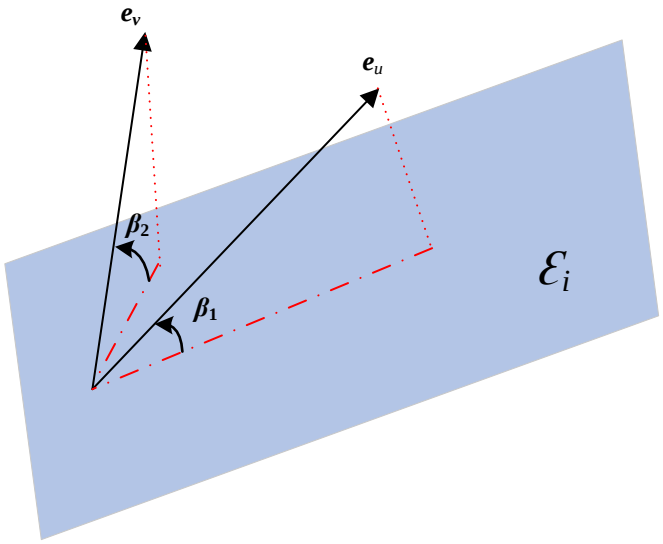

Fig. 5.2. Projection of different basis of $\mathbb{R}^n$ onto $\mathcal{E}_i$

For networks with a simple spectrum, i.e. no repeated eigenvalue for the Laplacian matrix, $\mathrm{Ker}(L - \lambda_i \mathrm{I}) = <\boldsymbol{x}_i>$, i.e. $\mathcal{E}_i$ is generated only by the eigenvector $\boldsymbol{x}_i$. This results in $E_i^{vv} = (\boldsymbol{x}_i^v)^2$ meaning that the v^{th} element of $\boldsymbol{x}_i^T \boldsymbol{x}_i$ reflects the impact of the removal of node v on λ_i. In chapter 3, we identified node v with the maximum $(\boldsymbol{x}_N^v)^2$, where $\boldsymbol{x}_N$ is associated with the largest eigenvalue, as the best node to be controlled for achieving synchrony over the widest range of coupling parameters. One can find that as a special case of our results in this chapter since results here are not restricted to any specific eigenvalue.

5.4 Discovering vital nodes in networks with different topologies

In this section, the local multiplicity technique is applied to synthetic networks with scale-free, Watts-Strogatz and random topologies to study the effect of node removal on their algebraic connectivity, spectral gap and the Laplacian energy.

5.4.1 Algebraic connectivity

Practically, modification of algebraic connectivity λ_2 by removing nodes is easier than by adding them (Watanabe and Masuda 2010). Therefore, targeted node removal for maximum increase in λ_2 is a matter of interest. We apply the maximum local multiplicity of λ_2 to identify the node whose removal causes the maximum influence on the algebraic connectivity. We first calculate $E_2 = U_2 U_2^T$ using eigen-decomposition of the Laplacian, and then rank nodes based on diagonal elements of E_2, i.e. E_2^{uu}. The performance is then compared with some heuristic methods including degree-, betweenness- and closeness-centrality. In order to study the precision of our proposed metric, the ground-truth is first obtained; the best node is obtained through examining all nodes and identifying the one which causes the maximum increase in the algebraic connectivity when removed. To this end, $\Delta\lambda_2$ is measured by removing nodes one-by-one. The nodes are ranked based on $\Delta\lambda_2$ with the node with the maximum $\Delta\lambda_2$ on the top. This is a time-consuming process and nearly impractical (if not impossible) in real large-scale networks and is only used to compare the performance of the proposed metric with the ground-truth. Then, $\Delta\lambda_2^v$ is calculated by removing the node v predicted by the proposed metric. This metric is computationally efficient and is calculated for all nodes using only a single eigen-decomposition of the Laplacian. Finally, precision of our metric is calculated as $P = \Delta\lambda_2^v / \max(\Delta\lambda_2)$. For example, 90% precision indicates that the effect of removal of the predicted node on the algebraic connectivity is 90% of the maximum possible influence. This precision is also calculated for heuristic centrality metrics. Although they are not directly related to the algebraic connectivity, they are still the first which come to mind when one is looking for an index to test the impact of node removal.

Figures 5.3 and 5.4 compare the precision of the proposed metric with that of heuristic centrality measures in terms of their correct prediction on λ_2 in networks with scale-free, Watts-Strogatz and Erdős-Rényi topologies. It is clearly shown that in scale-free networks (Fig. 5.3), using local multiplicity one can almost accurately identify the node with the maximum impact on λ_2 regardless of level of heterogeneity (see Fig. 5.3 (A) to (C)). None of the heuristic methods shows such a reliable performance. Betweenness and Closeness centrality measures have uniform performance when average degree of the network changes, while the former is more accurate. The precision of the degree centrality decreases almost linearly as average degree increases. Fig. 5.3 (D) shows how the ranking by the local multiplicity of λ_2 is correlated to the ground-truth. It shows the correlation between the ranking vector obtained by the proposed local multiplicity metric and the group-truth ranking vector. It is seen that regardless

of the level of heterogeneity, this correlation increases as average degree of the network increases.

The performance of the metric in Watts-Strogatz and Erdős-Rényi is again close to perfect, and much better than the heuristics (Fig. 5.4). We further consider Erdős-Rényi networks with different assortativity levels and study the performance (Fig. 5.5). By making the networks more assortative, the precision is slightly reduced, but it is still much higher than heuristics.

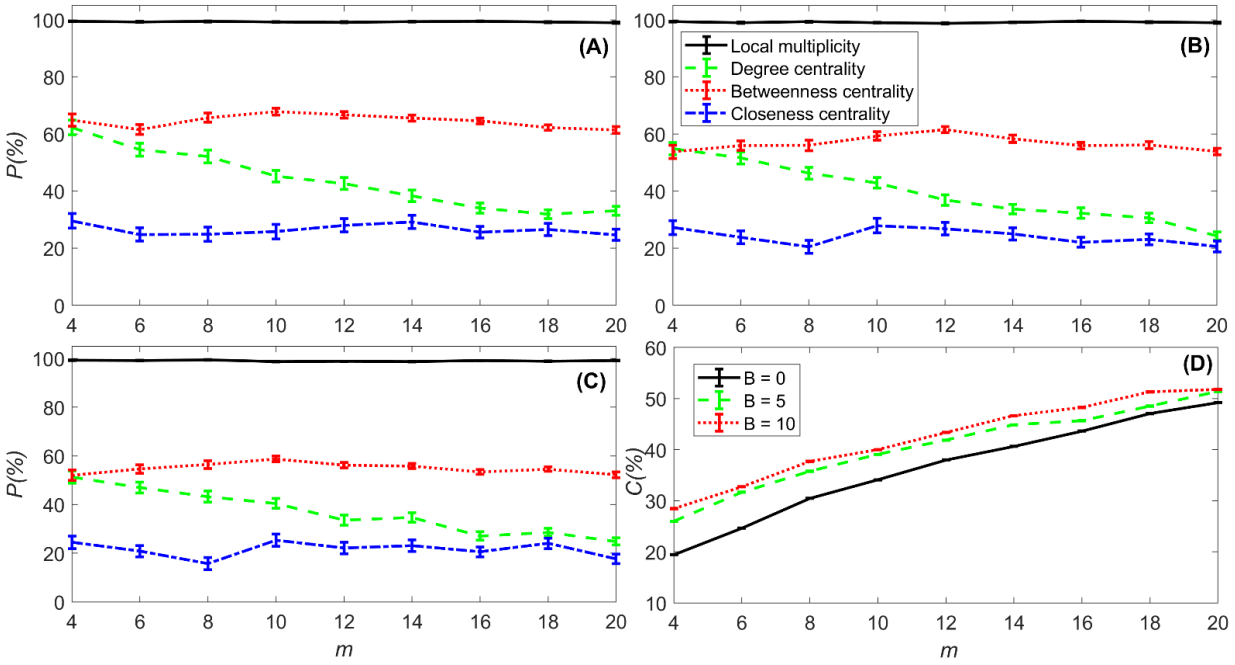

Fig. 5.3. The precision of the local multiplicity-based metric in scale-free networks.
The precision of the proposed metric (solid), maximum degree (dash-dot), maximum betweenness centrality (dot) and maximum closeness centrality (dashed) in finding the agent whose removal causes maximum impact on λ_2 in networks with $N = 200$ agents. Networks have scale-free structure with average degree m and (A) B=0, (B) B=5 and (C) B=10 (as B increases, the heterogeneity of the network decreases). Panel (D) shows correlation between Local multiplicity-based and the ground-truth rankings. Results are averaged over 100 realizations.

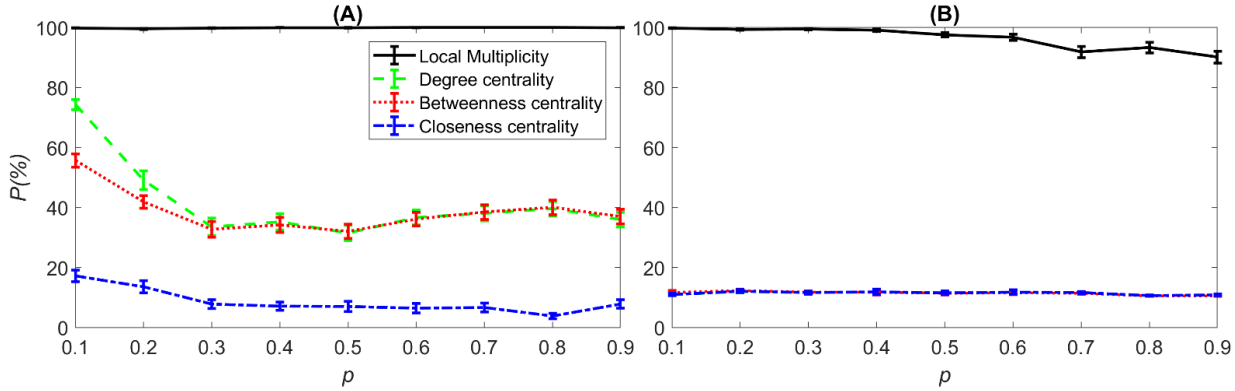

Fig. 5.4. The precision of the local multiplicity-based metric in small world and random networks. Networks have (A) Watts-Strogatz and (B) Erdős-Rényi topologies with $N = 200$ nodes. The precision of the proposed metric (solid), maximum degree (dash-dot), maximum betweenness centrality (dot) and maximum closeness centrality (dashed) in finding the node whose removal causes maximum impact on λ_2. Results are averaged over 100 realizations.

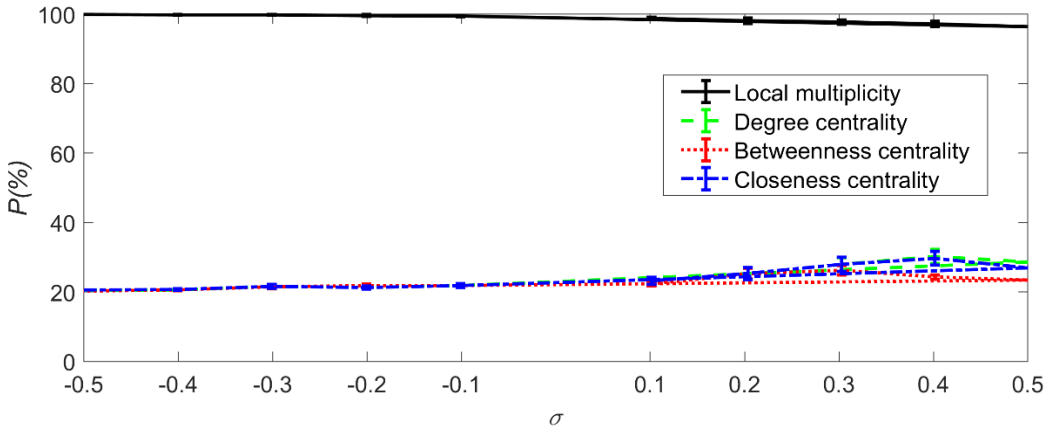

Fig. 5.5. The precision of the local multiplicity-based metric in random Erdős-Rényi networks with different assortativity σ.

5.4.2 Spectral gap

Here, finding the node whose removal causes the maximum reduction in the spectral gap is studied where precision of our proposed local multiplicity-based metric is compared with heuristic methods. The way of calculating precision P is exactly the same as what explained for algebraic connectivity. For example, P = 90% for a metric means that if the node suggested by that metric is removed, $\Delta\lambda_n$ will be 90% of maximum possible $\Delta\lambda_n$ that may cause by node removal in that network. Fig. 5.6 (A) and (B) depict this comparison in synthetic small-world networks with Watts-Strogatz and Erdős-Rényi topologies, respectively. Local multiplicity-based metric works more accurately than heuristics while its performance is more reliable in random Erdős-Rényi networks.

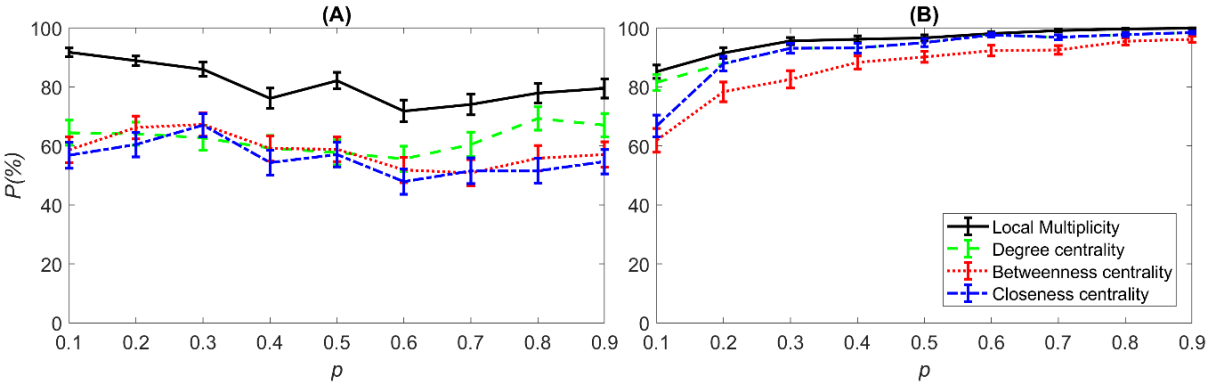

Fig. 5.6. Accuracy of the proposed metric in networks with Watts-Strogatz and Erdős-Rényi topologies. Accuracy of the proposed metric (solid), maximum degree (dash-dot), maximum betweenness centrality (dot) and maximum closeness centrality (dashed) in finding the agent whose removal causes a maximum reduction in spectral gap. Networks with N=200 nodes have A) Watts-Strogatz and B) Erdős-Rényi topologies. Results are averaged over 100 realizations.

5.4.3 Laplacian centrality

Laplacian centrality (Qi et al. 2012) of a node is defined based on Laplacian energy $E_L(G) = \Sigma_i\lambda_i^2$. Importance of a node in a network is quantified by the drop of the Laplacian energy

when that node is removed from the network. Therefore, to rank nodes based on their importance, the Laplacian energy should be calculated N times (N is the number of nodes), which needs eigen-decomposition of the Laplacian matrix to be repeated N times. Here, using the concept of local multiplicity, we define a new function $\bar{E}_L(G) = \Sigma_i E_i^{uu}$, where E_i^{uu} is the local multiplicity of the eigenvalue λ_i at node u. With this new function, one can rank nodes using a single eigen-decomposition of the Laplacian matrix. To study precision of $\bar{E}_L(G)$ in finding the most important node, we first calculate the drop in Laplacian energy $E_L(G)$ by removing nodes one-by-one and then rank nodes based on maximum energy drop, i.e. the node whose removal causes the maximum energy drop is ranked the highest. Then, we apply $\bar{E}_L(G)$ which can clearly rank nodes faster. Precision P of $\bar{E}_L(G)$ in identifying the node with the maximum energy drop is shown in the upper panels of columns (A) and (B) of Fig. 5.7 for scale-free, Watts-Strogatz and Erdős-Rényi networks, respectively. Correlation C between rankings given by $\bar{E}_L(G)$ and $E_L(G)$ are also shown in the bottom figures. Results show that in scale-free networks, $\bar{E}_L(G)$ can always predict the most important node with at least 60% precision regardless of heterogeneity level of the network. The ranking of nodes is at least 50% correlated to that of $E_L(G)$. Both these precision and correlation are higher than 70% in Watts-Strogatz and Erdős-Rényi networks (Fig. 5.7 (B)). This concludes that $\bar{E}_L(G)$ is accurate enough to rank nodes based on Laplacian centrality especially in random Erdős-Rényi networks.

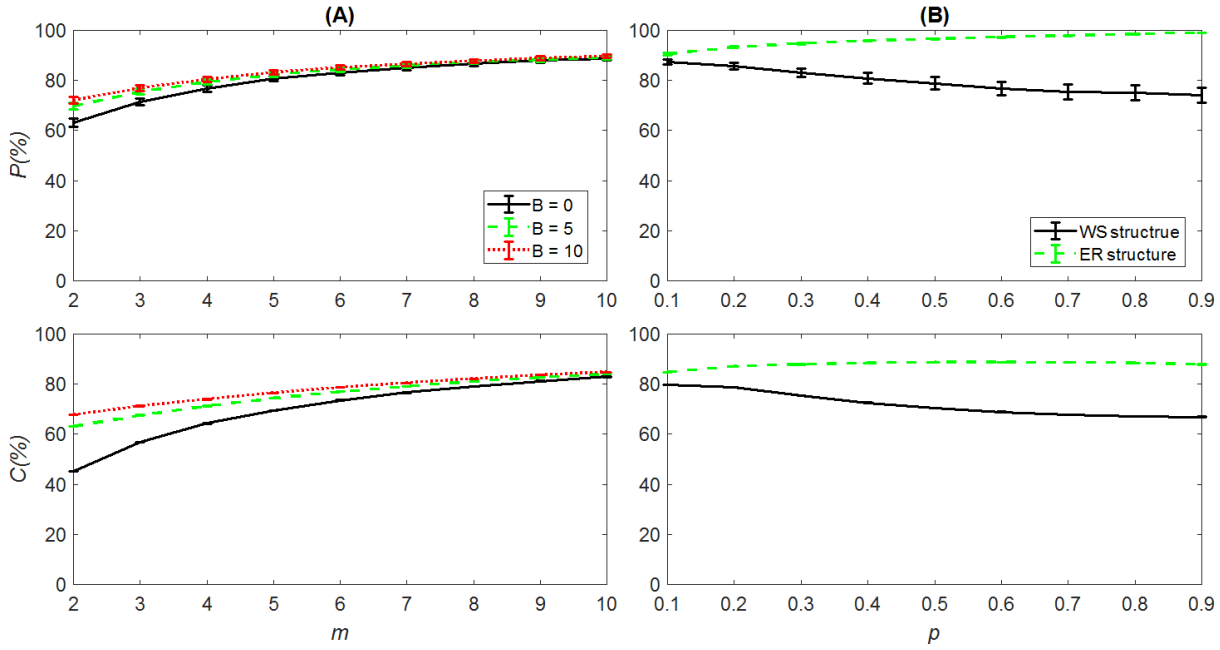

Fig. 5.7. The precision of the $\bar{E}_L(G)$ in predicting central nodes based on Laplacian centrality concept. Networks with N=200 nodes and scale-free topologies are reported in column (A) where those with Watts-Strogatz and Erdős-Rényi topologies are in column (B). In each column, the upper figure is precision of $\bar{E}_L(G)$ and the lower one is the correlation between rankings of $\bar{E}_L(G)$ and $E_L(G)$. Results are averaged over 100 realizations.

5.5 Summary

In this chapter, the problem of finding the node with the maximum influence on the spectrum of the Laplacian matrix was studied. An eigenvalue interlacing theorem was first derived to define upper and lower bounds on the variation of eigenvalues of the Laplacian matrix when one of its nodes is removed. Then, based on the concept of local multiplicities of the Laplacian matrix at each node, a metric was proposed to rank the nodes based on their effect on spectrum of the Laplacian matrix. It worked almost perfect in identifying the node whose removal results in the maximum change in the algebraic connectivity. The proposed metric for networks with Watts-Strogatz topologies could predict the most influential node almost perfectly. It also works accurate enough for scale-free and Erdős-Rényi networks and outperformed other heuristic methods. It also provides a reliable and easy to calculate approximation for the Laplacian energy of a network.

Chapter 6

Blocking failure propagation in complex networks: A formation control study

Formation control is one of the applications of synchronisation in the control community where the goal is typically to maintain the inter-agent distances constant over time. In this context, rigidity of the sensing network among agents is crucial to keep the formation stable using local data; hence, rigidity maintenance algorithms are of much interest. A rigidity maintenance algorithm should consider real-time constraints in applications, along with the limited range of sensing and limited power in each agent. In other words, it should work fast within a minimum sensing range for each agent to reduce its power consumption. Taking into account these constraints, a lattice-based distributed online reconfiguration approach is proposed in this thesis to maintain the rigidity of the sensing graph in a multi-agent formation control system. In this approach, the rigidity of the whole framework is related to the rigidity of all sub-frameworks, which are much smaller in scale and hence much easier to deal with. A lattice of configurations is applied to reconfigure the faulty sub-framework to a rigid configuration, which leads to the rigidity of the whole framework without any online adaptation

in control parameters. The proposed procedure satisfies real-time requirements and is applicable if at least one rigid configuration is available for each sub-framework, i.e. each agent and all its neighbours can always interact over at least one rigid sensing configuration. If such a configuration is not available for at least the agent affected by link breakage, formation goes to emergency, which may lead to loss of agent(s) if not well handled. This critical case is expected since constraint in power consumption may force the formation to move towards rigidity with a minimum number of sensing links, which is indeed not robust enough. This important situation has not been well studied to date. Motivated by the above observation, this thesis further proposes a technique to temporarily preserve the formation in the aforementioned emergency situation. A novel technique is introduced with a combination of sensing and communication networks, for which a sufficient condition for its desired performance is derived. Results of this chapter are submitted to IEEE Transactions on Control of Network Systems.

6.1 Rigidity Recovery Using Lattice of Configurations

Suppose that a formation in d-dimensional Euclidian space (d = 2 or 3) is modelled as a graph G while the i^{th} agent is associated with a point $\boldsymbol{p}_i \in \mathbb{R}^d$. The pair ($G$, $\boldsymbol{p}$), a combination of a graph of agents and the position vector $\boldsymbol{p} = [\boldsymbol{p}_1{}^T, \boldsymbol{p}_2{}^T, \ldots, \boldsymbol{p}_N{}^T]^T$, is referred to as a *framework*. This chapter focuses on frameworks in $\mathbb{R}^2$. For edge k, which relates node i to node j in G, a relative position is associated with $\boldsymbol{l}_k = \boldsymbol{p}_i - \boldsymbol{p}_j$, resulting in the relative position vector

$$Z = [\boldsymbol{l}_1^T \quad \boldsymbol{l}_2^T \quad \ldots \quad \boldsymbol{l}_M^T] = (H \otimes I_n)\boldsymbol{p}; \quad Z \in \mathbb{R}^{n \times m} \tag{6.1}$$

A framework (G, $\boldsymbol{p}$) is said to be *rigid* in $\mathbb{R}^d$ if there exists a neighbourhood U of $\boldsymbol{p}$ such that $r_G{}^{-1}(r_G(\boldsymbol{p})) \cap \mathrm{U} = r_K{}^{-1}(r_K(\boldsymbol{p})) \cap \mathrm{U}$, where $r_G(\boldsymbol{p})$ is a vector containing the lengths of all m edges of the graph, i.e. $r_G(\boldsymbol{p}) = [\ \ldots, \|\boldsymbol{p}_i - \boldsymbol{p}_j\|^2, \ldots]$ for all $(i,j) \in G$ and r_K is the same mapping considering a complete graph with the same nodes as G (Asimow and Roth 1979). The superscript "–1" means inverse mapping of a graph. In the following definitions, $\boldsymbol{p}^{\boldsymbol{0}}$ and $\boldsymbol{p}^{\boldsymbol{1}}$ are two different position vectors:

Definition 6.1: Frameworks (G, $\boldsymbol{p}^{\boldsymbol{0}}$) and ($G$, $\boldsymbol{p}^{\boldsymbol{1}}$) are *equivalent* if $\|\boldsymbol{p}_i{}^{\boldsymbol{0}} - \boldsymbol{p}_j{}^{\boldsymbol{0}}\| = \|\boldsymbol{p}_i{}^{\boldsymbol{1}} - \boldsymbol{p}_j{}^{\boldsymbol{1}}\|$ for all $(i,j) \in E$. They are *congruent* if $\|\boldsymbol{p}_i{}^{\boldsymbol{0}} - \boldsymbol{p}_j{}^{\boldsymbol{0}}\| = \|\boldsymbol{p}_i{}^{\boldsymbol{1}} - \boldsymbol{p}_j{}^{\boldsymbol{1}}\|$ for all $i,j \in V$.

Definition 6.2: A Framework (G, $\boldsymbol{p}^0$) is rigid if every framework (G, $\boldsymbol{p}^1$), which is equivalent to (G, $\boldsymbol{p}^0$) and satisfies $\|\boldsymbol{p}_j^0 - \boldsymbol{p}_j^1\| < \varepsilon$ for all $j \in V$ and for at least one $\varepsilon > 0$, is congruent to (G, $\boldsymbol{p}^0$).

For each node i, one can define a subgraph $G_i = (V_i, E_i)$, in which $V_i = \{i\} \cup N_i$ and $E_i = \{(k, j) \in E; k,j \in V_i\}$. In other words, each subgraph G_i is a cut of graph G which includes node i (i =1, 2, …, N) and all its neighbours. (G_i, $\boldsymbol{p}^0$) is called a sub-framework centred at node i. The following Lemmas help to define the proposed approach:

***Lemma* 6.1**: The framework (G, $\boldsymbol{p}^0$) is rigid if sub-frameworks (G_i, $\boldsymbol{p}^0$) are rigid for all $i \in \{1, 2, \ldots, N\}$.

Proof: To show the sufficiency, suppose that all (G_i, $\boldsymbol{p}^0$) are rigid. To prove that the framework (G, $\boldsymbol{p}^0$) will be rigid, it needs to show that if

$$\|\boldsymbol{p}_i^0 - \boldsymbol{p}_j^0\| = \|\boldsymbol{p}_i^1 - \boldsymbol{p}_j^1\|, \quad \forall (i,j) \in E$$
$$\exists \varepsilon > 0, \quad \|\boldsymbol{p}_j^0 - \boldsymbol{p}_j^1\| < \varepsilon \qquad (6.2)$$

then $\|\boldsymbol{p}_i^0 - \boldsymbol{p}_j^0\| = \|\boldsymbol{p}_i^1 - \boldsymbol{p}_j^1\|$ for all $i,j \in V$. For this purpose, denote the set of all sub-frameworks by $\mathcal{V} = \{(G_i, \boldsymbol{p}^0); i = 1, 2, \ldots, N\}$. Each $(i,j) \in E$ belongs to a subset of sub-frameworks $S \subset \mathcal{V}$, whose elements are all rigid. Thus, $\|\boldsymbol{p}_i^0 - \boldsymbol{p}_j^0\| = \|\boldsymbol{p}_i^1 - \boldsymbol{p}_j^1\|$ for all $i,j \in V_i$ when $(G_i, \boldsymbol{p}^0) \in S$. This is also valid for all $i \in \{1, 2, \ldots, N\}$ as condition (6.2) is satisfied for all edges in E, resulting in $\|\boldsymbol{p}_i^0 - \boldsymbol{p}_j^0\| = \|\boldsymbol{p}_i^1 - \boldsymbol{p}_j^1\|$ for all $i,j \in V$. This completes the proof. ■

Using *Lemma* 6.1, the rigidity property of the framework (G, $\boldsymbol{p}^0$) is decomposable to the rigidities of the sub-frameworks (G_i, $\boldsymbol{p}^0$), $i \in \{1, 2, \ldots, N\}$. This is useful to develop distributed algorithms for rigidity.

***Lemma* 6.2**: Suppose that the framework (G, $\boldsymbol{p}$) is rigid with $G = (V, E)$. The framework ($\bar{G}$, $\boldsymbol{p}$) with $\bar{G} = (V, E \cup P)$ is also rigid, where $P \subset (V \times V) \setminus E$.

Proof: It directly follows from the definitions, since adding an edge to a rigid framework will not affect its rigidity. ■

Definition 6.3: The sub-framework (G_i, $\boldsymbol{p}$) is defined as a cut of the framework (G, $\boldsymbol{p}$) centred at node i, in which $\|\boldsymbol{p}_i - \boldsymbol{p}_j\| < D^i_s$ where $D^i_s \in \mathbb{R}^+$ shows the sensing range. Inside this sub-framework, the *admissible sensing network* is defined as $\bar{G}_i = (\bar{V}_i, \bar{E}_i)$ where $\bar{V}_i$ includes all

agents in G_i and $\bar{E}_i$ is the set of all possible sensing links inside the cut, i.e. where agents are equipped with appropriate independent sensing channels. The *admissible communication network* is defined for each node i where the communication range is defined as $D^i_c \in \mathbb{R}^+$.

From this definition, one can conclude that each local framework (G_i, $\boldsymbol{p}$) can be implemented in $2^{\bar{E}i}$ configurations. On the other hand, *Lemma* 6.1 shows that one can preserve the rigidities of all sub-frameworks (G_i, $\boldsymbol{p}$), $i \in \{1, 2, \ldots, N\}$ to guarantee the rigidity of the whole framework (G, $\boldsymbol{p}$). It means that among the $2^{\bar{E}i}$ different configurations for sub-framework (G_i, $\boldsymbol{p}$), those rigid ones can contribute to the rigidity of the whole framework (G, $\boldsymbol{p}$).

Here, the objective is to develop an online distributed algorithm to locally preserve the rigidities of the sub-frameworks by adding a new link(s) in the case of failure in a sensing link. If failure in a sensing link of the rigid framework (G, $\boldsymbol{p}$) causes loss of rigidity, there exists at least one sub-framework (G_i, $\boldsymbol{p}$) whose rigidity is lost according to *Lemma* 6.1. The proposed approach is to reconfigure this sub-framework to make it rigid so as to recover the rigidity of (G, $\boldsymbol{p}$). This approach is developed here based on lattice of configurations and its monotonicity property.

6.1.1 Lattice of Configurations

This subsection explains how a lattice of configurations works. Recall that $\bar{E}_i$ represents the set of all admissible sensing links in sub-framework (G_i, $\boldsymbol{p}$). Denote by $|\bar{E}_i|$ the cardinality of $\bar{E}_i$.

Definition 6.4: Each subset $E^k_i \subset \bar{E}_i$; $k = 1, 2, \ldots, 2^{|\bar{E}i|}$, is a "configuration" for the framework (G_i, $\boldsymbol{p}$), where E^k_i is the k^{th} configuration. $\bar{E}_i$ is called the complete configuration.

Lattice is an abstract structure, which has been widely studied in the ordered sets theory in mathematics since the 1890s. It was originated from mathematical "Group Theory"; however, its properties (Davey and Priestley 2002) have been used in recent years to improve fault-tolerance performance in systems or to achieve fault-tolerant control (Staroswiecki and Amani 2015).

The notion of the lattice is introduced in the following: The set of all configurations of $\bar{E}_i$ is the power set of $\bar{E}_i$, i.e. $S(\bar{E}_i) = 2^{\bar{E}i}$. $S(\bar{E}_i)$ can be partially ordered by set-inclusion: for $A, B \in S(\bar{E}_i)$, $A < B$ if and only if $A \subset B$. In this sense, sets A and B are called comparable. The word

"partial" indicates that not all elements of $S(\bar{E}_i)$ are comparable. With this partial ordering, $S(\bar{E}_i)$ is a lattice, i.e. for each pair of elements of $S(\bar{E}_i)$ there exists a unique largest lower bound and a unique least upper bound, both in $S(\bar{E}_i)$. In other words, every pair $(E^k{}_i, E^p{}_i) \in S(\bar{E}_i) \times S(\bar{E}_i)$ has a minimal element, namely $\min(E^k{}_i, E^p{}_i) = E^k{}_i \cap E^p{}_i$, and a maximal element, namely $\max(E^k{}_i, E^p{}_i) = E^k{}_i \cup E^p{}_i$ (Davey and Priestley 2002).

A lattice is usually represented by an undirected graph. Each node represents a configuration, that is an element of $S(\bar{E}_i)$, and there exists a connection (link) between two nodes $E^k{}_i$ and $E^p{}_i$ if

$$\exists \Omega \in S(\bar{E}_i),\ \ E_i^k = E_i^p \cup \Omega \quad or \quad E_i^p = E_i^k \cup \Omega \tag{6.3}$$

The graph of a lattice is organised into levels. Each level contains configurations with the same number of elements. For example, in the lattice of configurations to be used below, configurations in each level have the same number of sensing links. The full configuration $\bar{E}_i$ is usually on the top of the lattice and the empty configuration Φ is on the bottom. Edges are available only between adjacent levels according to the partial ordering.

A lattice can be directed, either in top-down or in bottom-up orientation, considering cases in equation (6.3). In the latter case, moving from a node in an upper layer to a node in a lower layer means that a sensing link in the configuration is removed while adding a new link moves it up. It can be enriched by adding extra information to each node, such as the probability of the configuration to happen or the power consumption related to this configuration. The lattice to be used below will be enriched by adding the "rigidity" feature to each configuration.

Definition 6.5: The predecessors $P(E^k{}_i)$ of a configuration $E^k{}_i \subset S(\bar{E}_i)$ are denoted by

$$P\left(E_i^k\right) = \left\{\tilde{E} \in S(\bar{E}_i); E_i^k \subset \tilde{E}\right\} \tag{6.4}$$

Similarly, the set of successors $\Lambda(E^k{}_i)$ of a configuration $E^k{}_i \subset S(\bar{E}_i)$ is defined by

$$\Lambda\left(E_i^k\right) = \left\{\tilde{E} \in S(\bar{E}_i); \tilde{E} \subset E_i^k\right\} \tag{6.5}$$

Example: Suppose $\bar{E}_i = \{1, 2, 3\}$. Then, $S(\bar{E}_i) = \{\Phi, \{1\},\{2\},\{3\},\{1,2\},\{1,3\},\{2,3\},\{1,2,3\}\}$. The lattice shown in Fig. 6.1 represents $S(\bar{E}_i)$.

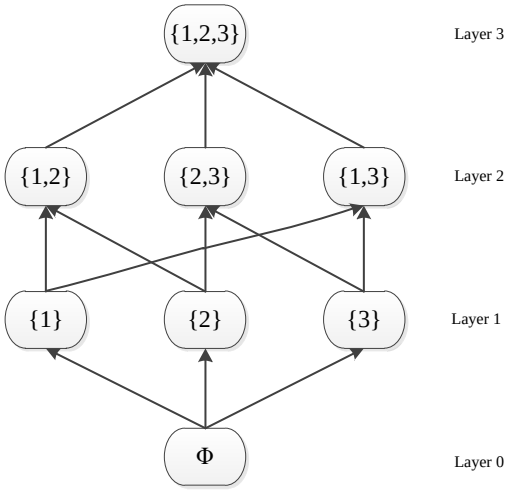

Fig. 6.1: Lattice graph of the example

In order to establish the lattice of configurations for a sub-framework, let's define the partial ordering ≥ for these configurations by

$$(G_i^k, \boldsymbol{p}) \geq (G_i^p, \boldsymbol{p}) \Leftrightarrow E_i^k \subset E_i^p \tag{6.6}$$

where $G^k{}_i = (\bar{V}_i, E^k{}_i)$ and $G^p{}_i = (\bar{V}_i, E^p{}_i)$ are two configurations. For each sub-framework $(G_i, \boldsymbol{p})$, $i \in \{1, 2, \ldots, N\}$, $2^{|\bar{E}i|}$ configurations can be constructed. The predecessors of a framework $(G^k{}_i, \boldsymbol{p})$ form the set

$$P\left(G_i^k, \boldsymbol{p}\right) = \left\{\left(G_i^p, \boldsymbol{p}\right); (G_i^k, \boldsymbol{p}) \geq (G_i^p, \boldsymbol{p})\right\} \tag{6.7}$$

while its successors from the set

$$\Lambda\left(G_i^k, \boldsymbol{p}\right) = \left\{\left(G_i^p, \boldsymbol{p}\right); (G_i^p, \boldsymbol{p}) \geq (G_i^k, \boldsymbol{p})\right\} \tag{6.8}$$

A framework is minimally rigid if it has no rigid successor. In order to construct the lattice of configurations for a sub-framework, all configurations should be arranged in different layers such that each framework is connected to all its successors while all its predecessors are connected to it. It is clear that if the framework is rigid for a specific configuration, it will be rigid for all its successors (*Lemma* 6.2).

In order to clarify the approach, the framework of Fig. 6.2 is considered, in which the circle $D_s{}^1$ shows the sensing range of agent 1. Suppose that the formation is well controlled using a distance-based control algorithm over the sensing network presented by solid links. As the sensing graph of this formation is rigid, the formation can be successfully achieved. Here, a lattice of configurations is developed for the sub-framework $(G_1, \boldsymbol{p})$; this process can also be repeated for all other agents. It is assumed in Fig. 6.2 that nodes 2, 3, 5 and 6 are in the sensing range of node 1. In the worst case of the analysis, consider that agent 1,2,3,5 and 6 are well

equipped to sense each other, i.e. all sensing links inside the sub-framework (G_1, $\boldsymbol{p}$) are admissible. This results in the maximum complexity in developing the lattice. Sensing graph of the sub-framework (G_1, $\boldsymbol{p}$) is $G_1 = (\bar{V}_1 \cup \{1\}, \bar{E}_1)$, $\bar{V}_1 = \{2,3,5,6\}$ and $\bar{E}_1 = \{a, b, c, d, e, f, g, h, r, m\}$. The number of all possible configurations is $2^{|\bar{E}1|} = 2^{10}$.

The lattice shown in Fig. 6.3 contains all possible sensing configurations of the framework (G_1, $\boldsymbol{p}$) in different layers. Layer i ($6 \leq i \leq 10$) contains all combinations of i links from $\bar{E}_i$. Due to space limitation, only a few configurations in layers 6, 7 and 8 are shown to explain the proposed algorithm. In addition, there is no need to consider layers 0 to layer 7 since all configurations in these layers are not rigid according to the following lemma.

***Lemma* 6.3** (Fidan et al. 2010): Any minimally d-rigid graph $G = (V, E)$ (d = 2 or 3) with at least d nodes satisfies $|E| = d|V| - d(d+1)/2$.

Dark nodes represent rigid configurations in this lattice. According to *Lemma* 6.3, configuration (G_1, $\boldsymbol{p}$) needs at least $2|\bar{V}_1 \cup \{1\}| - 3 = 7$ links to be rigid, which means that configurations in layer 6 and below are definitely non-rigid and there is no need for further investigation. On the other hand, as all configurations in layer 8 are all rigid, all configurations of layer 9 inherit the rigidity according to *Lemma* 6.2 and the properties of the lattice diagram. Therefore, there is no need to check the rigidity of configurations in layer 9. These techniques considerably reduce the computational cost in constructing the lattice, where only configurations in layers 7 and 8 need to be studied for rigidity, while the rigidity status of other configurations is clear.

After the lattice is established offline and programmed in a node (here, node 1), it can be used to preserve the rigidity of the sub-framework (G_1, $\boldsymbol{p}$) in the following manner. As shown in Fig. 6.2, the implemented configuration of this sub-framework is $E_1^1 = \{a, b, c, d, e, g, h\}$, which is marked by "*" in layer 7 of Fig. 6.3. It is dark, meaning that the sub-framework is rigid with this configuration.

Suppose that for some reason such as the line-of-sight constraint, sensing through link h becomes impossible. This link break reduces $|E_1^1|$ by one and the sensing configuration goes to its successor configuration in layer 6 of the lattice, which is marked by "*1". The lattice shows that the recent configuration is not rigid, thus node 1 needs to activate new link(s) to recover the rigidity. According to the lattice, the configuration "*1" has two predecessors (other than E_1^1) in layer 7, which are: $\{a, b, c, d, e, g, r\}$ and $\{a, b, c, d, e, g, f\}$. The lattice shows that

the first one is rigid and the second one is not. Therefore, node 1 selects the first one in order to preserve the rigidity, i.e. it activates the sensing link *r* instead of the failed link *h* in order to recover the rigidity of the affected sub-framework and, consequently, the whole framework. In this way, node 1 can easily switch the local configuration to a rigid one thereby recovering the rigidity of the framework. As shown, once the lattice is established and programmed in the agents, the process of finding the rigid configuration to which the sub-framework should be switched is fast, which satisfies the real-time requirement.

As another example, suppose that the rigid sub-framework (G_1, $\boldsymbol{p}$) has the configuration marked by ▲ in the lattice of Fig. 6.3. A link break in *f* forces the sub-framework to configuration {*a, b, c, d, e, g, r*}, which is marked by "*2" in the lower layer. The new configuration is still rigid (it is dark in the lattice), meaning that failure in *f* has not affected the rigidity of the sub-framework, and consequently, the whole framework according to *Lemma* 6.1. Therefore, there is no need to add any new sensing link. In this way, the configuration of the faulty sub-framework can be switched easily and fast in order to achieve the best (in the sense of adding the minimum number of links) new configuration which preserves the rigidity. One lattice per agent should be developed and pre-programmed based on its sensing range and potential neighbours.

The proposed algorithm has a number of advantages as follows. The algorithm is implemented in a distributed manner and is independent of the control law. The lattice can be developed offline and pre-programmed in each agent resulting in huge reduction in online computational cost. Nodes in the lattice can be also weighted based on practical constraints such as the power required for measuring; the farther the node, the more power required for sensing. The decision of each node thus goes towards options with more constraint satisfaction, if available. The approach has some drawbacks, however. Although the lattice (e.g. Fig. 6.3) can be built for each individual node in the framework, the proposed lattice does not enable a fully decentralized recovery approach for rigidity maintenance. Each node needs information about the links within its neighbours. The algorithm may also lead to a conservative configuration as Lemma 6.1 only offers a sufficient condition.

6.1.2 Complexity analysis

One may feel that establishing such a lattice for all sub-frameworks (G_i, $\boldsymbol{p}$), $i = 1, 2, \ldots, N$, is a complex and time- consuming process. Actually, it is not. The lattice for each node can be issued offline and the only online task is to update the current configuration of the subgraph

related to it, i.e. the location of the sign ▲ in Fig. 6.3, which is manageable in each individual node. Before proceeding, a complexity analysis is provided.

***Lemma* 6.4** (Nourine and Raynaud 1999): Let X be a set and F be a set of subsets of X. The algorithm of developing the lattice has $O((|X| + 1)|F|)$ time complexity.

The number of elements of $\bar{E}_i$, which is the set of all admissible sensing links for the framework $(G_i, \boldsymbol{p})$, is at most $d_i(d_i+1)/2$ where d_i is the degree of node i. From *Lemma* 6.3, a rigid sub-framework must have at least $2d_i - 1$ links. Therefore, one should examine all k_i combinations ($2d_i - 1 \leq k_i < d_i(d_i+1)/2$) of elements of $\bar{E}_i$ for rigidity. By using *Lemma* 7.4 and considering $X = \bar{E}_i$ and F as the set of k_i combinations of elements of $\bar{E}_i$, the time complexity of developing lattice of configurations for all nodes becomes $O\left(\sum_{i=1}^{N}\sum_{k_i=2di-1}^{n_i}(n_i+1)\binom{n_i}{k_i}\right)$.

where N is the number of agents. Calculating k-combinations of a set of n elements, i.e. $\binom{n}{k} = \frac{n!}{k!(n-k)!}$ has a complexity of order $O(n^k)$ if $k \leq n\text{-}k$ and of order $O(n^{n-k})$ otherwise. Therefore, this calculation has $O(n^{\min\{k,n-k\}})$ time complexity. The subset of links E_i for the sub-framework (G_i, p) has $n_i = \binom{d_i+1}{2} = \frac{d_i(d_i+1)}{2}$ elements, each of which is a potential link between two nodes. In view of *Lemma* 7.3, the rigidity of configurations generated by the set of k_i links of $\bar{E}_i$ should be studied where $(2d_i - 1) \leq k_i < d_i(d_i+1)/2$. Note that one needs at least $2d_i - 1$ links for the two-dimensional sub-framework (G_i, p) to be rigid. As $n_i = d_i(d_i+1)/2$, the computational complexity depends more on the degree distribution of the network rather than the number of agents. From network theory, it is known that even if the number of nodes increases gradually, the power-law distribution (in scale-free networks) or Poisson distribution (in random small-world networks) limits the largest degree of the network.

The lattice of configurations method can successfully recover the rigidity of a faulty framework if at least one rigid configuration is available to cover the affected sub-framework. When such a configuration is not available, the whole framework will not be recoverable. This case, which is not usually considered in the literature, may lead to loss of node(s), and thus can be considered as an emergency for the framework. In the next section, a technique is developed to recover the framework in such an emergency state through the utilization of the communication network.

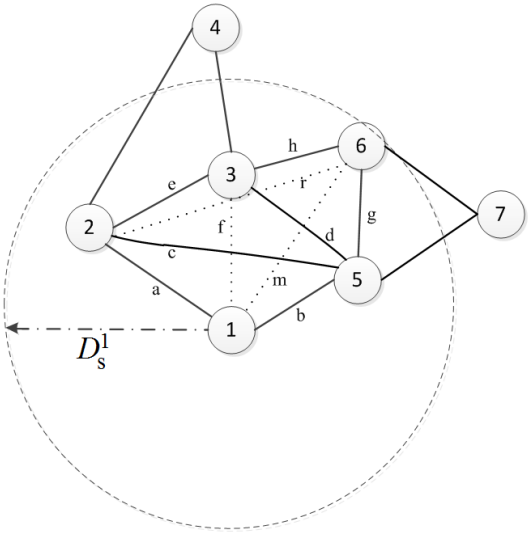

Fig. 6.2. A rigid formation of agents. Solid and dotted lines are active and potential sensing links among agents, respectively.

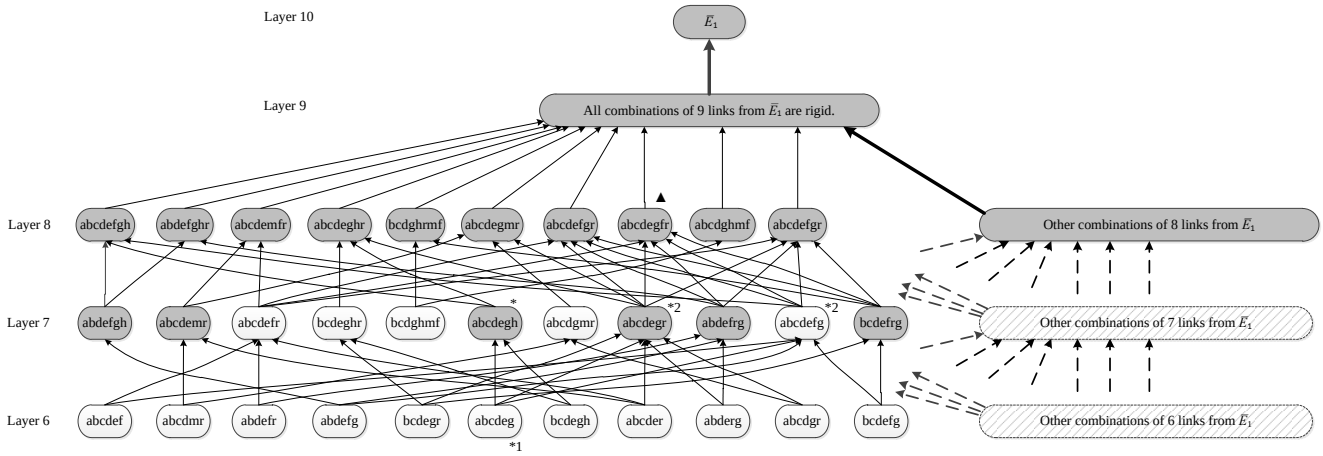

Fig. 6.3: Lattice of configurations for sub-graph (G_1, $\boldsymbol{p}$) in Fig. 6.2.

6.2 Formation Recovery in Emergency

Here, the rigidity maintenance problem in the emergency case is studied. This is the case when a link failure causes loss of rigidity that is not recoverable using the above lattice approach due to the unavailability of local rigid configurations. A technique is proposed that uses a combination of sensing and communication networks. In doing so, the locally non-rigid framework becomes "virtually rigid" by using the communication network.

Suppose that in a formation of N agents in the d-dimensional space, every agent is modelled as a single-integrator:

$$\dot{\boldsymbol{p}}_i = \boldsymbol{u}_i; \quad i = 1,2,\dots,N, \tag{6.9}$$

where $\boldsymbol{p}_i \in \mathbb{R}^d$ and $\boldsymbol{u}_i \in \mathbb{R}^d$ are the position and control signals for agent i, respectively. The objective of formation control is to maintain all inter-agent distances constant over time, i.e.

$$\left\|\boldsymbol{p}_i - \boldsymbol{p}_j\right\| = \left\|\boldsymbol{p}_i^* - \boldsymbol{p}_j^*\right\|; \quad \forall i,j \in \{1,2,\dots,N\}, \tag{6.10}$$

where $\boldsymbol{p}^* = [(\boldsymbol{p}_1{}^*)^T, (\boldsymbol{p}_2{}^*)^T, \dots, (\boldsymbol{p}_N{}^*)^T]^T$ is the nominal position vector of agents and $\|\boldsymbol{p}_i{}^* - \boldsymbol{p}_j{}^*\|$ represents the desired distance between agents i and j, $\forall i,j \in \{1,2,\dots,N\}$. Asymptotic stability of such a formation can be obtained using the following gradient-based distributed controller (Krick et al. 2009):

$$\boldsymbol{u}_i = \sum_{\boldsymbol{l}_j \in E_i} e_j \boldsymbol{l}_j; \quad i = 1,2,\dots,N \tag{6.11}$$

where E_i is the set of sensing links adjacent to node i and $e_j = \|\boldsymbol{l}_j\|^2 - \|\boldsymbol{l}_j^*\|^2$. Let's denote the sensing network among agents by G. Controller (6.11) for each agent is independent of any global coordinates; that is, each agent can use its own coordinate system to measure relative positions and to implement the controller (Krick et al. 2009). Applying it to the system (6.9) results in

$$\dot{\boldsymbol{p}}(t) = -\mathcal{R}^T \boldsymbol{e}(t), \tag{6.12}$$

in the global coordinate with $\boldsymbol{e} = [e_1, e_2, \dots, e_M]^T$, $\mathcal{R}$ is the rigidity matrix of the framework (G, $\boldsymbol{p}$), which is defined as the Jacobian matrix $\mathcal{R}(\boldsymbol{p}) = \partial r_G(\boldsymbol{p})/\partial \boldsymbol{p}$ and can be written as

$$\boldsymbol{\mathcal{R}}_{M\times nN}(\boldsymbol{p}) = diag([\boldsymbol{l}_1, \boldsymbol{l}_2, \dots, \boldsymbol{l}_M])^T (H \otimes I_n) \tag{6.13}$$

Here '*diag*([.])' represents a diagonal matrix with elements defined in the vector [.]. Consequently, since $Z(t) = [\boldsymbol{l}_1{}^T, \boldsymbol{l}_2{}^T, \dots, \boldsymbol{l}_M{}^T]^T = (H \otimes I_n)\boldsymbol{p}(t)$, the dynamical equation of the relative position vector $Z(t)$ is

$$\dot{Z}(t) = (H \otimes I_n)\dot{\boldsymbol{p}}(t) = -(H \otimes I_n)(H^T \otimes I_n) diag([\boldsymbol{l}_1, \boldsymbol{l}_2, \dots, \boldsymbol{l}_M])\boldsymbol{e}(t) \tag{6.14}$$

Defining $\Gamma(\boldsymbol{e}) = diag([\boldsymbol{e}_1, \boldsymbol{e}_2, \dots, \boldsymbol{e}_M])$, equation (6.14) can be written as

$$\dot{Z}(t) = -(H \otimes I_n)(H^T \otimes I_n)\Gamma(\boldsymbol{e})Z(t) \tag{6.15}$$

The formation of agents defined in (6.9) and controlled by the gradient-based controller (6.11) is locally stable (Krick et al. 2009).

Now, suppose that a link break happens to the sub-framework (G_i, $\boldsymbol{p}$), say at the link $\boldsymbol{l}_\alpha$, causing loss of rigidity of the whole framework. Also, suppose that there is no rigid configuration available for the sub-framework (G_i, $\boldsymbol{p}$) after this failure. As a result, the controller of node i cannot satisfy the desired performance due to the lack of information, therefore the formation is at risk of loss of node(s). The idea is to compensate for the lack of data using the communication network. To this end, the following procedure, called "indirect

position sensing", is proposed (see Fig. 6.4). The procedure is tailored for node 1, but it is similar for all other nodes:

1) Any break in the links adjacent to node 1 in the sub-framework (G_i, $\boldsymbol{p}$) should be detectable by this node. In this example, suppose that a link break between agents 1 and 4 is detected.

2) By investigating the lattice, it is concluded that node 1 cannot establish any locally rigid configuration.

3) Node 1 thereafter initiates a search algorithm over the communication network among its adjacent nodes, so as to find the shortest path towards node 4, which had link break. It would be found as $1 \rightarrow 3 \rightarrow 4$ (see Fig. 6.4).

4) Node 1 initiates a common local coordinate system for those nodes in the shortest path. This should be done through the communication network and results in the nodes in the shortest path to have a common coordinate temporarily.

5) All nodes in the shortest path can measure the positions of their successors; hence node 1 calculates the vector $\boldsymbol{l}_\alpha$ by reading these position vectors through the shortest path.

As a result, $\boldsymbol{l}_\alpha$ can be calculated by node 1 using "indirect position sensing", and the lack of data for local control at this node can be compensated. The proposed approach is simple and technically implementable; however, there are two major constraints. First, a local common coordinate system for nodes in the shortest path should be implemented. It needs another algorithm by each node, resulting in further communication load. A simple algorithm to achieve such oriented coordinates is described in *Remark* 6.1. Second, $\boldsymbol{l}_\alpha$ calculated through such a successive measuring approach is subject to the delay induced by the communication network and calculating process. This delay, as inserted into the control system, may destabilise the formation.

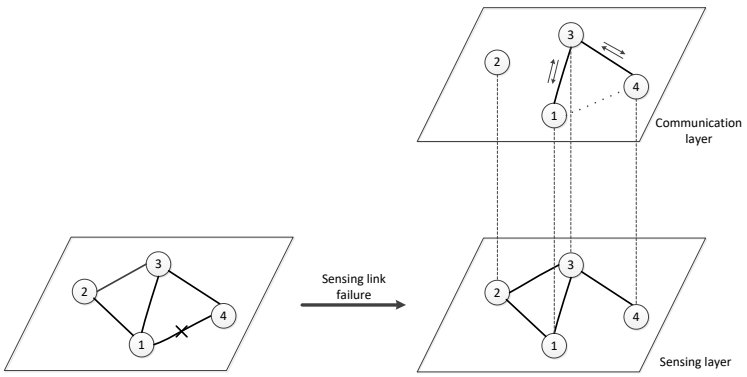

Fig. 6.4. Indirect position sensing

To obtain the maximum communication delay that can be tolerated by the control system with equation (6.15), suppose that the controller at node *i*, after indirect position sensing, becomes

$$\boldsymbol{u}_i(t) = -\sum_{\boldsymbol{l}_j \in E_i^h} e_j \boldsymbol{l}_j - e_\alpha \boldsymbol{l}_\alpha(t - h_\alpha) \tag{6.16}$$

where $E_i^h = E_i \setminus \{\boldsymbol{l}_\alpha\}$ is the set of sensing links adjacent to node *i* after the break, i.e. the links which are still working, and $e_\alpha(t) = \|\boldsymbol{l}^f_\alpha(t - h_\alpha)\|^2 - \|\boldsymbol{l}_\alpha^*\|^2$. In this case, Equation (6.15) becomes

$$\begin{aligned}\dot{Z}_R(t) = &-(H \otimes I_n)(H_+^T \otimes I_n)\Gamma(\boldsymbol{e})Z_R(t) \\ &- (H \otimes I_n)(H_-^T \otimes I_n)\Gamma(\boldsymbol{e})Z_R(t - h_\alpha)\end{aligned} \tag{6.17}$$

Suppose that the link break splits the configuration $G_i = (V_i, E_i)$ into $(V_i, E^h{}_i)$ and $(V_i, \{\boldsymbol{l}_\alpha\})$ with incidence matrices $\boldsymbol{H}_+$ and $\boldsymbol{H}_-$, respectively, and $\boldsymbol{H} = \boldsymbol{H}_- + \boldsymbol{H}_+$, where $\boldsymbol{H}$ is the incidence matrix of G_i. Then, a condition will be derived, under which equation (6.17) remains stable.

The failure-free formation is supposed to be locally stable, i.e. any local deformation around the nominal formation is compensated by the control system. It is also proved in (Cortés 2009) that if the node affected by link failure uses the last recorded information about the relative position of its neighbour, the formation still remains around the target. Thus, one can linearize equation (6.17) around the nominal relative position vector $Z^* = [\boldsymbol{l}_1{}^{*T}, \boldsymbol{l}_2{}^{*T}, \ldots, \boldsymbol{l}_M{}^{*T}]$ for stability analysis after link break, thereby obtaining the time-delay dynamical system, as

$$\begin{aligned}\frac{d(\Delta Z_R)}{dt} = &-(H \otimes I_n)(H_+^T \otimes I_n)\Lambda(Z^*)\Delta Z_R \\ &-(H \otimes I_n)(H_-^T \otimes I_n)\Lambda(Z^*)\Delta Z_R(t - h_\alpha)\end{aligned} \tag{6.18}$$

where

$$\begin{aligned}&\Delta Z_R(t) = Z_R(t) - Z^*, \\ &\Lambda(Z^*) = diag([\boldsymbol{l}_1^* \quad \boldsymbol{l}_2^* \quad \ldots \quad \boldsymbol{l}_M^*])\end{aligned} \tag{6.19}$$

which may be written as

$$\frac{d(\Delta Z_R)}{dt} = A\Delta Z_R + A_1 \Delta Z_R(t - h_\alpha) \tag{6.20}$$

$$\mathrm{A} = -(\mathrm{H} \otimes \mathrm{I_n})(\mathrm{H_+^T} \otimes \mathrm{I_n})\Lambda(\mathrm{Z}^*)$$

$$\mathrm{A_1} = -(\mathrm{H} \otimes \mathrm{I_n})(\mathrm{H_-^T} \otimes \mathrm{I_n})\Lambda(\mathrm{Z}^*)$$

Consequently, the following dynamical equation, derived from equations (6.15) and (6.20), characterizes the error vector $\varepsilon(t) = \Delta Z(t) - \Delta Z_R(t)$:

$$\dot{\varepsilon}(t) = -(HH_+^T \otimes I_n)\Lambda(Z^*)\varepsilon(t)$$
$$-(HH_-^T \otimes I_n)\Lambda(Z^*)[\Delta Z(t) - \Delta Z_R(t - h_\alpha)] \quad (6.21)$$

which can be written as

$$\dot{\varepsilon}(t) = (A + A_1)\varepsilon(t) + A_1\Delta Z_R(t) - A_1\Delta Z_R(t - h_\alpha) \quad (6.22)$$

Defining a new state vector, $x(t) = [e^T(t), \Delta Z_R{}^T(t)]^T$, equations (6.15) and (6.22) can be augmented to the following dynamical equation:

$$\dot{x}(t) = \begin{bmatrix} A + A_1 & A_1 \\ 0 & A \end{bmatrix} x(t) + \begin{bmatrix} 0 & -A_1 \\ 0 & A_1 \end{bmatrix} x(t - h_\alpha) \quad (6.23)$$

The characteristic equation of this system is

$$\Delta(s) = det\left(sI - \begin{bmatrix} A + A_1 & A_1 \\ 0 & A \end{bmatrix} - \begin{bmatrix} 0 & -A_1 \\ 0 & A_1 \end{bmatrix} e^{-h_\alpha s}\right)$$
$$= \det(sI - A - A_1) \cdot \det(sI - A - A_1 e^{-h_\alpha s}) \quad (6.24)$$

Therefore, the affected formation remains stable under indirect position sensing if all roots of equation (6.24) have negative real parts. The first term in this equation is related to the system before the link break, which was supposed to be stable originally. The next theorem establishes the condition under which all zeros of the second term, i.e. $\det(sI - A - A_1 e^{-h_\alpha s}) = 0$, have negative real parts. To prove the theorem, the following lemma is first needed.

***Lemma* 6.5**: Suppose that $H_{M\times N}$ is the incidence matrix of an arbitrary edge orientation in an undirected graph $G = (V, E)$ with the set of n nodes V and set of m edges E, $m > n$. The eigenvalues of HH^T are the same as the eigenvalues of the Laplacian matrix of G, while the eigenvalue $\lambda = 0$ of HH^T has a multiplicity of $m - n + 1$.

Proof: Suppose that $\boldsymbol{v}_i$ is an eigenvector of the Laplacian matrix L associated with the eigenvalue λ_i:

$$L\boldsymbol{v}_i = \lambda_i \boldsymbol{v}_i; \quad i = 1,2, \dots, n$$
$$\rightarrow H^T H\boldsymbol{v}_i = \lambda_i \boldsymbol{v}_i; \quad i = 1,2, \dots, n$$
$$\rightarrow HH^T(H\boldsymbol{v}_i) = \lambda_i(H\boldsymbol{v}_i); \quad i = 1,2, \dots, n$$

It follows that the n eigenvalues of HH^T are exactly the same eigenvalues as the Laplacian matrix. From linear algebra, one has rank (L) = rank (H^TH) = rank (HH^T). Therefore, the other $m - n$ eigenvalues of HH^T are zero. This completes the proof. ■

Theorem 6.1: Suppose that a formation of N agents with equations of motion (6.9) is achieved by the gradient-based distributed control law (6.11) over a minimally rigid sensing graph. The formation remains locally stable in the case of a break to the sensing link $\boldsymbol{l}_\alpha$ if the delay h_α in the indirect position calculation satisfies

$$h_\alpha < \frac{\pi}{2\lambda_m \|\boldsymbol{l}_\alpha^*\|^2} \tag{6.25}$$

where $\|\boldsymbol{l}^*_\alpha\|$ is the desired length of $\boldsymbol{l}_\alpha$ and λ_m is the largest eigenvalue of the Laplacian matrix of the sensing graph.

Proof: Without loss of generality, suppose that the broken link $\boldsymbol{l}_\alpha$ corresponds to the last row of the incidence matrix H. To study the positions of roots of the second term of (6.24), consider a system with the following transfer function:

$$\begin{aligned} G_h(s) &= sI - A - A_1 e^{-h_\alpha s} \\ &= sI + (HH_+^T \otimes I_n)\Lambda(Z^*) + (HH_-^T \otimes I_n)\Lambda(Z^*)e^{-h_\alpha s} \end{aligned} \tag{6.26}$$

All zeros of $G_h(s)$ should have negative real parts in order to guarantee stability. It can be simplified by some algebraic manipulations as follows:

$$\begin{aligned} G_h(s) &= sI + (HH_+^T \otimes I_n)\Lambda(Z^*) + (HH_-^T \otimes I_n)\Lambda(Z^*)e^{-h_\alpha s} \\ &= sI + (H \otimes I_n)[(H_+^T \otimes I_n) + (H_-^T \otimes I_n)e^{-h_\alpha s}]\Lambda(Z^*) \\ &= sI + (H \otimes I_n)(H^T I_h \otimes I_n)\Lambda(Z^*) \\ &= sI + (HH^T I_h \otimes I_n)\Lambda(Z^*) \end{aligned} \tag{6.27}$$

where

$$I_h = \begin{bmatrix} I_{(M-1)\times(M-1)} & 0 \\ 0 & e^{-h_\alpha s} \end{bmatrix}$$

For simplicity of formulation, consider the roots of the characteristic function $G'_h(s) = sI + (HH^TI_h)\Lambda(Z^*)$. By *Lemma* 6.5, eigenvalues of HH^T are the same as those of the Laplacian matrix L with different multiplicities of $\lambda = 0$. Here, without loss of generality, suppose that eigenvalues of HH^T are $0 = \lambda_1 < \lambda_2 \leq \ldots \leq \lambda_M$ when the sensing network G is connected. Let

ω_1^T be the left eigenvector of HH^T associated with $\lambda_1 = 0$. $s = 0$ is a transmission zero of $G'_h(s)$ in the direction of ω_1^T because

$$\omega_1^T G'_h(0) = \omega_1^T (HH^T I_h)\Lambda(Z^*) = \lambda_1 \omega_1^T I_h \Lambda(Z^*) = 0 \tag{6.28}$$

However, $G'_h(s)$ goes back to the fault-free setting when $s = 0$, which was assumed to be locally stable; thus, $s = 0$ is a stable zero for $G'_h(s)$. Next, we show that all other zeros of $G'_h(s)$ are located on the left-hand side of the complex plane. Let (s, ω_k^T) be a transmission zero of $G'_h(s)$. Then,

$$\begin{aligned}
&\omega_k^T G'_h(s) = 0 \rightarrow \omega_k^T s + \omega_k^T (HH^T) I_h \Lambda(Z^*) = 0 \\
&\rightarrow \omega_k^T s + \lambda_k \omega_k^T I_h \Lambda(Z^*) = 0 \\
&\rightarrow \omega_k^T \big(sI + \lambda_k I_h \Lambda(Z^*)\big) = 0
\end{aligned} \tag{6.29}$$

Since $\omega_k^T \neq 0$, one has $sI + \lambda_k I_h \Lambda(Z^*) = 0$, which yields negative roots $s = -\lambda_k \|\boldsymbol{l}^*_k\|^2 < 0$ for all $k \neq \alpha$; but for $k = \alpha$,

$$s + \lambda_k \|\boldsymbol{l}^*_\alpha\|^2 e^{-h_\alpha s} = 0 \tag{6.30}$$

An upper bound for the time delay h_α can be estimated by using the technique proposed in (Olfati-Saber and Murray 2004). Suppose that $\bar{h}_\alpha$ is the smallest value of the delay that puts the zeros of (6.30) on the imaginary axis. Thus,

$$\begin{aligned}
&j\omega + \lambda_k \|\boldsymbol{l}^*_\alpha\|^2 e^{-j\omega \bar{h}_\alpha} = 0 \\
&-j\omega + \lambda_k \|\boldsymbol{l}^*_\alpha\|^2 e^{j\omega \bar{h}_\alpha} = 0
\end{aligned} \tag{6.31}$$

After some algebraic manipulations, one obtains

$$(\omega - \lambda_k \|\boldsymbol{l}^*_\alpha\|^2)^2 + 2\lambda_k \|\boldsymbol{l}^*_\alpha\|^2 \big(1 - \sin(\omega \bar{h}_\alpha)\big) = 0 \tag{6.32}$$

This equation holds when

$$\omega = \lambda_k \|\boldsymbol{l}^*_\alpha\|^2, \;\; \sin(\omega \bar{h}_\alpha) = 1 \tag{6.33}$$

The minimum value of $\omega \bar{h}_\alpha$ that satisfies the second condition is $\pi/2$. In addition, (6.33) should be satisfied for all $k = 1, 2, \ldots, m$. Therefore, the stability condition becomes

$$\omega \bar{h}_\alpha < \frac{\pi}{2} \longrightarrow \bar{h}_\alpha < \frac{\pi}{2\lambda_m \|\boldsymbol{l}^*_\alpha\|^2} \tag{6.34}$$

Consequently, the formation subjected to the loss of rigidity due to the link break remains locally stable if condition (6.34) is satisfied. This completes the proof. ■

***Remark* 4.1**: As mentioned earlier, a common orientation of local reference frameworks should be executed through the shortest path between nodes affected by the link break. Here, a simple procedure based on the distributed implementation of the flooding algorithm proposed in (Peleg 2000) is described. Suppose G is a connected undirected graph in $\mathbb{R}^2$. A sensing link failure happens between nodes N_1 and N_2. N_1 applies an indirect position sensing procedure and find the shortest path towards N_2. In order to orient reference frameworks of all agents through the path, node N_1 moves a unit in the positive direction of its x-axis. All its neighbours, including the ones in the path, measure the relative displacement in their local frameworks and rotate them to align with the direction of displacement. This process is repeated until the frameworks of all agents in the path are aligned.

In summary, the formation can still be preserved even if there is no locally rigid sub-framework available after failure in a sensing link if condition (6.25) is satisfied. Clearly, nothing can be said about the stability of the formation if this sufficient condition is violated. The right-hand side of condition (6.25) depends on the desired distance between agents affected by link failure (which is usually constant) as well as the largest eigenvalue λ_M of the Laplacian matrix of the graph representing the sensing network. If the sensing graph is static, the right-hand side of condition (6.25) is fixed and can be calculated offline. Therefore, the condition can be easily checked. However, if it is not static, each node should be able to at least estimate λ_M individually. This requires a distributed algorithm, like the one developed in (L. Kempton et al. 2016).

Finally, checking the condition (6.25) needs the delay in indirect position sensing to be calculated. This implicitly means that the agents should be time-synchronised.

6.3 Simulation Results

A formation of four agents with single-integrator motion equation (6.9) is illustrated in Fig. 6.4. This formation is supposed to be well controlled using the gradient-based control law (6.11) and the desired performance, i.e. $\|\boldsymbol{l}^*_{12}\| = \|\boldsymbol{l}^*_{23}\| = \|\boldsymbol{l}^*_{34}\| = \|\boldsymbol{l}^*_{41}\| = 5$, can be achieved. The sensing graph shown in Fig. 6.4 is originally rigid in $\mathbb{R}^2$. It is also supposed that position measurements of all nodes are subject to Gaussian noise of different mean values (between 0.1 and 0.3) and different variance values (between 0.1 and 0.15). Figure 6.5A shows the formation before link breaking.

Now, suppose that the link between agents 1 and 4 is broken, thus neither agent 1 nor 4 can measure the position of the other, yet both of them need this measurement for their control laws. If node 2 is in the sensing range of node 4, a link between these two nodes will recover the rigidity. This can be investigated and activated by node 4 using its lattice of configurations. However, if it is not in the range, there is no configuration to recover the rigidity of the sub-framework centred at node 4, thus the whole framework becomes non-rigid. In this case, the formation starts diverging from the desired framework.

Figures 6.5A and 6.5B show the formation 'before' and '100 seconds after' the link failure, respectively. Clearly, the distance between agents 1 and 4 as shown in Fig. 6.5B is far from ideal, meaning that the formation is diverging. To recover the formation, agent 4 starts an "indirect position sensing" process. First, it initiates the shortest-path finding algorithm to find a path towards node 1 which results in $1 \rightarrow 3 \rightarrow 4$. Then, it activates a process to temporarily generate a common coordinate with node 3. Finally, node 4 can calculate the position of node 1 using the position of node 3 as well as the position of node 1 in coordinates of 3. Clearly, the common coordinate should remain active when the formation is in emergency. According to Theorem 1, maximum admissible delay in this measurement process is

$$\bar{h} < \frac{\pi}{2\times4\times25} \approx 0.016$$

Figures 6.5C and 6.5D compare cases when the delay in indirect sensing is $h = 0.015 < \bar{h}$ and $h = 0.04 > \bar{h}$, respectively. The formation is clearly recovered when $h < \bar{h}$ (Fig. 6.5C), while it starts rotating and diverging when $h > \bar{h}$ (Fig. 6.5D).

Figure 6.6 shows the deviation in the distance between agents 1 and 4 when the sensing link between them breaks at T = 50 seconds. Simulation results are averaged over 100 runs while bars represent standard deviations. It is supposed that "Indirect Position Sensing" (including finding the shortest path, alignment of coordinates, etc.) takes 100 seconds. During this time, i.e. between T = 50 and T = 150 seconds, the distance between agents 1 and 4 is almost 9, which is far from the desired value 5. The amplitude of the bars also shows a higher variation in this distance. However, after activation of the proposed rigidity maintenance algorithm at T = 150 seconds, the distance returns back to the normal, meaning that the formation is well recovered. The delay in "Indirect Position Sensing" is supposed to be h = 0.01 second. To further study the effect of variation in h on the performance of the proposed formation recovery technique, in Fig. 6.7, use $e = \sum (||\boldsymbol{l}_{ij}|| - ||\boldsymbol{l}_{ij}^*||)^2$ as a metric for how far the

formation is from the desired framework. As expected, the formation diverges as the delay h in the indirect position sensing increases.

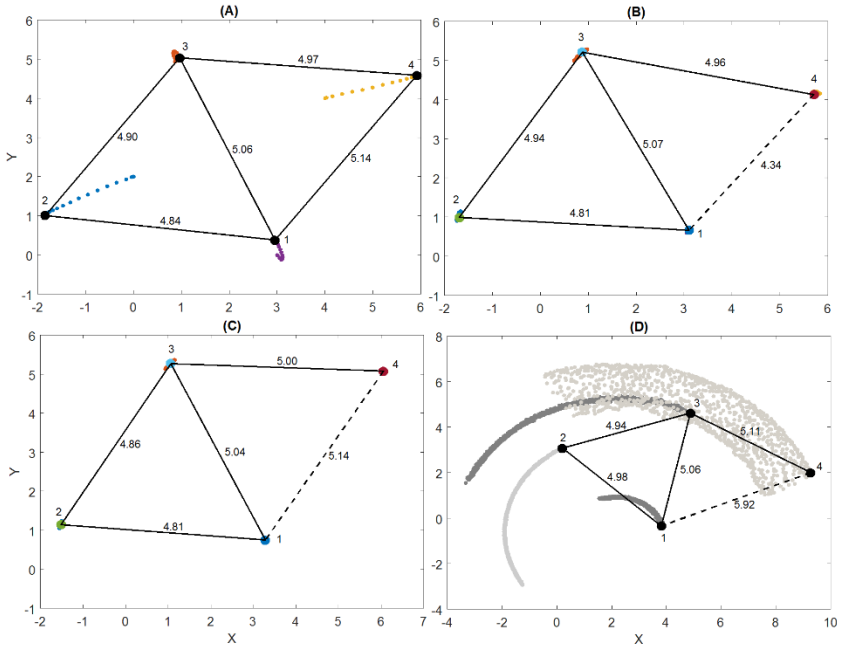

Fig. 6.5: A formation control example (A) Formation in normal condition (controlled using a distributed gradient-based control system); (B) Formation at 100 seconds after failure of the sensing link between agents 1 and 4; (C) Formation is recovered by applying indirectly the measured positions in the control system of agent 4 when delay in this measurement is $h = 0.015 < \bar{h}$ (satisfies Theorem 1); (D) Formation becomes unstable by applying indirectly measured position in the control system when delay in this measurement is $h = 0.015 > \bar{h}$ (violates Theorem 1). Numbers on links show distances between agents.

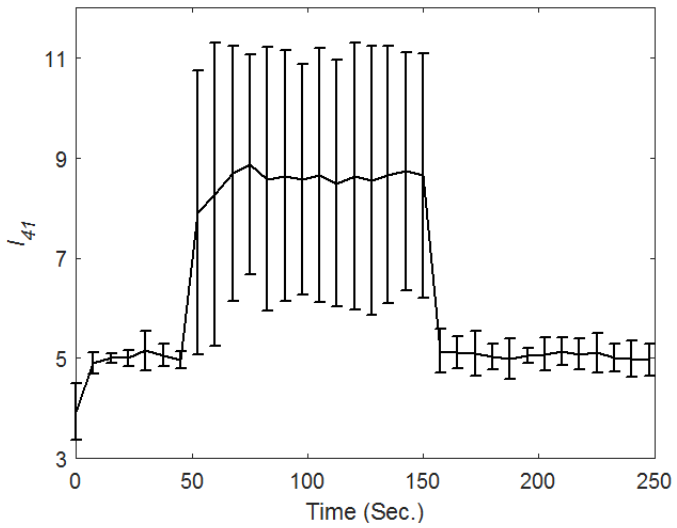

Fig. 6.6: Variation of the distance between nodes 1 and 4 when the sensing link between them breaks at T = 50 seconds. Indirect Position Sensing is activated at T = 150 seconds. Data are averaged over 100 realizations. The solid line shows the mean value and bars indicate standard deviation.

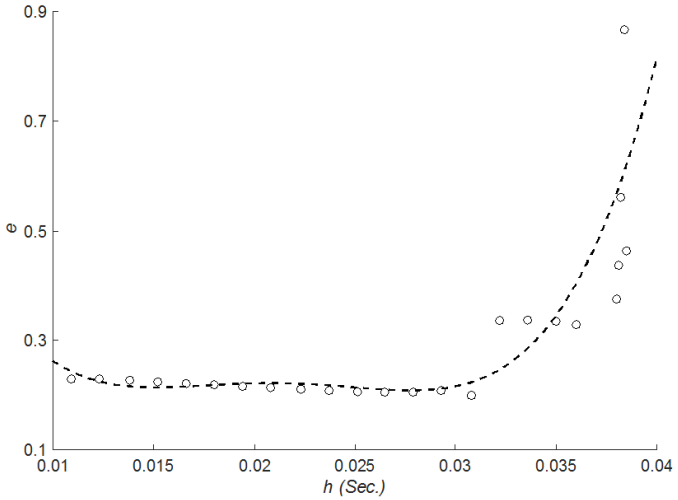

Fig. 6.7: Effect of delay *h* in Indirect Position Sensing on the performance of a formation.

6.4 Summary

The practical problem of increasing the robustness of a formation of multi-agents against sensing failures and constraints, such as line-of-sight requirements and power limitations, is addressed in this chapter. When inter-agent distances are controlled using a distributed gradient-based controller over a minimally rigid measuring graph, the formation would diverge in the case of failure at a sensing link. To handle such situations, a lattice of configurations is proposed in this thesis to be used locally for each agent, which includes all possible configurations among the agent and its sensible neighbours, subject to the rigidity requirement that guarantees the formation. In the proposed algorithm, each agent establishes an appropriate configuration through the lattice and activates it to recover failed rigidity of the sensing framework locally, which achieves rigidity recovery of the whole framework. In the case that such a rigid local framework is not available, the affected node calculates the relative positions indirectly using a multi-layer rigidity recovery technique, i.e. using a combination of sensing and communication networks. Although simple to implement, the proposed algorithm is subject to delays in measurements. An upper bound on measurement time delays is then estimated, ensuring the stability of the formation to be maintained under the link breaking condition. Simulation results support and validate the theoretical analysis and demonstrate the good performance of the proposed control algorithm.

Chapter 7

Conclusions and outlooks

Complex networks are abundant in many critical systems including some of the most important infrastructures, such as transportation and communication systems. Academic and industry communities are much interested in modelling and control of these complex systems. Existing theories cannot address ever-increasing complicated dynamics of these systems and a paradigm shift is required. From the control theory perspective, the state-space approach, which has been used for more than half a century to model and to control dynamical systems, should be revised considering networked structures. In addition, computational efficiency is a requirement when networks with millions of nodes are to be studied. Although the field of control of networked systems has been subject to heavy investigation in the last two decades, we are still far from the point to say that we have overcome the complexity of these systems. This thesis aimed at addressing some of the open questions in this field.

7.1 Findings

Coupled dynamical systems can develop spontaneous collective behaviours, such as synchronisation, under some conditions. The coupling might also facilitate unwanted effects, such as failure propagation through the complex network. These behaviours are highly

dependent on the structure of the interaction network as well as the dynamics of agents. Optimal network topology for collective behaviours and network robustness can be achieved by intelligently modifying the network topology, which is termed as “engineering network structure” in the thesis.

This thesis first started with engineering a complex network by controlling its nodes. The goal was to identify the best drivers which facilitate synchronisation of the network over the widest range of coupling strengths. Central nodes could be good candidates and heuristic centrality measures such as degree, betweenness or closeness centrality can be considered, although they are not related to dynamics of networks. We proposed a new controllability centrality to find the best driver node(s). In order to engineer a network for better collective behaviour, this metric was proposed to identify the most influential set of driver nodes on controllability of a dynamical network. The metric is based on single eigen-decomposition of the Laplacian matrix of the graph; thus, it is computationally efficient and applicable on large-scale networks. Simulation results prove the precision of this metric in networks with different scale-free, Watts-Strogatz and random topologies. Interestingly, controllability centrality shows the sub-modularity feature. It means that by only one eigen-decomposition of the Laplacian matrix, the best subset of nodes with any desired size can be identified. As an application, this metric successfully predicted the best frequency leader in secondary frequency control of distributed generation systems. This is one of the real-time requirements of future power management systems, where there are a lot of small capacity generators. The metric was also applied to identify brain areas of activation which may prevent disease to propagate in dementia networks. Results for these applications should prove of interest to the network community.

The second contribution of this thesis was to find the vital nodes based on their impact on the Laplacian spectrum of a network. Recent research has shown that spectral analysis of complex networked systems is an important tool in describing their functional properties. Therefore, network spectral analysis has found many applications in science and engineering. Although there have been some research articles reporting the importance of nodes and links for the spectrum, there is still lack of a solid mathematical framework to study impact of nodes on the spectrum of a network. In this thesis, a weak interlacing theorem was first proved in a simple way. The main contribution of the thesis for this part was to propose a novel centrality metric which ranks nodes based on their impact on any desired eigenvalue of the Laplacian matrix. This computationally cost-effective metric is based on the local multiplicity concept

and requires only a single eigen-decomposition to identify vital nodes. As such, it could be applied to networks of any size. Consequently, one can identify central nodes considering any desired spectral property of the Laplacian matrix of a graph, such as algebraic connectivity, spectral gap or Laplacian energy. Numerical simulations supported the analytic results.

Finally, the problem of preventing failure propagation in a complex network using rewiring was considered. Interaction between nodes might facilitate the propagation of failures thorough the network, resulting in degradation of the quality of collective behaviours. One strategy against this undesired effect is to re-engineer the network once failure happens in order to either restrict its impact or recover the faulty network. In order to theoretically study this problem, the class of failure and the desired collective behaviour should be clearly defined. In this thesis, formation was considered as collective behaviour in a network of agents. It is known that local controllers can stabilise a formation while the sensing framework is rigid. Failure of sensing links may affect rigidity of the sensing framework, thus affecting stability of the formation. Therefore, the rigidity maintenance problem is considered when failure of a sensing link between two agents results in loss of rigidity in the sensing network. In order to engineer the network to recover its rigidity, an online distributed rigidity maintenance algorithm based on “Lattice of Configuration” was proposed, which prevents the formation instability in the case of link breakage. The proposed technique activates new configuration for the local frameworks by adding a few extra sensing links which results in the rigidity of the local framework, and thus the whole framework. This problem was also solved in an emergency condition when no extra sensing link could be activated, using a combination of sensing and communication networks.

7.2 Future directions

With increasing large-scale complex systems in the real-world, modern tools for their analysis and control should be developed. The existing algorithms for control systems should be properly revised considering network connections between dynamical agents. To this end, computationally efficient and accurate enough algorithms should be developed. Complex network approach which is well-supported by mathematical graph theory seems a promising approach to handle this complexity.

This thesis was the first step towards optimal pinning control of complex networks. The interpretation of being “optimal” is slightly different from the optimal control theory, widely

studied in control society. Here, for instance, for a network with fixed topology, we should select the best control nodes and design appropriate control gains for them in order to achieve optimal pinning control performance. This thesis proposed a metric to find the best drivers, which is easy to compute. As it needs only an eigen-decomposition of the Laplacian matrix, it is also applicable to some classes of evolving networks. The next step could be to extend the proposed technique to solve the optimal control problem, i.e. addressing the trade-off between the number and location of driver nodes and their gains, which may convert the problem into a combinatorial optimisation one. Practical constraints, such as limits on control gains or delay in interaction, can also be considered to make it more applicable to real-world scenarios. Using controllability centrality, one may also think about extracting the backbone of a network and extending results to recommender systems. To this end, extension of controllability centrality to directed networks might be required.

Inspired from the master stability function formalism, this thesis showed that one approach to study the effect of failures in nodes/links on network synchronisability is through spectral graph theory. Using this approach, a simple metric was proposed to measure the impact of node removal on the spectrum of a graph, hence on its collective behaviours of a class of complex systems. This problem can be further studied for another class of systems where synchronisability is measured using $R = \lambda_N/\lambda_2$ metric. The proposed metric in this thesis can also be studied in networks with different topologies such as community-based and multi-layer networks and networks with load redistribution. In addition to finding vulnerable nodes and links, making a complex network tolerant to faults can be studied in the context of spectral graph theory. We particularly considered formation of agents and proposed an online recovery algorithm in the case of link break. This problem is a special case of distributed fault tolerant control of complex networks. It can be comprehensively studied using spectral graph theory by developing distributed algorithms to recover λ_2 or λ_N/λ_2 of a complex network in the case of failure in nodes or links. The problem becomes more interesting when real-time constraints of different application are also considered.

Bibliography

1. Albert, R., H. Jeong and A. Barabasi (2000). "Error and attack tolerance of complex networks." Nature 406: 5.

2. Amaral, L. A. and J. M. Ottino (2004). "Complex networks." The European Physical Journal B 38(2): 147-162.

3. Arenas, A., A. Díaz-Guilera, J. Kurths, Y. Moreno and C. Zhou (2008). "Synchronization in complex networks." Physics Reports 469(3): 93-153.

4. Asimow, L. and B. Roth (1979). "The rigidity of graphs, II." Journal of Mathematical Analysis and Applications 68(1): 171-190.

5. Barabasi, A.-L. and Z. N. Oltvai (2004). "Network biology: understanding the cell's functional organization." Nature reviews genetics 5(2): 101.

6. Barabasi, A. L. and R. Albert (1999). "Emergence of Scaling in Random Networks." Science 286: 509-512.

7. Belykh, I., M. Hasler, M. Laurent and H. Nijmeijer (2005). "Synchronization and graph topology." International Journal of Bifurcation and Chaos 15(11): 3423-3433

8. Bevrani, H., M. Watanabe and Y. Mitani (2014). Power system monitoring and control, John Wiley & Sons.

9. Bidram, A. and A. Davoudi (2012). "Hierarchical structure of microgrid control system." IEEE Transactions on Smart Grid 3(4): 1963-1976.

10. Bidram, A., F. L. Lewis and A. Davoudi (2014). "Distributed control systems for small-scale power networks." IEEE Control Systems Magazine 34(6): 56-77.

11. Bidram, A., F. L. Lewis, Z. Qu and A. Davoudi (2013). "Secondary control of microgrids based on distributed cooperative control of multi-agent systems." IET Generation, Transmission & Distribution 7(8): 822-831.

12. Boccaletti, S., V. Latora, Y. Moreno, M. Chavez and D. Hwang (2006). "Complex networks: Structure and dynamics." Physics Reports 424(4-5): 175-308.

13. Bornholdt, S. and H. G. Schuster (2006). Handbook of graphs and networks: from the genome to the internet, John Wiley & Sons.

14. Buldyrev, S. V., R. Parshani, G. Paul, H. E. Stanley and S. Havlin (2010). "Catastrophic cascade of failures in interdependent networks." Nature 464(7291): 1025-1028.

15. Carboni, D., R. K. Williams, A. Gasparri, G. Ulivi and G. S. Sukhatme (2015). "Rigidity-Preserving Team Partitions in Multiagent Networks." IEEE Transactions on Cybernetics 45(12): 2640-2653.

16. Chavez, M., D. U. Hwang, A. Amann, H. G. Hentschel and S. Boccaletti (2005). "Synchronization is enhanced in weighted complex networks." Physical Review Letters 94(21): 218701.

17. Chen, C.-T. (1998). Linear system theory and design, Oxford University Press, Inc.

18. Cheng, J., W. Cheng and R. Nagpal (2005). Robust and self-repairing formation control for swarms of mobile agents. AAAI. 5**:** 59-64.

19. Cortés, J. (2009). "Global and robust formation-shape stabilization of relative sensing networks." Automatica 45(12): 2754-2762.

20. Costa, L. d. F., F. A. Rodrigues, G. Travieso and P. R. Villas Boas (2007). "Characterization of complex networks: A survey of measurements." Advances in Physics 56(1): 167-242.

21. Cowan, N. J., E. J. Chastain, D. A. Vilhena, J. S. Freudenberg and C. T. Bergstrom (2012). "Nodal dynamics, not degree distributions, determine the structural controllability of complex networks." PLoS One 7(6): e38398.

22. Crucitti, P., V. Latora and M. Marchiori (2004). "Model for cascading failures in complex networks." Physical Review E 69(4): 045104.

23. Cui, L., S. Kumara and R. Albert (2010). "Complex Networks: An Engineering View." IEEE Circuits and Systems Magazine 10(3): 10-25.

24. Cvetković, D. and M. Doob (1985). "Developments in the theory of graph spectra." Linear and Multilinear Algebra 18(2): 153-181.

25. Das, A. K., R. Fierro, V. Kumar, J. P. Ostrowski, J. Spletzer and C. J. Taylor (2002). "A vision-based formation control framework." IEEE Transactions on Robotics and Automation 18(5): 813-825.

26. Davey, B. A. and H. A. Priestley (2002). Introduction to lattices and order, Cambridge university press.

27. De Lellis, P., M. di Bernardo and F. Garofalo (2008). "Synchronization of complex networks through local adaptive coupling." Chaos 18(3): 037110.

28. Erdős, P. and A. Rényi (1960). "On the evolution of random graphs." Publications of the Mathematical Institute of the Hungarian Academy of Science 5: 17-61.

29. Eren, T. (2012). "Formation shape control based on bearing rigidity." International Journal of Control 85(9): 1361-1379.

30. Eren, T., B. D. O. Anderson, A. S. Morse, W. Whiteley and P. N. Belhumeur (2003). "Operations on Rigid Formations of Autonomous Agents." Communications in Information and Systems 3(4): 223-258.

31. Eren, T., P. N. Belhumeur, B. D. O. Anderson and A. S. Morse (2002). "A Framework for Maintaining Formations Based on Rigidity." IFAC Proceedings Volumes 35(1): 499-504.

32. Estrada, E. and J. A. Rodriguez-Velazquez (2005). "Subgraph centrality in complex networks." Physical Review E 71(5): 056103.

33. Euler, L. (1741). "Solutio problematis ad geometriam situs pertinentis." Commentarii academiae scientiarum Petropolitanae: 128-140.

34. Fathian, K., D. I. Rachinskii, T. H. Summers, M. W. Spong and N. R. Gans (2017). Distributed formation control under arbitrarily changing topology. American Control Conference**:** 271-278.

35. Fidan, B., J. M. Hendrickx and B. D. O. Anderson (2010). "Closing ranks in rigid multi-agent formations using edge contraction." International Journal of Robust and Nonlinear Control 20(18): 2077-2092.

36. Fiedler, M. (1973). "Algebraic connectivity of graphs." Czechoslovak Mathematical Journal 23(2): 298-305.

37. Fiol, M. A. (2002). "Algebraic characterizations of distance-regular graphs." Discrete Mathematics 246(1-3): 111-129.

38. Fiol, M. A. and E. Carriga (1997). "From local adjacency polynomials to locally pseudo-distance-regular graphs." Journal of Combinatorial Theory, Series B 71(2): 162-183.

39. Gaeini, N., A. Moradi Amani, M. Jalili and X. Yu (2016). Roles of node dynamics and data network structure on cooperative secondary control of distributed power grids. 42nd Annual Conf. IEEE Indust. Elec. Society (IECON), Italy.

40. Gao, J., Y.-Y. Liu, R. M. D'souza and A.-L. Barabási (2014). "Target control of complex networks." nature communications 5: 5415.

41. Gates, A. J. and L. M. Rocha (2016). "Control of complex networks requires both structure and dynamics." Scientific Report 6: 24456.

42. Ge, X., F. Yang and Q.-L. Han (2015). "Distributed networked control systems: A brief overview." Information Sciences.

43. Gershgorin, S. A. (1931). "Uber die abgrenzung der eigenwerte einer matrix." Известия Российской академии наук. Серия математическая(6): 749-754.

44. Godsil, C. and G. Royle (2001). Graduate Texts in Mathematics. Algebraic graph theory, Springer-Verlag New York. 207.

45. Goh, K. I., B. Kahng and D. Kim (2001). "Universal behavior of load distribution in scale-free networks." Physical Review Letters 87(27): 278701.

46. Guerrero, J. M., M. Chandorkar, T.-L. Lee and P. C. Loh (2013). "Advanced Control Architectures for Intelligent Microgrids Part I: Decentralized and Hierarchical Control." IEEE Transactions on Industrial Electronics 60(4): 1254-1262.

47. Iyer, S., T. Killingback, B. Sundaram and Z. Wang (2013). "Attack robustness and centrality of complex networks." PLoS One 8(4): e59613.

48. Jahanpour, E. and X. Chen (2013). "Analysis of complex network performance and heuristic node removal strategies." Communications in Nonlinear Science and Numerical Simulation 18(12): 3458-3468.

49. Jalili, M. (2013). "Enhancing synchronizability of diffusively coupled dynamical networks: A survey." IEEE Transactions on Neural Networks and Learning Systems 24(7): 1009-1022.

50. Jalili, M., O. A. Sichani and X. Yu (2015). "Optimal pinning controllability of complex networks: Dependence on network structure." Physical Review 91.

51. Jalili, M., O. A. Sichani and X. Yu (2015). "Optimal pinning controllability of complex networks: Dependence on network structure." Physical Review E 91: 012803.

52. Jamakovic, A. and P. Van Mieghem (2008). "On the robustness of complex networks by using the algebraic connectivity." Networking 2008 Ad Hoc and Sensor Networks, Wireless Networks, Next Generation Internet: 183-194.

53. Kailath, T. (1980). Linear systems, Prentice-Hall Englewood Cliffs, NJ.

54. Kalman, R. E., Y. C. Ho and S. K. Narendra (1963). "Controllability of linear dynamical systems." Contrib. Differ. Equ. 1(2): 189– 213.

55. Kar, S. and J. M. F. Moura (2009). "Distributed Consensus Algorithms in Sensor Networks With Imperfect Communication: Link Failures and Channel Noise." IEEE Transactions on Signal Processing 57(1): 355-369.

56. Katiraei, F. and M. R. Iravani (2006). "Power management strategies for a microgrid with multiple distributed generation units." IEEE Transactions on Power Systems 21(4): 1821-1831.

57. Kinney, R., P. Crucitti, R. Albert and V. Latora (2005). "Modeling cascading failures in the North American power grid." The European Physical Journal B - Condensed Matter and Complex Systems 46(1): 101-107.

58. Klamka, J. (2013). "Controllability of dynamical systems. A survey." Bulletin of the Polish Academy of Sciences: Technical Sciences 61(2): 335-342.

59. Krick, L., M. E. Broucke and B. A. Francis (2009). "Stabilisation of infinitesimally rigid formations of multi-robot networks." International Journal of Control 82(3): 423-439.

60. Kundur, P., N. J. Balu and M. G. Lauby (1994). Power system stability and control, McGraw-hill New York.

61. L. Kempton, G. Herrmann and M. d. Bernardo (2016). Distributed adaptive optimization and control of network structures. IEEE 55th Conference on Decision and Control. Las Vegas, USA, IEEE**:** 5839-5844.

62. Laman, G. (1970). "On graphs and rigidity of plane skeletal structures." Journal of Engineering Mathematics 4(4): 331-340.

63. Latora, V. and M. Marchiori (2001). "Efficient behavior of small-world networks." Physical Review Letter 87(19): 198701.

64. Lewis, M. A. and K.-H. Tan (1997). "High Precision Formation Control of Mobile Robots Using Virtual Structures." Autonomous Robots 4(4): 387-403.

65. Lin, C.-T. (1974). "Structural controllability." IEEE Transactions on Automatic Control 19(3): 201-208.

66. Liu, X. and L. Pan (2015). "Identifying driver nodes in the human signaling network using structural controllability analysis." IEEE/ACM Transactions on Computational Biology and Bioinformatics 12(3): 467-472.

67. Liu, Y., J. Slotine and A. Barabasi (2011). "Controllability of complex networks." Nature 473.

68. Liu, Y., Y. Zhao and G. Chen (2016). "Finite-time formation tracking control for multiple vehicles: A motion planning approach." International Journal of Robust and Nonlinear Control 26(14): 3130-3149.

69. Lopes, J. A. P., C. L. Moreira and A. G. Madureira (2006). "Defining control strategies for microgrid islanded operation." IEEE Trans. Power Syst. 21(2): 916-924.

70. Lotker, Z. (2007). "Note on deleting a vertex and weak interlacing of the Laplacian spectrum." Electronic Journal of Linear Algebra 16(1).

71. Lovasz, L. (2007). Eigenvalues of graphs. Available: www.cs.elte.hu/~lovasz/eigenvals-x.pdf.

72. M. Jalili and X. Yu (2016). "Enhancement of synchronizability in networks with community structure through adding efficient inter-community links." IEEE Transactions on Network Science and Engineering 3(2): 106-116.

73. M. Profiri and M. di Bernardo (2008). "Criteria for global pinning-controllability of complex networks." Automatica 44(12): 3100-3106.

74. Machowski, J., J. Bialek and J. Bumby (2011). Power system dynamics: stability and control, John Wiley & Sons.

75. Marwali, M. N., J.-W. Jung and A. Keyhani (2004). "Control of distributed generation systems - Part II: load sharing control." IEEE Transactions on Power Electronics 19(6): 1551-1561.

76. Mesbahi, M. and M. Egerstedt (2010). Graph theoretic methods in multiagent networks, Princeton University Press.

77. Meyer-Bäse, A., A. Moradi Amani, U. Meyer-Bäse, S. Foo, A. Stadlbauer and W. Yu (2019). "Pinning observability of competitive neural networks with different time–constants." Neurocomputing 329: 97-102.

78. Mieghem, P. V. (2011). Graph Spectra for Complex Networks, Cambridge University Press.

79. Milanese, A., J. Sun and T. Nishikawa (2010). "Approximating spectral impact of structural perturbations in large networks." Physical Review E 81(4): 046112.

80. Moradi Amani, A., G. Chen, M. Jalili, X. Yu and L. Stone "Distributed rigidity maintenance in distance-based formations using configuration lattice." IEEE Transaction on Control of Network Systems (under revision).

81. Moradi Amani, A., N. Gaeini, A. Afshar and M. B. Menhaj (2013). "A new approach to reconfigurable load frequency control of power systems in emergency conditions." IFAC Proceedings Volumes 46(13): 526-531.

82. Moradi Amani, A., N. Gaeini, M. Jalili and X. Yu (2017). "Which generation unit should be selected as control leader in secondary frequency control of microgrids?" IEEE Journal on Emerging and Selected Topics in Circuits and Systems 7(3): 393-402.

83. Moradi Amani, A., M. Jalili, X. Yu and L. Stone (2017). "Finding the most influential nodes in pinning controllability of complex networks." IEEE Transactions on Circuits and Systems - II: Express Briefs 64(6): 685-689.

84. Moradi Amani, A., M. Jalili, X. Yu and L. Stone (2018). "Controllability of complex networks: Choosing the best driver set." Physical Review E 98(3): 030302.

85. Moradi Amani, A., M. Jalili, X. Yu and L. Stone (2018). A New Metric to Find the Most Vulnerable Node in Complex Networks. 2018 IEEE International Symposium on Circuits and Systems (ISCAS), Florence, Italy: 1-5.

86. Motter, A. E. and Y. C. Lai (2002). "Cascade-based attacks on complex networks." Physical Review E 66(6 Pt 2): 065102.

87. Nelson, R. B. (1976). "Simplified calculation of eigenvector derivatives." AIAA Journal 14(9): 1201-1205.

88. Newman, M. (2010). Networks: an introduction, Oxford university press.

89. Nourine, L. and O. Raynaud (1999). "A fast algorithm for building lattices." Information processing letters 71(5-6): 199-204.

90. Oh, K.-K., M.-C. Park and H.-S. Ahn (2015). "A survey of multi-agent formation control." Automatica 53: 424-440.

91. Olfati-Saber, R., J. A. Fax and R. M. Murray (2007). "Consensus and cooperation in networked multi-agent systems." Proceedings of the IEEE 95(1): 215 - 233.

92. Olfati-Saber, R. and R. M. Murray (2004). "Consensus problems in networks of agents with switching topology and time-delays." IEEE Transactions on Automatic Control 49(9): 1520-1533.

93. Orouskhani, Y., M. Jalili and X. Yu (2016). "Optimizing dynamical network structure for pinning control." Scientific Report 6: 24252.

94. Ortiz, A., J. Munilla, I. Álvarez-Illán, J. M. Górriz, J. Ramírez and A. s. D. N. Initiative (2015). "Exploratory graphical models of functional and structural connectivity patterns for Alzheimer's disease diagnosis." Frontiers in computational neuroscience 9: 132.

95. Pasqualetti, F., S. Zampieri and F. Bullo (2014). "Controllability metrics, limitations and algorithms for complex networks." IEEE Transactions on Control of Network Systems 1(1): 40-52.

96. Pecora, L. M. and T. L. Carroll (1998). "Master stability functions for synchronized coupled systems." Physical Review Letters 80(10): 2109.

97. Peleg, D. (2000). "Distributed computing." SIAM Monographs on discrete mathematics and applications 5.

98. Pham, T. T. H., Y. Bésanger and N. Hadjsaid (2009). "New challenges in power system restoration with large scale of dispersed generation insertion." IEEE Transactions on Power Systems 24(1): 398-406.

99. Pikovsky, A., M. Rosenblum and J. Kurths (2003). Synchronization: a universal concept in nonlinear sciences, Cambridge university press.

100. Porfiri, M. and M. di Bernardo (2008). "Criteria for global pinning-controllability of complex networks." Automatica 44(12): 3100-3106.

101. Posfai, M., Y. Y. Liu, J. J. Slotine and A. L. Barabasi (2013). "Effect of correlations on network controllability." Scientific Report 3: 1067.

102. Q. Song and J. Cao (2010). "On pinning synchronization of directed and undirected complex dynamical networks." IEEE Transactions on Circuits and Systems I: Regular Papers 57(3): 672-680.

103. Qi, X., E. Fuller, Q. Wu, Y. Wu and C.-Q. Zhang (2012). "Laplacian centrality: A new centrality measure for weighted networks." Information Sciences 194: 240-253.

104. Rad, A. A., M. Jalili and M. Hasler (2008). "Efficient rewirings for enhancing synchronizability of dynamical networks." CHAOS 18(3): 037104.

105. Ramazani, S., R. Selmic and M. de Queiroz (2017). "Rigidity-based multiagent layered formation control." IEEE Trans. Cybernetics 47(8): 1902-1913.

106. Restrepo, J. G., E. Ott and B. R. Hunt (2006). "Characterizing the dynamical importance of network nodes and links." Physical Review Letters 97(9): 094102.

107. Rocabert, J., A. Luna, F. Blaabjerg and P. Rodr´ıguez (2012). "Control of power converters in AC microgrids." IEEE Transactions on Power Electronics 27(11): 4374-4749.

108. Schafer, B., M. Matthiae, M. Timme and D. Witthaut (2015). "Decentral smart grid control." New Journal of Physics 17(5): 015002.

109. Scharf, D. P., F. Y. Hadaegh and S. R. Ploen (2004). A survey of spacecraft formation flying guidance and control. Part II: control. American Control Conference. 4**:** 2976-2985.

110. Schiano, F. and P. R. Giordano (2017). Bearing rigidity maintenance for formations of quadrotor UAVs. IEEE International Conference on Robotics and Automation (ICRA)**:** 1467-1474.

111. Scott, J. (2017). Social network analysis, Sage.

112. Slootweg, J. G. and W. L. Kling (2002). Impacts of distributed generation on power system transient stability. Power Engineering Society Summer Meeting. 2**:** 862-867 vol.862.

113. Sorrentino, F., M. di Bernardo, F. Garofalo and G. Chen (2007). "Controllability of complex networks via pinning." Physical Review E 75: 046103.

114. Sorrentino, F., M. di Bernardo, F. Garofalo and G. Chen (2007). "Controllability of complex networks via pinning." Physical Review E 75(4): 046103.

115. Staroswiecki, M. and A. M. Amani (2015). "Fault-tolerant control of distributed systems by information pattern reconfiguration." Int. J. Adapt. Control Signal Process. 29(6): 671-684.

116. Staroswiecki, M. and A. M. Amani (2015). "Fault-tolerant control of distributed systems by information pattern reconfiguration." International Journal of Adaptive Control and Signal Processing 29(6): 671-684.

117. Summers, T. H., F. L. Cortesi and J. Lygeros (2016). "On submodularity and controllability in complex dynamical networks." IEEE Transactions on Control of Network Systems 3(1): 91-101.

118. Sun, J. and A. E. Motter (2013). "Controllability transition and nonlocality in network control." Physical Review Letters 110(20): 208701.

119. Tahmassebi, A., A. M. Amani, K. Pinker-Domenig and A. Meyer-Baese (2018). Determining disease evolution driver nodes in dementia networks. SPIE Medical Imaging. Houston, Texas, USA. 10578.

120. Tang, Y., H. Gao and J. Kurths (2013). "Multiobjective identification of controlling areas in neuronal networks." IEEE/ACM Trans. Comput. Biol. Bioinf. 10(3): 708-720.

121. Tang, Y., F. Qian, H. Gao and J. Kurths (2014). "Synchronization in complex networks and its application – A survey of recent advances and challenges." Annual Reviews in Control 38(2): 184-198.

122. Tielens, P. and D. Van Hertem (2012). Grid inertia and frequency control in power systems with high penetration of renewables. Young Researchers Symposium in Electrical Power Engineering. Netherlands.

123. Uhlhaas, P. J. and W. Singer (2006). "Neural synchrony in brain disorders: relevance for cognitive dysfunctions and pathophysiology." neuron 52(1): 155-168.

124. Vasquez, J. C., J. M. Guerrero, M. Savaghebi, J. Eloy-Garcia and R. Teodorescu (2013). "Modeling, analysis and design of stationary-reference-frame droop-controlled parallel three-phase voltage source inverters." IEEE Transactions on Industrial Electronics 60(4): 1271-1280.

125. Wang, X. F. and G. Chen (2002). "Pinning control of scale-free dynamical networks." Physica a: Statistical mechanics and its applications 310(3): 521-531.

126. Wang, X. F. and G. Chen (2003). "Complex networks: Small-world, scale-free and beyaond." IEEE Circuits and Systems Magazine 3(1): 6-20.

127. Wasserman, S. and K. Faust (1994). Social network analysis: Methods and applications, Cambridge university press.

128. Watanabe, T. and N. Masuda (2010). "Enhancing the spectral gap of networks by node removal." Physical Review E 82(4 Pt 2): 046102.

129. Watts, D. J. and S. H. Strogatz (1998). "Collective dynamics of 'small-world' networks." Nature 393: 440-442.

130. Wiener, N. (1965). Cybernetics or Control and Communication in the Animal and the Machine, MIT press.

131. Wilkinson, J. H. (1965). The algebraic eigenvalue problem, Clarendon Press Oxford.

132. Winfree, A. T. (1967). "Biological rhythms and the behavior of populations of coupled oscillators." Journal of theoretical biology 16(1): 15-42.

133. Wu, J., M. Barahona, Y. J. Tan and H. Z. Deng (2011). "Spectral Measure of Structural Robustness in Complex Networks." IEEE Transactions on Systems, Man, and Cybernetics - Part A: Systems and Humans 41(6): 1244-1252.

134. Wu, Y., W. Wei, G. Li and J. Xiang (2009). "Pinning control of uncertain complex network to a homogeneous orbit." IEEE Transactions on Circuits and Systems II: Express Briefs 56(3): 235-239.

135. Xiao Fan, W. and C. Guanrong (2002). "Synchronization in scale-free dynamical networks: robustness and fragility." IEEE Transactions on Circuits and Systems I: Regular Papers 49(1): 54-62.

136. Yan, G., J. Ren, Y. C. Lai, C. H. Lai and B. Li (2012). "Controlling complex networks: how much energy is needed?" Physical Review Letters 108(21): 218703.

137. Yu, W., G. Chen and J. Lü (2009). "On pinning synchronization of complex dynamical networks." Automatica 45(2): 429-435.

138. Yu, W., J. Lu, X. Yu and G. Chen (2013). A step forward to pinning control of complex networks: finding an optimal vertex to control. Asian Control Conference, Istanbul, Turkey.

139. Yu, W., G. Wen, G. Chen and J. Cao (2017). Distributed Cooperative Control of Multi-agent Systems, John Wiley & Sons.

140. Yu, W., G. Wen, X. Yu, Z. Wu and J. Lu (2014). "Bridging the gap between complex networks and smart grids." Journal of Control and Decision 1(1): 102-114.

141. Yu, X., C. Cecati, T. Dillon and M. G. Sim (2011). "The new frontier of smart grids." IEEE Control System Magazine 5(3): 49-63.

142. Zelazo, D., A. Franchi, H. H. Bülthoff and P. Robuffo Giordano (2015). "Decentralized rigidity maintenance control with range measurements for multi-robot systems." Int. J. Robotics Research 34(1): 105-128.

143. Zhou, M.-Y., Z. Zhuo, H. Liao, Z.-Q. Fu and S.-M. Cai (2015). "Enhancing speed of pinning synchronizability: low-degree nodes with high feedback gains." Scientific Reports 5: 17459.